SEISMIC VULNERABILITY OF OLDER REINFORCED CONCRETE FRAME STRUCTURES IN MID-AMERICA

A Thesis

by

LAUREN RAE BEASON

Submitted to the Office of Graduate Studies of
Texas A&M University
in partial fulfillment of the requirements for the degree of

MASTER OF SCIENCE

May 2004

Major Subject: Civil Engineering

SEISMIC VULNERABILITY OF OLDER REINFORCED CONCRETE FRAME STRUCTURES IN MID-AMERICA

A Thesis

by

LAUREN RAE BEASON

Submitted to Texas A&M University
in partial fulfillment of the requirements
for the degree of

MASTER OF SCIENCE

Approved as to style and content by:

Joseph Bracci (Chair of Committee)	Mary Beth Hueste (Member)
Terry Kohutek (Member)	Paul Roschke (Interim Department Head)

May 2004

Major Subject: Civil Engineering

ABSTRACT

Seismic Vulnerability of Older Reinforced Concrete Frame Structures in Mid-America.

(May 2004)

Lauren Rae Beason, B.S., Texas A&M University

Chair of Advisory Committee: Dr. Joseph Bracci

This research quantifies the seismic vulnerability of older reinforced concrete frame structures located in Mid-America. After designing a representative three-story gravity load designed reinforced concrete frame structure, a nonlinear analytical representation was used evaluate inter-story drift demands from simulated earthquake time histories that were representative for the region. Limit state story drift capacities were identified for FEMA 273 guidelines, nonlinear pushover analyses, and incremental dynamic analyses. Integrating these two quantities allowed for the creation of fragility curves which relates the probability of exceeding a particular limit state given an imposed spectral acceleration at the fundamental building period. These curves were then used to evaluate the seismic vulnerability of the representatively designed structure. The structure as originally designed was found to be inadequate to resist large lateral loading that would be typical for the Memphis area. So structural retrofit performed by increasing the column-to-beam strength ratio was evaluated by increasing the strength of the column members in the analytical model. The first retrofit raised the column-to-beam strength ratio to 1.2, which is currently required by the ACI code provisions. The second retrofit raised the column-to-beam strength ratio to 1.8, as suggested in previous studies. The story capacity, demand, and fragility curves were once again created for these retrofitted structures. Comparison of these fragility curves is discussed in relation to the retrofit strategy of column strengthening for older reinforced concrete frame structures in Mid-America.

ACKNOWLEDGMENTS

I would like to thank my committee chair, Dr. Joe Bracci, for giving me the opportunity to do such interesting research and giving me the guidance to get it done. I would also like to thank Dr. Mary Beth Hueste and Dr. Terry Kohutek for the advice and suggestions with this thesis.

This work was supported in part by the Mid-America Earthquake Center through the Earthquake Engineering Research Center Program of the National Science Foundation under award number EEC-9701785. Funding was also provided by the Department of Civil Engineering and the Texas Engineering Experiment Station at Texas A&M University. The support from each of these sources is gratefully acknowledged.

.

.

TABLE OF CONTENTS

CHAPTER Page

LIST OF FIGURES

LIST OF TABLES

CHAPTER I
INTRODUCTION

BACKGROUND

The possible risks and hazards associated with earthquakes has been a topic of much discussion since the San Fernando California earthquake of 1971. Since this time much work has been done pertaining to earthquake events, as well as the damage that these events cause to the built environment. This built environment consists of anything manmade such as bridges and structures. While much research has been done, much remains to be done in order to fully understand the seismic risks and hazards present. The Mid-America region of the country is an area that needs further study to fully quantify the character of the earthquake events and the damage that they cause to the built environment. Current code provisions have Memphis, Tennessee located in the largest magnitude earthquake region in the continental United States, however, this is not the case in older code provisions. The older code provisions either neglected or underestimated the current earthquake hazard in this region of the country. For this reason, older structures, reinforced concrete frame structures in particular in this work, are believed to be particularly susceptible to damage from lateral loading caused by large magnitude earthquakes. Therefore, the older reinforced concrete frame structures in the Mid-America region should be studied to fully understand the damage potential for earthquakes.

RESEARCH OBJECTIVES

The research undertaken in this project is a study of the vulnerability of older reinforced concrete frame structures located in the Mid-America region, specifically Memphis, due to potential earthquakes.

This thesis follows the style and format of the *Journal of Structural Engineering.*

The purpose of this study is to quantify the fragility, or probability of exceeding a particular limit state given an imposed seismic demand parameter, of these structures. One set of these fragility curves will plot the probability of exceedance versus the spectral acceleration of the earthquake event at the fundamental period of the structure under consideration. The other set of fragility curves will plot the probability of exceedance versus spectral displacement at the fundamental period of the structure under consideration. Additionally, the research attempts to quantify the vulnerability of retrofitted reinforced concrete structures using column strengthening.

SCOPE OF WORK

A literature review on the performance of reinforced concrete frame structures during earthquakes is first presented in Chapter II. This information validates the research performed, as well as placing this research with respect to other related studies. Following this, a structure representative of older reinforced concrete frame structures located in Mid-America was designed according to past practice. The prototype structure is a three story; four bay reinforced concrete frame structure. The design procedures specified in ACI 318-99 in conjunction with IBC 2000 were utilized in the design of the representative structure. The design procedures and calculations are outlined in Chapter III of this thesis.

Chapter IV documents the numerical structural model used to represent the designed structure through the use of IDASS, a nonlinear time history dynamic analysis program (Kunnath, 2003). Three different groups of analyses were run to fully quantify the behavior of the prototype structure. The first of these were the pushover analyses that were used to define the story capacity limit states of the modeled structure. Six different pushover analyses were run to determine quantitative limit states for inter-story drift and define the reserve strength available in a given structure. These limit states are first yield, plastic mechanism initiation, and strength degradation. Incremental dynamic analyses were also performed to quantify the incipient capacity resistance, or story

capacity, of the designed structure. These analyses utilized ground motion files for the Memphis area on representative soft soil (Wen, 2003). All analyses utilized in defining the story capacity of the modeled structure are discussed in detail in Chapter IV.

Chapter V presents the inter-story drift demands of the building when excited by the ground motions for Memphis, as in Chapter IV, using inelastic time history dynamic analyses. A best-fit line following the power law equation is used to represent the structural demand for varying amplitudes of ground motion for Memphis.

Fragility curves are created from integrating the results of the demand and capacity analyses discussed above and are presented in Chapter VI. Several sets of fragility curves were developed, including limits states based on immediate occupancy, life safety, collapse prevention, incipient collapse, first yield and plastic mechanism initiation. In addition, fragility curves were created both including and excluding the second-order effects of p-delta. Different levels of uncertainty were also tested to determine their significance to the overall fragility of the prototype structure.

Having created the desired fragility curves, the next step was to determine whether or not the prototype structure was adequate. Taking the typical earthquake acceleration design values for the region at the fundamental period of the prototype structure from IBC 2000, one would be able to assess the seismic vulnerability of the structure. If the prototype structure has a high probability of exceeding a limit state, then retrofitting may need to be considered. Based on previous research, structures with column-to-beam strength ratios on the order of 0.60 are prone to story mechanisms during large magnitude earthquakes (Bracci, 1995). Therefore, a retrofit scheme based on increasing the column strength was evaluated for improved performance. Based on the research done by Dooley and Bracci (2001) and others, the performance of gravity load designed reinforced concrete frame structures can be significantly improved through the use of column strengthening. An initial retrofit increased this ratio from that

of the originally designed prototype structure to 1.2, which is the current ACI minimum requirement (ACI 318-99, 1999), and a second retrofit option increased this ratio to 1.8, as recommended by Dooley and Bracci (2001). The initial retrofit involving a 1.2 column-to-beam strength ratio is discussed in Chapter VII and the second retrofit involving a column-to-beam strength ratio of 1.8 is discussed in Chapter VIII. By combining these design options, adequacy of the originally designed structure can be determined, as well as any column strengthening retrofits of the original prototype structure. Chapter IX combines all of the information in previous chapters to determine applicable conclusions and opportunities for future work.

CHAPTER II
LITERATURE REVIEW

SEISMIC RISK

Earthquakes that occur at the boundary between two tectonic plates, such as in California, are called interplate earthquake events (Powell, 2003). Locations prone to these types of earthquakes have historically been classified as areas of high seismic risk. Due to this high risk, the seismic effects and susceptibility these areas are likely to encounter has been studied and well defined. However, earthquakes can also occur within the boundaries of a single tectonic plate and are referred to as intraplate earthquakes. The New Madrid Seismic zone, near Memphis, is one such intraplate earthquake area. Intraplate regions have been historically described as areas of low to moderate seismic hazard. The effects and risks involved with intraplate earthquakes have been studied, but are not yet fully understood (Olshansky, 1993). In response to this lack of information, research efforts have been performed to better understand the activity occurring in these areas, of particular interest is the central and eastern portion of the United States referred to here as Mid-America. This region of the country has been defined as an area where large magnitude earthquakes occur at long recurrence periods (Nuttli, 1987). This means that large intensity earthquakes occur infrequently.

The most dramatic examples of the earthquake hazards present in this area are the New Madrid events of 1811 and 1812, which took place at various locations along the New Madrid fault line. Earthquake magnitudes occurring during this time period ranged from moderate to great based on Richter magnitude scale (Nuttli, 1987). One of the largest of these earthquakes occurred in 1811, starting in the portion of the New Madrid seismic zone located in the lower sector of Arkansas. The effects of this earthquake were felt as far away as Washington D.C.

To quantify this, an earthquake magnitude of six or greater would be felt within 800,000 square miles of the epicenter. Additionally, an earthquake of magnitude eight or greater was felt within 100,000 square miles of the epicenter. Fig. 1 shows the seismic intensity on the Modified Mercalli scale that would be felt throughout the New Madrid fault zone should an earthquake of magnitude 7.6 occur at the mid point of the fault. It is clear that the damage caused by such an earthquake would occur throughout numerous Mid-America states.

Earthquakes of magnitude equivalent to those seen in 1811 and 1812 have recently been discovered to occur not only during these time periods, but also in 1450 and 900 A.D. (Tuttle, 2002). This was determined through efforts of seismologists, archeologists, and geologists working in combination to date sand blows, which are common occurrences in earthquakes in this area of the country (Tuttle, 2002). This research suggests that a recurrence period of 200 to 800 years, a much shorter return period than previously believed, is a more accurate estimation for the Mid-America region. The earthquake history of this region combined with the recent knowledge of a shorter earthquake return period means that earthquakes should be a topic of concern to all engineers and building owners in Mid-America.

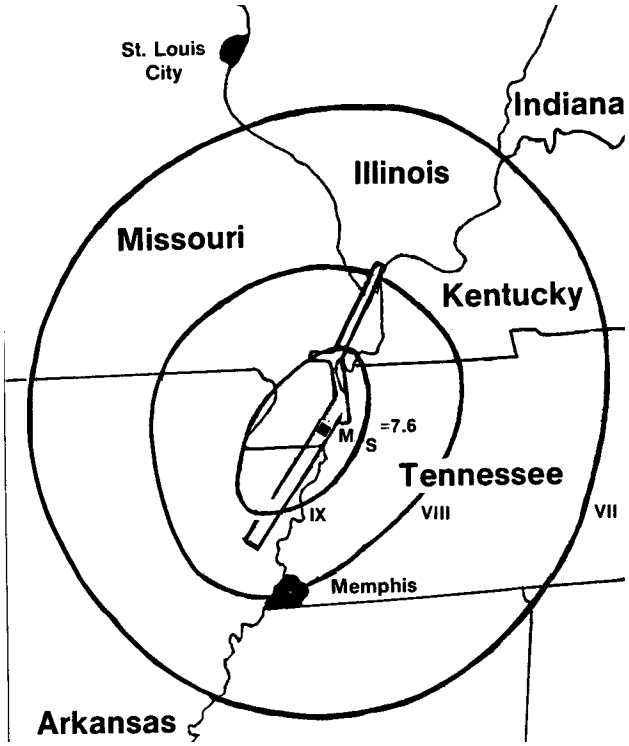

FIGURE 1 Intensity Map (Nuttli, 1987)

NON-STRUCTURAL DAMAGE

Before structural design issues for older reinforced concrete (RC) frame structures are discussed, an overview of other earthquake non-structural implications is presented to fully document the potential consequences of an earthquake strike in this region of the country. Non-structural issues include economic, social, and physical well-being effects including loss of life and severe injuries. As far as injuries and deaths are concerned, the actual tolls of an earthquake in this region are not known, since no earthquake events have occurred in this region since 1812 (Jones, 1993). Deaths occurred due the 1811 and 1812 events, but were few since the population was sparse. A study presented at the National Earthquake conference in 1993 shows that the built environment is the most important aspect affecting the deaths and injuries associated with earthquakes (Jones, 1993). While the built environment is of great concern, the

behavior, placement, and age of people within structures after a potential earthquake are also important considerations. Once damage has occurred and the earthquake event has ceased, the next main factor in preserving life safety of the individuals involved is through medical care and search and rescue operations. The sooner that trapped individuals are located and removed, the lower the risk of death and injury to these individuals. Combining all of the above listed considerations, it is estimated that a large, magnitude 8, earthquake occurring in this region of the country during the day would cause 3,300 fatalities in Memphis alone (Litan, 1993).

Another non-structural consideration when discussing earthquakes is the effect that these events may cause to the economy. When discussing the economy, two different portions must be accounted for. The first portion of the economy is the economy in the specific region where the earthquake event occurs and the second portion pertains to the economy of the nation as a whole. Studies have shown that the economic impact of a severe earthquake event occurring in the Mid-America region would cause $10 billion worth of damage to buildings from shaking alone (Litan, 1993). This number, while large, does not account for the after effects of such an earthquake event and their economic losses. These after effects include, but are not limited to the effects of fires, floods, and mudslides. In addition, other studies have shown that the Memphis region is much more economically vulnerable to earthquakes than California (Cochrane, 1993). Although these studies are pertinent, the economic losses and the effects that they cause are quite complex and not yet fully understood (Kim, 1999). However, they do pose a large problem and therefore are deemed necessary in a discussion considering earthquake events occurring in any region.

All of these non-structural damages in conjunction with the seismic risk present in this region lead to a concern for engineers and building owners when dealing with older structures located in the Mid-America region of the country. To aid and reduce

these problems, it is necessary to understand the structural problems with older buildings located in this region.

CODE PROVISIONS

An overview of the seismic procedures and design requirements for the Mid-America region is presented first. The earliest code provisions for seismic design can be found in the 1927 Uniform Building Code standards (Olshansky, 1993). Following the San Fernando California earthquake event of 1971, earthquake resistant design took center stage in areas of high seismic risk (Nordenson, 1993). Since this time, seismic provisions have been added to current codes. For example, the 1988 version of the Southern Building Code provided seismic design provisions (Olshansky, 1993). Unfortunately, these provisions are only enforced in the design process when adopted by a state, county, or locality. Tennessee, the region focused on throughout the entirety of this project, did not adopt these code revisions until 1990, and specified their region with a lower seismic risk than was done in the model code provisions. This resulted in a design where the lateral load forces are small in comparison to the gravity load forces (Nordenson, 1993). Therefore, it can be concluded that buildings located in the Mid-America region have not been designed for current seismic hazards present in this region. Therefore, the potential vulnerability of such structures to earthquakes may be high.

In this research, a closer look is taken at the design procedures for reinforced concrete frame structures with respect to seismic loading. The code discussion for concrete design will be limited to the American Concrete Institute (ACI) 318 code provisions, because it is the leading code used throughout the country for structural concrete design. Seismic provisions were established for concrete structures following the San Fernando earthquake event in 1971. One provision in this code was that the column moment capacity needed to be greater than the beam moment capacity at a beam-column joint intersection (ACI 318-71, 1971). However, this provision was vague

when defining the member moment capacities (Dooley, 2001). It was also vague in defining the beam sections when discussing whether to include or exclude the section of the slab acting with the beam due to monolithic construction. The lack of clarity led to a variation in the final design of buildings. The ACI seismic provisions were refined in 1983 and this time the code required the column design flexure strength to be 1.2 times the beam design flexure strength (ACI 318-83, 1983). However, there was still no definition of the beam section and design strength was considered debatable. ACI committee 445 suggested a solution to the beam section problem as well as recommending that the column strength be 1.4 times greater than beam strength (Dooley, 2001). In the ACI 318-99, as well as the current version in 2002, the nominal flexural strength of columns should exceed the nominal flexural strength of beams at beam-column joint faces by at least 20%, where the beam section should consider the contribution of the slab and slab reinforcement.

OLDER REINFORCED CONCRETE FRAME STRUCTURES

Buildings studied in this research are older RC frame structures located in regions historically considered to be of low to moderate seismic risk and were typically designed without consideration of seismic loading. In addition, the lateral load due to wind on a low-rise structure was typically negligible. Therefore, such structures have been categorized as a gravity load designed, or GLD structures.

In general, GLD RC frame structures have no special reinforcing details in either the beams, columns, lap splices, or in the joint regions (El-Attar, 1997). These detailing problems have been identified and studied in other research projects, specifically the work done by Pessiki (1990), Aycardi (1994), and Bracci (1995). Another characteristic that distinguishes these structures from others designed in areas of higher seismic risk is the existence of strong beams and weak columns, which can lead to soft story failure mechanisms that are composed primarily of column hinging. The problem of weak columns has also been studied, and was found to be the main cause of collapse in

buildings that are designed for gravity loading only (Bracci, 1995). The lack of sufficient column strength in these buildings leads to column hinging at relatively low lateral loads, causing the formation of a story mechanism once all columns located on one story have hinged. Once the mechanism has developed, the building's resistance is provided solely by the post-yield strength of the hinging column ends and inherent section ductility. In addition to this lack of sufficient column strength, a lack of member section and overall system ductility is also present in these non-seismically designed columns (Aycardi, 1994). This lack of ductility is due to a lack of confinement in the column hinge, as well as buckling of longitudinal reinforcement bars in the interior columns. The column detailing deficiencies may also lead to brittle soft story failure mechanisms.

Combining the seismic threat present in the Mid-America region and the lack of seismic design and detailing of older reinforced concrete frame structures justifies, the objective of this thesis is to quantify the seismic fragility, or vulnerability, of older RC frame structures due to potential earthquakes in Mid-America.

CHAPTER III
BUILDING DESIGN

DESIGN EQUATIONS

The first task of this research was to design an older three-story reinforced concrete (RC) frame structure located in an area historically considered to be of low-to-moderate seismicity. As previously discussed, buildings located in areas of low to moderate seismicity have historically been designed for gravity loads only. A characteristic of these buildings is that they have weak columns and strong beams with typical column-to-beam strength ratios being less than 1.0. The column-to-beam strength ratio of the structure should be noted because it is a measure often used in the design process for earthquake resistant structures (Dooley, 2001). The wind loads present on the prototype structure located in Memphis were calculated and placed into the load equations provided by ACI 318-99. It was found through analysis of the structure that the controlling load equation, or the load equation that caused the most severe moments throughout the structure, did not contain wind loading. ACI 318-99 design procedures were utilized in conjunction with IBC 2000 procedures to design an appropriate structure. The controlling load equation used for design was:

$$U = 1.4D + 1.7L \qquad \text{(ACI 318-99, 1999)} \qquad \text{(EQ-1)}$$

Where: U = Factored Demand Loading
D = Dead Load
L = Live Load

BUILDING OVERVIEW

The final designed structure was three stories tall and had four symmetric bays in each direction. The plan and elevation views are shown in Fig. 2. The building used concrete strength of 4000 psi and reinforced steel with yield strength of 60,000psi.

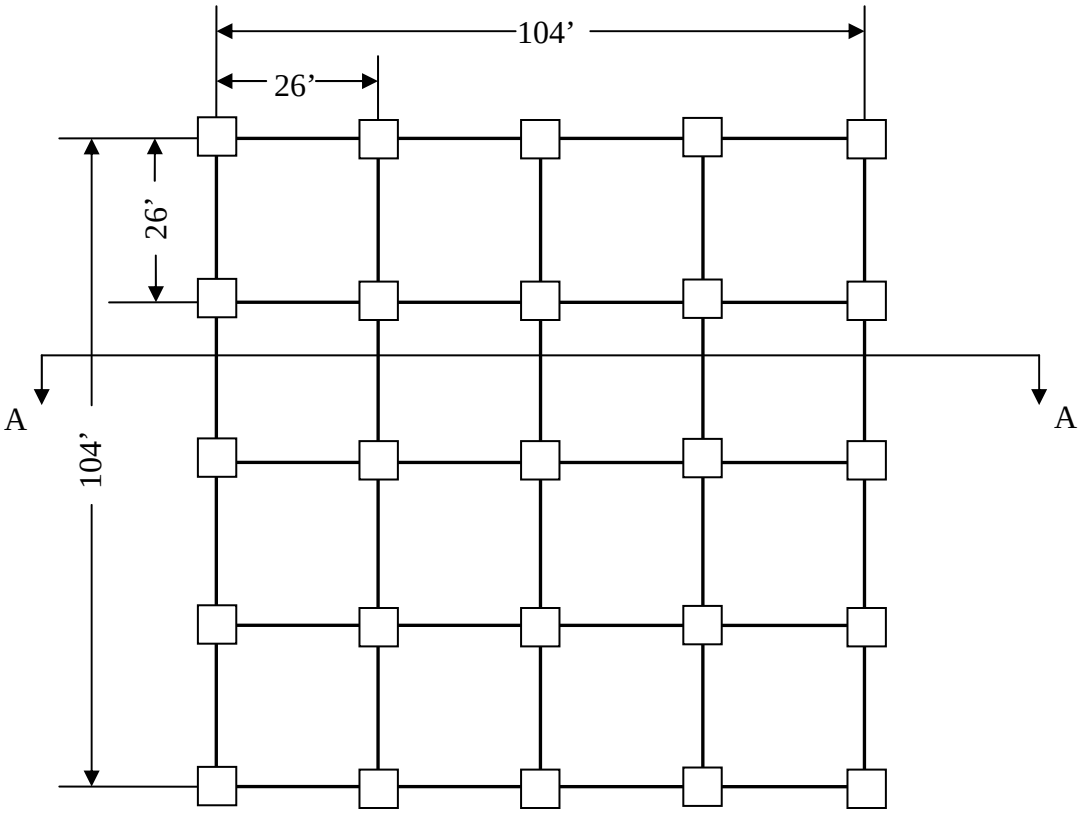

a) Plan View

FIGURE 2 Prototype Structure

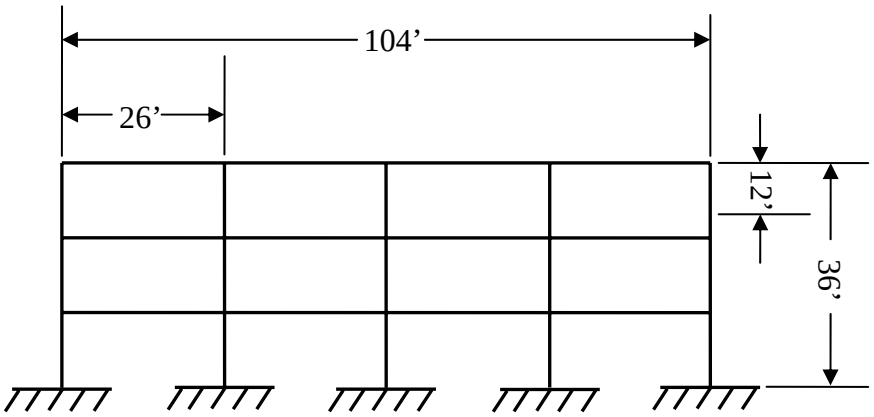

b) Section A-A

FIGURE 2 (Continued)

The story heights for the prototype structure were 12 ft. and each bay had columns spaced at 26 ft., maximizing the column spacing for an 8 in. thick slab. A superimposed dead load of 20 psf that included mechanical, HVAC, false work, cladding weight, and a live load of 50 psf, and the self-weight of the structure were the gravity loads considered for determining factored demands for the building. The geometry, member properties, and loading of the designed structure were then placed into SAP 2000 (1999), a commercial structural analysis program. This program provided the necessary factored demand moments, shear forces, and axial loads needed for beam and column design. A sample moment diagram for an interior frame of the structure is shown in Fig. 3 (a). Fig. 3 (b) shows the critical moment envelope for a beam located in this interior frame.

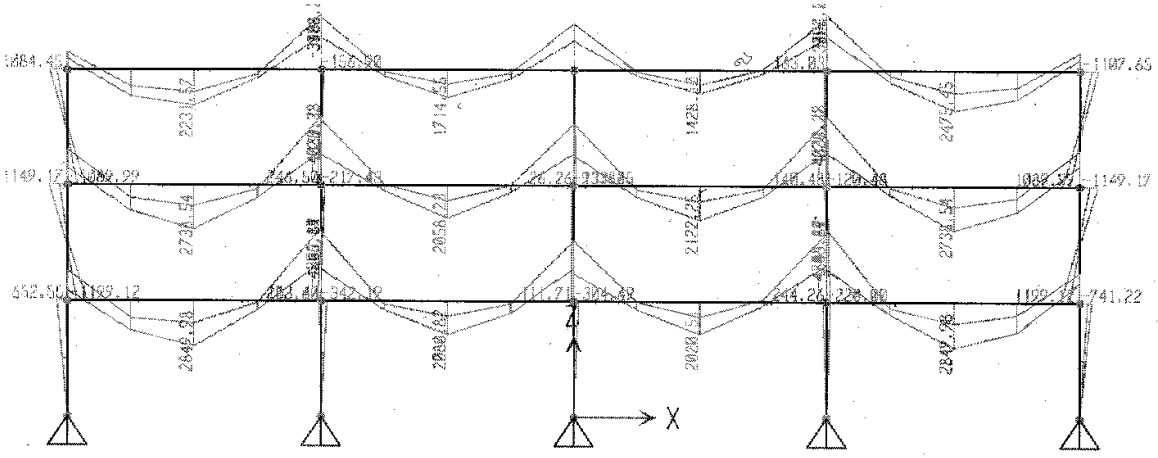

a) Moment Envelope Diagram

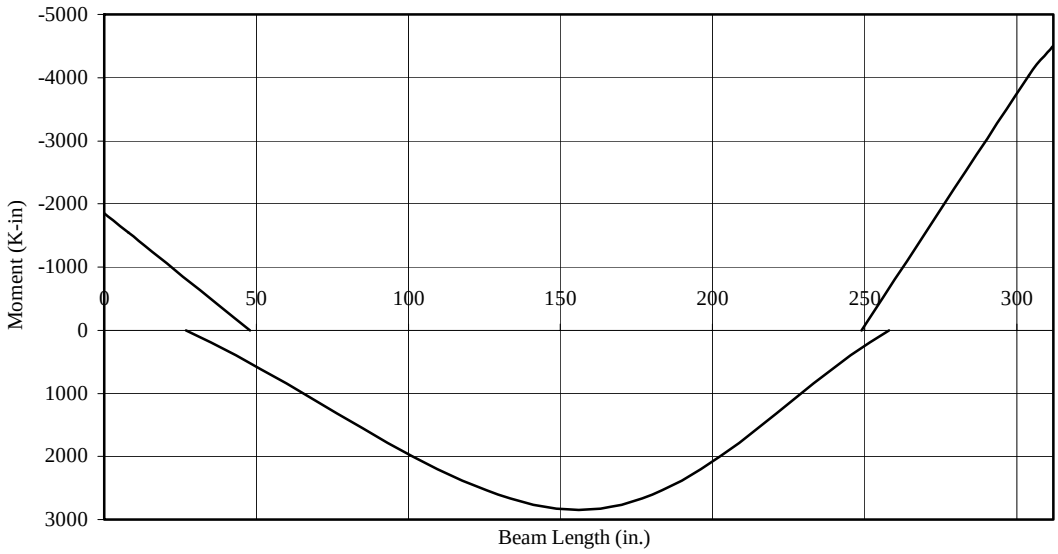

b) Critical Beam Moment Demand (Interior Span)

FIGURE 3 Sample Demand Moments

SLAB DESIGN

The slab was designed according to the direct design method specified in ACI 318-99 section 13.6, provisions for two-way slabs. Designing a two-way slab section is similar to designing a beam section once the demand moments have been calculated.

The most rigorous portion of the design process deals with defining the moment demands that will be placed onto a slab segment. Before this can be done, the slab must be subdivided into column and middle strips. For this particular building, it was found that the column and middle strips were equivalent in width, due to the symmetry of the structure. Following the definition of the strips, the positive and negative moments acting on the slab were determined. These moment values were then divided into the portion that must be resisted by the column strip and the portion that must be resisted by the middle strip. This division of the moment required the calculation of the multiplication factors shown in the sample calculations section. With the moments defined, the reinforcement necessary to resist these demands were calculated. As shown in the Appendix B, this was the same procedure followed for designing beam reinforcement. Due to the loading requirements and span lengths, an 8" thick slab was selected, and shown in conjunction with the beam section in Fig. 4. It was found that the minimum allowable reinforcement for this slab, # 4 bar at 12” center to center spacing, was adequate throughout both the column and middle strip of the slab.

BEAM DESIGN

The beams were designed according to ACI 318-99 provisions as T-beams, ACI 318-99 section 8.10 and Chapter 9. A sample beam design is shown in Appendix B. The first step in designing a beam section, according to ACI 318-99 section 8.10 is to determine the portion of the slab that is acting in conjunction with the beam. Following the previously mentioned provisions, an effective width of 78” was required for the interior beams. An effective width of 42” was required for the exterior beams. The final beam sections at the column faces (see Fig. 4) were 24” deep and 16” wide based on the moment envelope presented above.

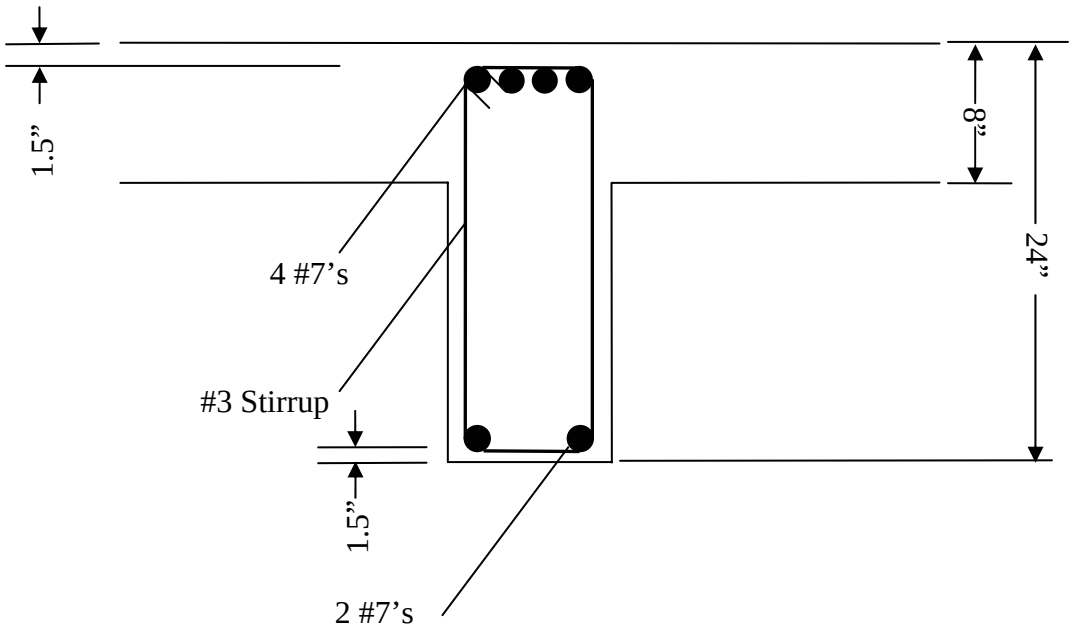

FIGURE 4 T-Beam Section

COLUMN DESIGN

Based on the factored demands, column sections were determined to be 16” by 16” with 4 #8 bars, as shown in Fig. 5. The computer program, PCACOL, was utilized as a design aid to obtain the final column dimensions and reinforcement (PCACOL, 1992). It was found that the column-to-beam strength ratio for the prototype building was approximately 0.60, which is typical for older RC frame structures. Based on an average level of axial loading among columns and consideration of the slab and slab reinforcement within the effective flange width for the beams, the approximate column-to-beam strength ratio for the prototype building was 0.6, which is well below the current ACI 318 seismic requirement of 1.2. From an eigenvalue analysis, the fundamental period of the building is about 0.9 seconds.

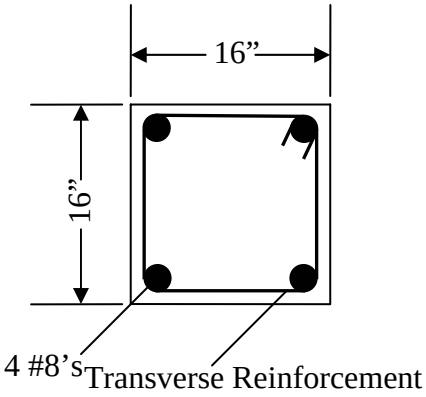

FIGURE 5: Column Section

CHAPTER IV
LIMIT STATE STORY DRIFT CAPACITES

INTRODUCTION

As previously discussed, there are numerous limit states (capacities) that can be considered in fragility curve development. Based on previous research, inter-story drift has been well-correlated with structural damage and is utilized as the key variable in the fragility development. Three different methods for developing structural capacities were used in conjunction with different models of uncertainty. The first set of limit state capacities was based on qualitative descriptions and general suggestions in FEMA-273 (1997). The second set of fragility curves used the quantitative results from the nonlinear pushover analyses performed for this research. Finally, incremental dynamic analyses were used to obtain incipient collapse limit state. Each of these capacity options are discussed in depth below.

FEMA-273 LIMITS

The limitations discussed in Chapter 2 of FEMA-273 correspond with common, qualitatively defined, structural performance requirements (NEHRP, 1997) and are Immediate Occupancy (IO), Life Safety (LS), and Collapse Prevention (CP). There are other intermediate limit states provided, but not considered in this research. In addition to these qualitatively defined limit states, appropriate inter-story drift limit suggestions are 1%, 2% and 4% for Immediate Occupancy, Life Safety, and Collapse Prevention, respectively. Although these suggested limits are approximate, they are considered fairly accurate for buildings properly designed for seismic loading. For GLD buildings, the limits for life safety and collapse prevention are probably not conservative due to insufficient section detailing for needed ductility.

PUSHOVER ANALYSES

Background

Pushover analyses are commonly used in seismic design and evaluation of structures as indicators of the structural yielding and potential failure mechanisms of the structure (Mwafy, 2001). This type of analysis subjects a nonlinear numerical model of a designed structure to prescribed forces or displacements until failure is considered to occur. These analyses have proven to be good predictors of building behavior when care is taken in the modeling of the structure and the proper definition of the prescribed loading is utilized (Bracci, 1995). FEMA 273 recommends the pushover analysis as a reasonable approximation of the internal forces experienced during a design earthquake (NEHRP, 1997). Results of pushover analyses demonstrate a building's story shear force versus the inter-story deformation, as well as identifying potential failure mechanisms.

When executing a force control pushover analysis, forces are placed on the stories of the structure up to a user specified maximum value and a realistic maximum building drift value. Specified forces are placed onto the structure incrementally until either the total maximum base shear force is reached or the building drift has exceeded the imposed maximum drift limit. In this work, forces were placed on the stories of the structure in two ways, uniformly on each story and in an inverted triangular fashion.

Displacement control pushover analyses impose incremental story displacements until a prescribed limit is reached. There are numerous options for applying story displacements on a given structure. In other words, displacements can be applied or restricted on any story of the structure. In particular to identify critical story mechanisms, an analysis is done for each story where the story in consideration is pulled to a very large displacement and the story beneath it is restrained to maintain zero displacement. Individual story capacities are of importance because; the lateral resistance of an entire structure is often dependent on the performance of a single story

of the structure, especially for GLD buildings. In addition, the upper most story is pulled for identifying beam side sway mechanisms.

Geometry and Member Properties

The basic geometry of the building was the first input required by this program. The geometry of the structure was specified by assigning numbers to the different members of the structure and connecting these numbered members into nodes. The weight of the structural members must be accounted for, so nodal masses were assigned. These weights were defined as nodal masses due to the lack of member size and shape definition in the program. The nodal masses were intended to assign the appropriate amount of mass to each node of the modeled structure. Therefore, the mass of the slab, column, and beams cast from normal weight reinforced concrete were calculated and placed in their appropriate positions throughout the building. A sample of this is shown below:

Nodal Mass for an Interior Reinforced Concrete Column with Specific Weight of 0.15kpf:

Columns:

$$L = 144'', h = 16'', b = 16''$$
$$Weight = h \cdot b \cdot Load = 32k$$

Beams:

$$L = 312'', h = 16'', b = 16''$$
$$Weight = \cdot h \cdot b \cdot Load \cdot 2 = 13.9k$$

Slab:

$$L = 312'', h = 8''$$
$$Weight = L^2 \cdot h \cdot Load = 67.6k$$

Dead Load:

$$L = 312"$$
$$Load = 20lb/\,ft^2$$
$$Weight = L^2 \cdot Load = 13.5k$$

Wall Load:

$$L = 312"$$
$$Load = 500lb/\,ft$$
$$Weight = 0lbs$$

$$TotalWeight = 32 + 13.9 + 67.6 + 13.5 + 0 = 98.19k$$
$$Mass = \frac{Weight}{Acceleration} = 0.25\frac{k}{in/s^2}$$

There was no wall load for the interior columns, because no walls were present in the interior of the structure. However, when considering the exterior columns, the wall load was included. Calculations for the edge columns, corner columns, interior roof columns, and exterior roof columns are similar to the above except that the final mass were 0.17 k/in/s^2 for the edge columns, 0.17 k/in/s^2 for the corner columns, 0.30 k/in/s^2 for the interior roof columns, and 0.17 k/in/s^2 for the exterior roof columns.

After defining the nodal masses, the hysteretic behavior of the structural member was defined. Often in dynamics this is discussed in terms of a hysteretic loop. This loop changes as a building structure is cycled in each direction from lateral loading, which is typical of RC sections. The hysteretic parameters specified for this program define the loss of stiffness, strength reduction, and also the slip occurring within a structural member (Kunnath, 2003). The stiffness degrading, target slip or crack closing, and energy based strength decay parameters were set to 0.7, 0.7, and 0.05, respectively. The ductility strength decay was neglected for these analyses. These parameters define the behavior that the structure would follow during inelastic cyclic lateral loading, and were calibrated for GLD buildings based on the experimental shaking table tests performed in previous research (Bracci, 1995). Another important specification when performing

pushover analyses is whether to include or neglect the second-order effects of p-delta. For this research, pushover analyses were done both considering and neglecting p-delta effects.

Tri-linear moment-curvature relationships were utilized to quantify the behavior of the individual structural members by defining three critical points, cracking, yield, and ultimate. The first portion of the input deals with column properties. The column number, the column height, any rigid portion of the column, such as the joint area, and the axial load that the column must withstand were defined. The rigid zones for the columns were defined as the region of a column that falls within the connecting beam depth. At the base of the first story columns, no rigid zone was applied. However, all other columns were defined as rigid both above and below a story at a level equivalent to the depth of the connecting member. The flexural rigidity, axial stiffness, and shear stiffness were defined, followed by the cracking, yield, and ultimate moments and curvatures. A similar approach was taken for the beam definitions and a sample is shown below.

Calculations for Negative Beam Moment:

Givens:

$$f'c = 4ksi$$
$$hf = 8"$$
$$beff = 78"$$
$$h = 16"$$
$$b = 16"$$

Calculation of Moment of Inertias:

TABLE 1 Moment of Inertia

	t	B	A	y_{bar}	I	Ad^2	I_{gc}
Flange	8”	78”	624 in.^2	4”	3328 in.^4	7600 in.^4	10928 in.^4
Web	16”	16”	256 in.^2	16”	5461 in.^4	18540 in.^4	24001in.^4
Total			880 in.^2	7.49”	8789 in.^4	26140 in.^4	34929in.^4

Tri-linear backbone curve:

First Linear Section: Initial Flexural Rigidity

$$EIo = 0.5 \cdot E \cdot Ig$$

$$EIo = 0.5 \cdot 3605 \cdot 34929.26 = 6.3x10^{7}\, k \cdot in^{4}$$

Second Linear Section:

$$0.5EIo = 0.5 \cdot 6.3x10^{7} = 3.2x10^{7}\, k \cdot in^{4}$$

Third Linear Section:

$$0.01Io = 0.01 \cdot 6.3x10^{7} = 6.3x10^{5}\, k \cdot in^{4}$$

Shear Stiffness (IDASS):

$$nu = 0.2$$

$$G = \frac{E}{2 \cdot (1 + nu)}$$

$$G = \frac{3605}{2 \cdot (1 + 0.2)} = 1502.1$$

$$G \cdot A = 1502.1 \cdot 3605 = 1.3x10^{6}$$

Moment and Curvature Values:

Curvature:

$$\phi o = \frac{Mcr}{Io} = 0.0000352438 \, {}^{in}\!/_{in}$$

$$\phi y = \frac{My - Mcr}{0.5Io + \phi o} = 0.00010573 \, {}^{in}\!/_{in}$$

$$\phi u = 20 \cdot \phi y = 0.002112646 \, {}^{in}\!/_{in}$$

Moment:

$$Mcr = \frac{My}{2} = 2218.95k - in$$

$$My = Mn = 4437.891k - in$$

$$Mu = 0.01Io \cdot (\phi u - \phi y) + My = 5702.69k - in$$

Table 1 displays the moment of inertia calculations utilized for the calculations presented above. All of these calculations were repeated for the positive moment beam sections and for the column sections. When considering the column sections, the calculations were similar but included the axial load and axial stiffness of the column member as well as a 2% post-yield stiffness utilized for calculating Mu. The backbone curve determined for the column sections are shown below.

Tri-linear backbone curve:

$$EIo = 0.7 \cdot E \cdot Ig$$

$$EIo = 0.5 \cdot 3605 \cdot 5461.3 = 1.37x10^7 \, k \cdot in^4$$

Second Linear Section:

$$0.5EIo = 0.5 \cdot 1.37x10^7 = 6.9x10^6 \, k \cdot in^4$$

Third Linear Section:

$$0.02EIo = 0.2 \cdot 1.37x10^7 = 2.8x10^5 \, k \cdot in^4$$

Imposed Loading

Dead loading was first placed onto the structure. For modeling purposes, an equivalent dead load was provided to correspond to the same maximum moment based on unfactored dead loading. For further description of the input files used for IDASS the reader is referred to the IDASS user's manual (Kunnath, 2003).

Force Control Loading

Two different force control pushover analyses were used to evaluate building response. The force was applied either uniformly or in an inverted triangular fashion. These analyses incrementally applied loading on the stories until a specified force or displacement limit was reached, 10% of the building's weight. These analyses were intended to give an overview of the entire building's behavior under monotonically increasing lateral loads. All results from the pushover analyses are presented in terms of story shear force vs. inter-story drift as shown in Fig. 6. First yield, plastic mechanism initiation, and strength degradation are the quantitative limit states defined in this research and displayed on these charts. First yield occurs when the first member in a structure yields. Plastic mechanism initiation occurs when a story mechanism develops. At this stage, the building is relying on the post-yield stiffness of the yielding members. Throughout this research, the beams had 1% post yield stiffness, while the columns had 2% post yield stiffness. Strength degradation is the final quantitative limit state defined for this research. This limit state can only be quantified when discussing analyses including the effects of p-delta, since member responses in IDASS are defined in first order analysis with positive slope. Strength degradation occurs when the building's story shear value drops by 20% of the maximum story shear force response. At this point, the building is considered to be near structural failure

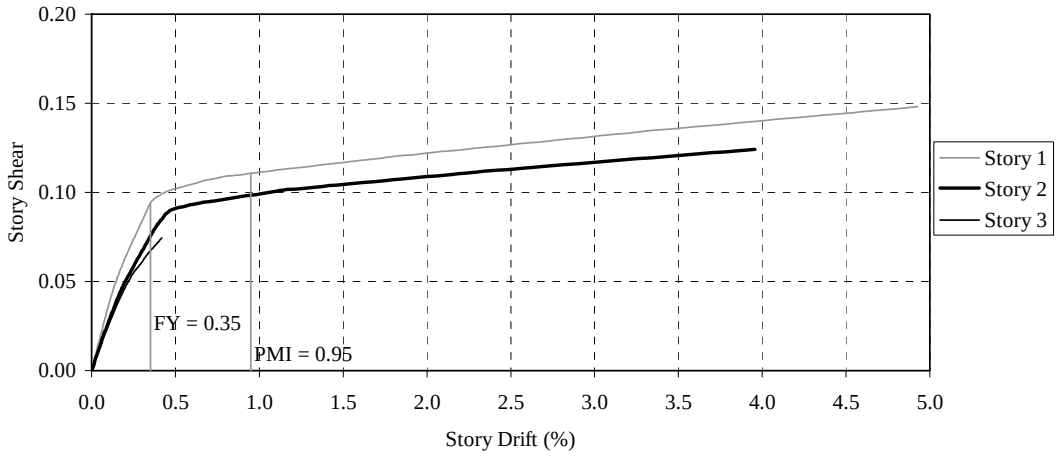

a) Inverted Triangular Distribution – Neglecting the Effects of P-Delta

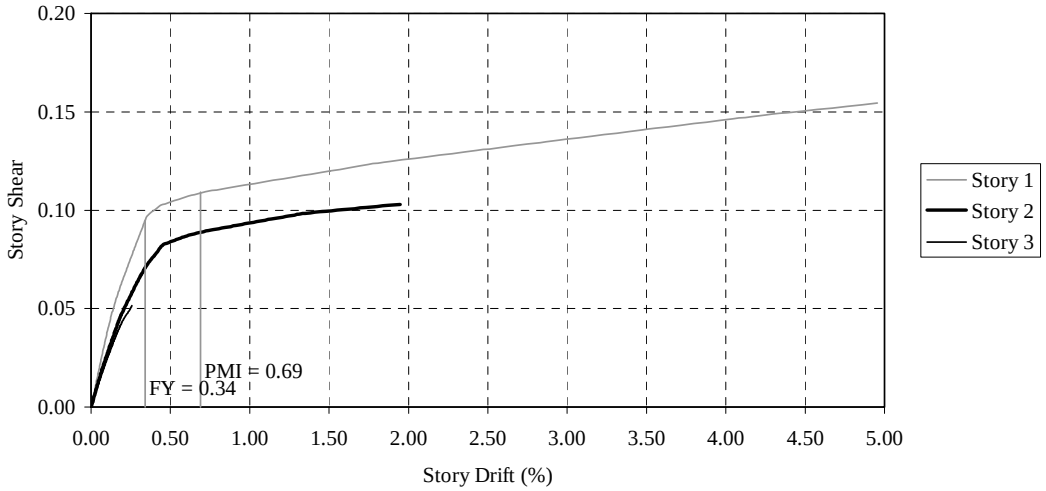

b) Uniform Distribution – Neglecting the Effects of P-Delta

FIGURE 6 Force Control Pushover Results

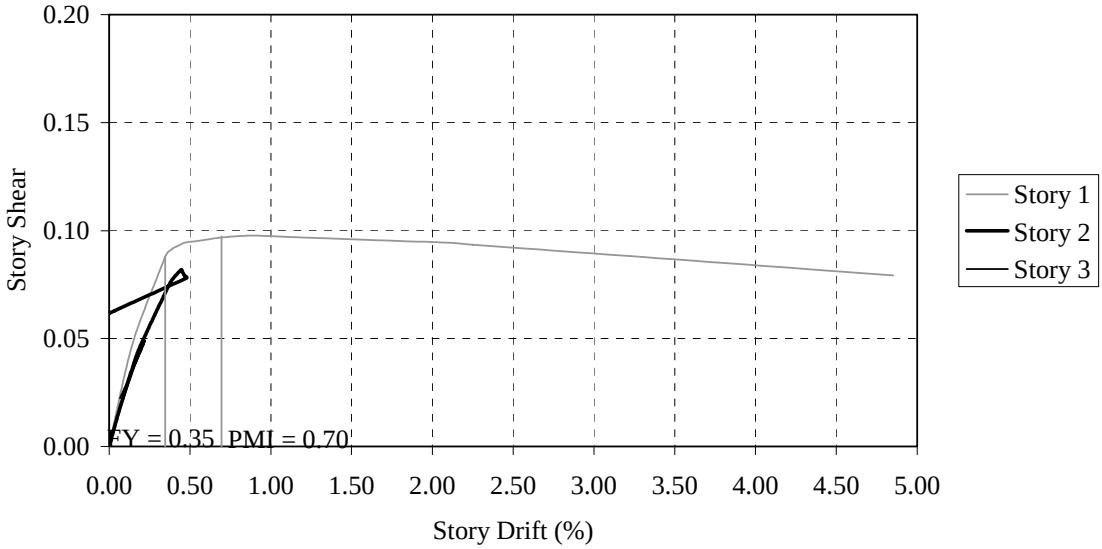

c) Inverted Triangular Distribution – Including the Effects of P-Delta

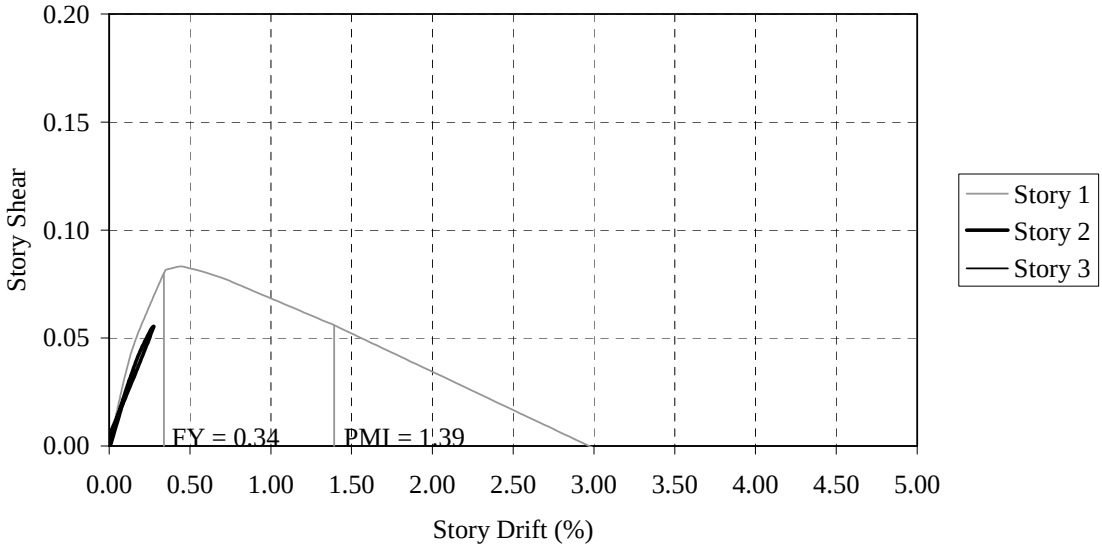

d) Uniform Distribution – Including the Effects of P-Delta

FIGURE 6 (Continued)

The force control analyses provide information about individual story behavior, as well as the behavior of the building as a whole. The load is placed onto the structure, and the building is allowed to react with no restrictions. Thereby, the most critical story

in the structure can be determined. It was found in all force control pushover analyses that the first story controlled the behavior of the structure. This means that the first story yielded before the other stories. Therefore, the behavior of this story is of particular interest.

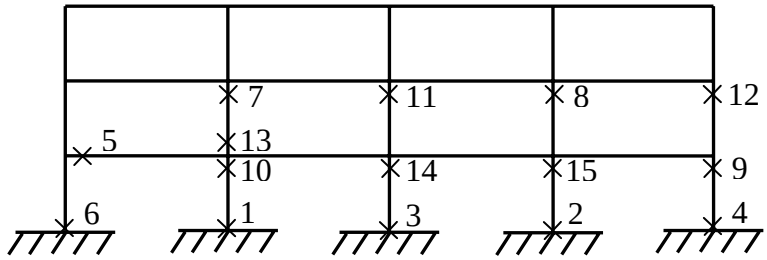

a) Inverted Triangular - Yielding Points

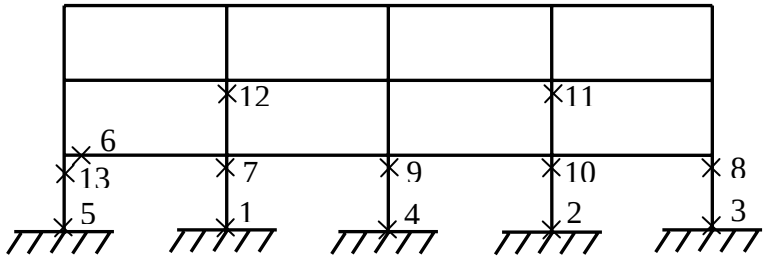

b) Uniform Distribution - Yielding Points

FIGURE 7 Yielding Points – Force Control

A few things should be noted about the results obtained from these force control analyses. First, almost all of the members found to yield under loading were column members. This was expected due to the design procedure used and the small column-to-beam strength ratio, 0.6. Since this building is representative of structures already in existence, this warrants notice. Second, the uniform force control analysis caused plastic mechanism initiation more rapidly that the inverted triangular force control analysis, and

the yielding was mainly restricted to the first story, as shown in Fig. 7. This means that the first story of the structure is particularly important due to the potential first story column side sway mechanism.

Displacement Control Loading

Displacement control analyses were also run, placing drifts up to 10% of the building height onto the structure. These analyses were run by incrementally imposing this drift on the third story while allowing the rest of the stories to move without restriction, placing the drift on the third story and restricting the motion of the second story, placing the drift on the second story while restricting the first, and finally placing the drift on the first story only. The last three analyses were intended to show the worst case scenario of the earthquake loads being confined to single story, allowing an investigation into individual story weaknesses and mechanisms. The first displacement control analysis can be compared with the force control analyses, since the displacement was applied on the third story and the building was allowed to move freely. The displacement control analysis also demonstrated the impact of the first story on the behavior of the structure as a whole. The remaining displacement control analyses were significant because of their impact on the limit state definitions. The results from these pushover analyses were displayed in the same manner as those of the force control pushover analyses and are displayed in Fig. 8.

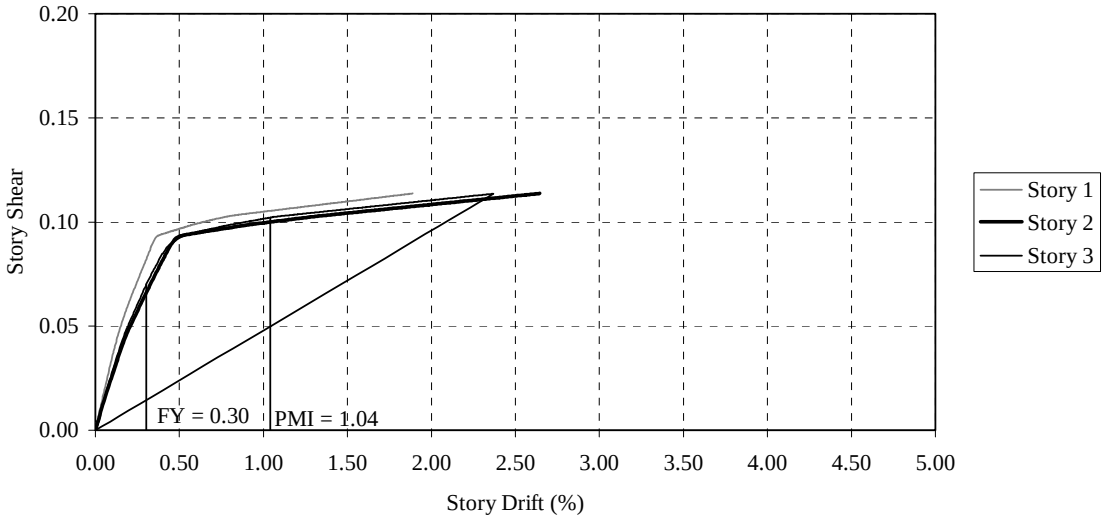

a) 10% on 3rd Story

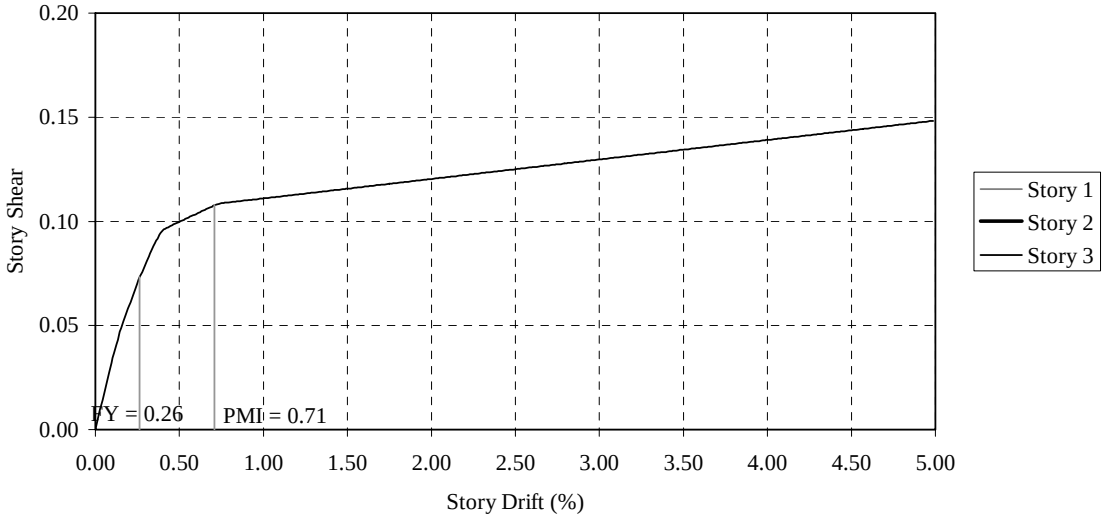

b) 10% on 3rd Story and 0% on 2nd Story – Neglecting the Effects of P-Delta

FIGURE 8 Displacement Control Pushover Results

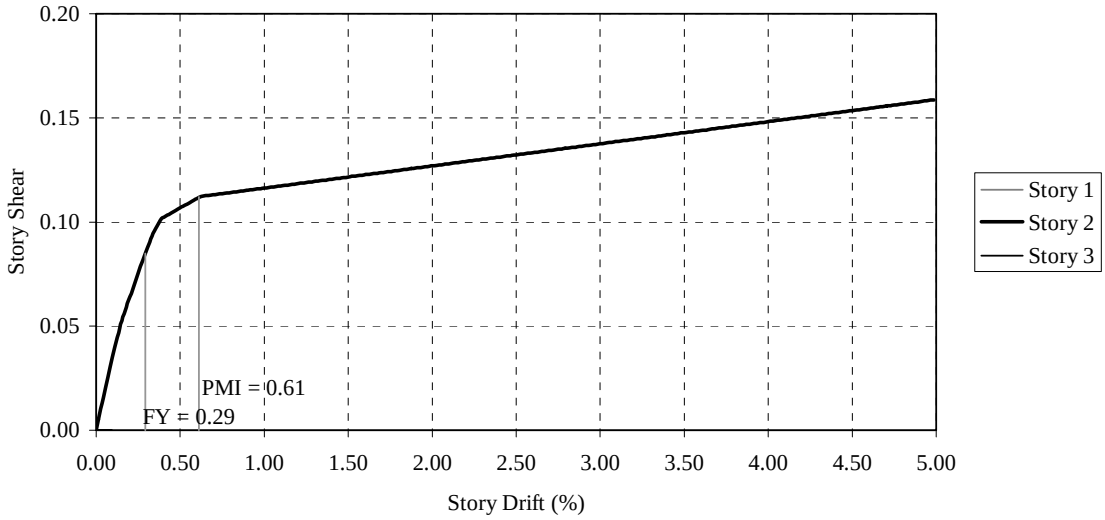

c) 10% on 2nd Story and 0% on 1st Story – Neglecting the Effects of P-Delta

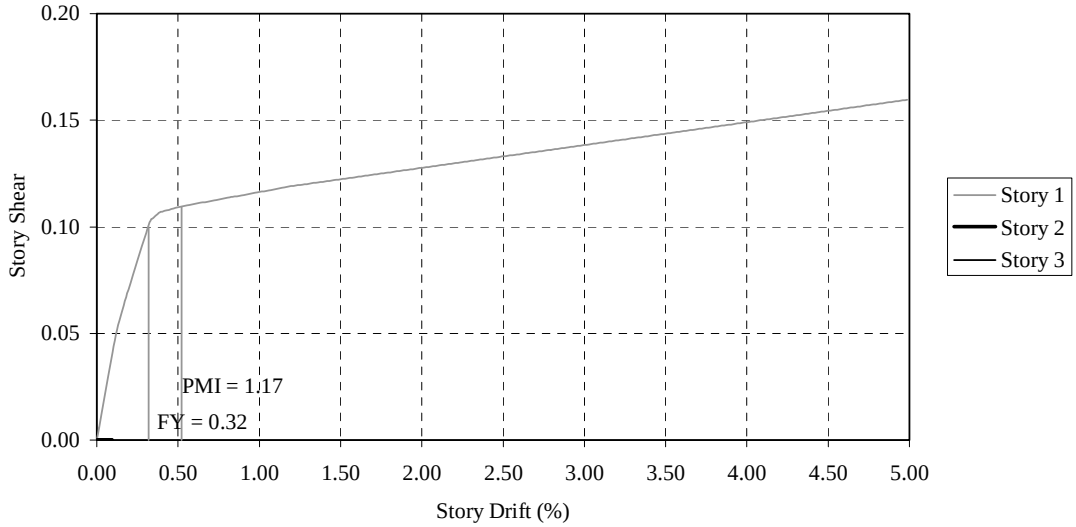

d) 10% on 1st Story – Neglecting the Effects of P-Delta

FIGURE 8 (Continued)

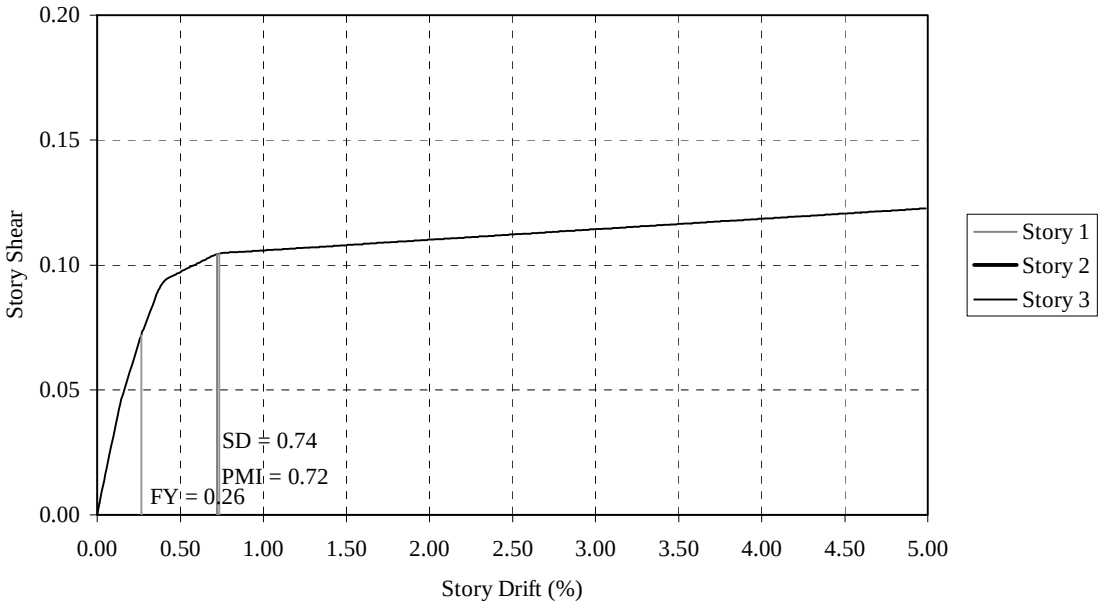

e) 10% on 3rd Story and 0% on 2nd Story – Including the Effects of P-Delta

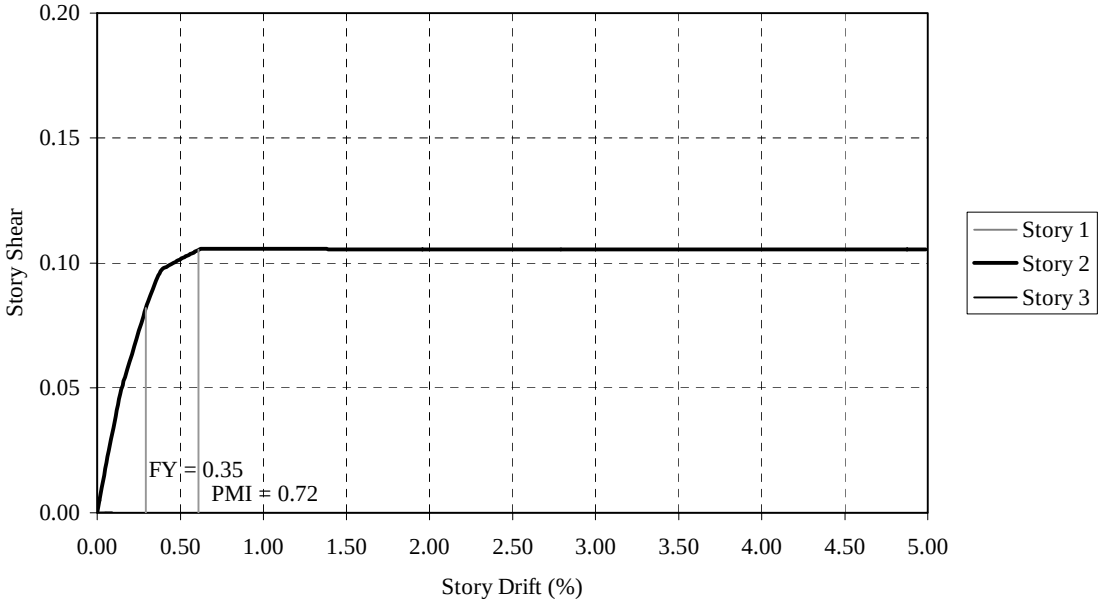

f) 10% on 2nd Story and 0% on 1st Story – Including the Effects of P-Delta

FIGURE 8 (Continued)

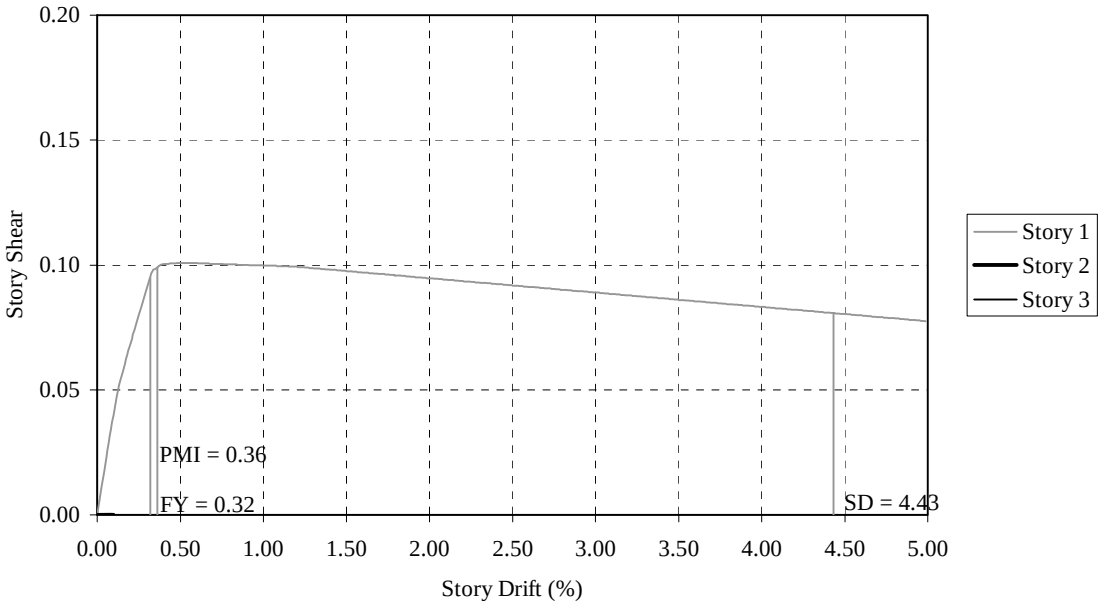

g) 10% on 1st Story – Including the Effects of P-Delta

FIGURE 8 (Continued)

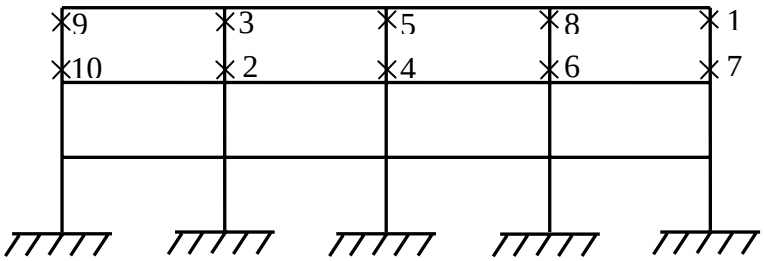

a) 10% on 3rd Story and 0% on 2nd Story - Yielding Points

FIGURE 9 Yielding Points – Displacement Control

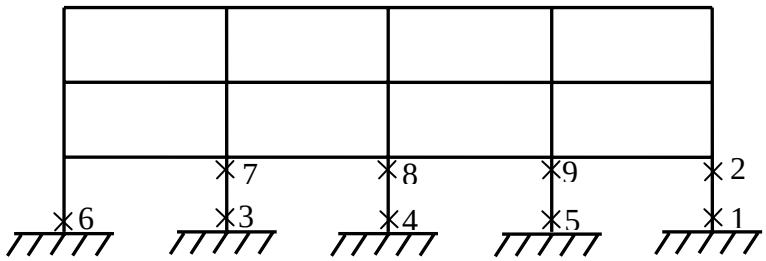

b) 10% on 1st Story – Yielding Points

FIGURE 9 (Continued)

Shown in Fig. 9 are the yielding points associated with some of the displacement control pushover analyses. When considering a building's response and collapse, applying the load to one story is the harshest loading scenario. The analyses requiring a single story to resist the lateral load placed onto the structure are used to determine the limit states to ensure safety under the most critical loading scenarios. The values obtained for the limit states are calculated by averaging the limit state values from the three remaining displacement analyses, discussed above. The value obtained for the first yield limit states excluding the effects of p-delta is 0.29% drift. The value for plastic mechanism initiation is 0.61% drift. It should be noted when averaging the limit state values for plastic mechanism initiation, that the analysis placing the load only on the first story had the smallest drift value, 0.52% drift, versus the other two analyses which displayed much better behavior and had limit state values of 0.71% drift and 0.61% drift. These analyses were also run including the effects of p-delta. The value calculated for the first yield limit state is 0.31% drift. The limit state value for plastic mechanism initiation is 0.6% drift. The final strength degradation limit state value obtained was 2.59% drift. The values obtained from each different displacement analysis varied greatly from 0.74% drift when placing the displacement on only the third story to a limit state value that is never reached when considering displacement applied only to the

second story for this final limit state. Additionally, it should be noted that in these analyses, as in the force control analyses, the yielding was confined mainly to the column members. These analyses provide vital information about quantifying the behavior and fragility of the designed structure.

INCREMENTAL DYNAMIC ANALYSES

Background

The results obtained from the incremental dynamic analyses are used as the capacity of the final fragility curves based on incipient collapse. This type of analysis utilizes the files and inputs created for the inelastic time history dynamic analyses, which is discussed later in Chapter V. This means that the ground motion files and required input data for these two types of analyses will be the same. The incremental dynamic analyses are used to determine the incipient collapse capacity of the numerically modeled structure under representative loading. The suite of twenty ground motions utilized for the dynamic analyses were once again used as the representative ground motions in these analyses. Each of these 19 records was run both including and excluding the effects of p-delta.

Procedures

The inputs required for this analysis are identical to those for the dynamic analyses, discussed in the following chapter. However, the horizontal peak ground acceleration multiplier is incrementally varied. This multiplier scales the horizontal accelerations provided in the ground motion file. The final goal of this analysis is to create an understanding of the numerically modeled structure under representative loading. To obtain this, the response of the structure under incrementally increasing peak ground accelerations is necessary. In this research the peak ground acceleration was varied incrementally from a value close to zero until the building was considered failed. As in all of the other analyses, failure was discerned when a story drift exceeded 5%.

At each different horizontal peak ground acceleration value, the story drift and story shear of the structure was recorded. The largest story drift values were used to determine the controlling story of the structure at failure. For all analytical simulations, the first story was the controlling story at failure and is used in the fragility curves based on incipient collapse.

Results

The first set of results obtained from these analyses is displayed in Fig. 10. This figure shows the incremental story drift versus the spectral acceleration at the fundamental period of the building for the controlling story of each earthquake record. This information shows the trend of each controlling story response as the peak ground acceleration is increased. The behavior of the controlling story throughout each earthquake record is fairly similar.

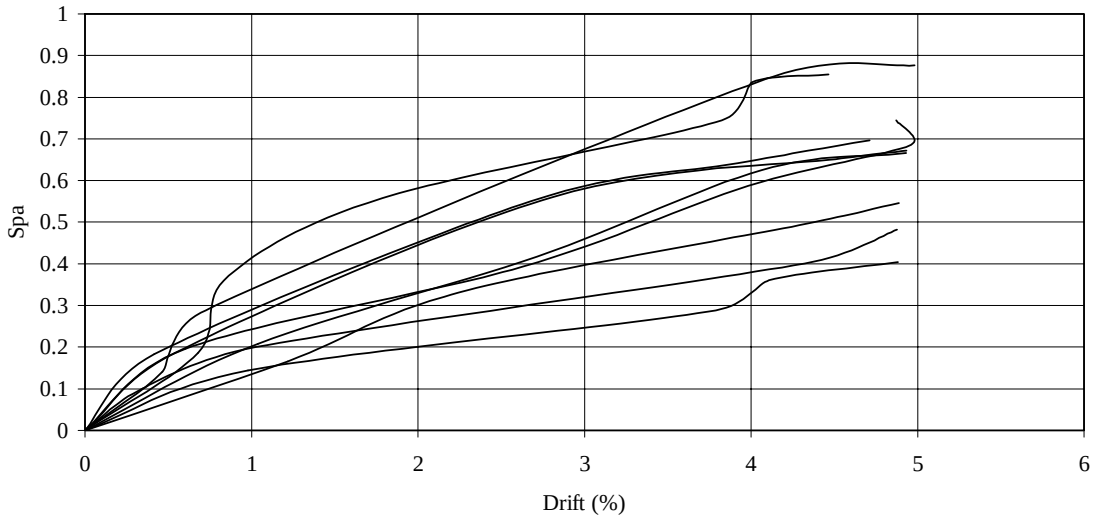

FIGURE 10 IDA - Controlling Story Response

The spectral acceleration of each earthquake record is calculated throughout this research using a response spectra analysis program. The response spectra analysis program required the acceleration for a given ground motion to be placed into a file. This file was then read by the program and the results were provided. The results consisted of two vertical lists of numbers. The first of these numbers was the period of the structure and the second was the spectral acceleration of the building given the period. This analysis was run on each of the 19 ground motion records. The period of the structure was displayed as an output in both the pushover and dynamic analyses and was approximately 0.90 seconds. From this information the spectral acceleration for each ground motion file at a period of 0.9 seconds was recorded.

With the spectral acceleration for each earthquake record defined, calculations could be made to find the spectral acceleration peak ground acceleration multiplier value. This was done by taking the peak ground acceleration multiplier and dividing it by the peak ground acceleration for the given earthquake record. This number was then multiplied by the spectral acceleration determined in the response spectra analysis and the individual spectral accelerations were determined. Incipient collapse is defined as a 20 or 50% drop in slope (Wen et al, 2004). In this research, the 50% drop in slope was used to define incipient collapse. This point was calculated for each ground motion record by calculating the slope between each set of data points obtained in the incremental dynamic analyses. This slope was then reduced by 50% and compared to the slope between the next two points. This process was repeated until a 50% drop in slope was found to occur. Having found the two points between which the slope drops 50%, these two points were averaged in order to obtain a value of incipient collapse for spectral acceleration and drift. These points are displayed in Fig. 11. Also displayed in Fig. 11 is a lognormal distribution function fitting the data. This function is calculated using the lognormal distribution function provided in Microsoft Excel in combination with the standard deviation and mean of the natural log of drift. Values for this function were plotted in conjunction with the incipient collapse points to demonstrate the

correlation between a lognormal fit and these data points. This correlation is the basis for the incipient collapse fragility curves discussed in the following chapter.

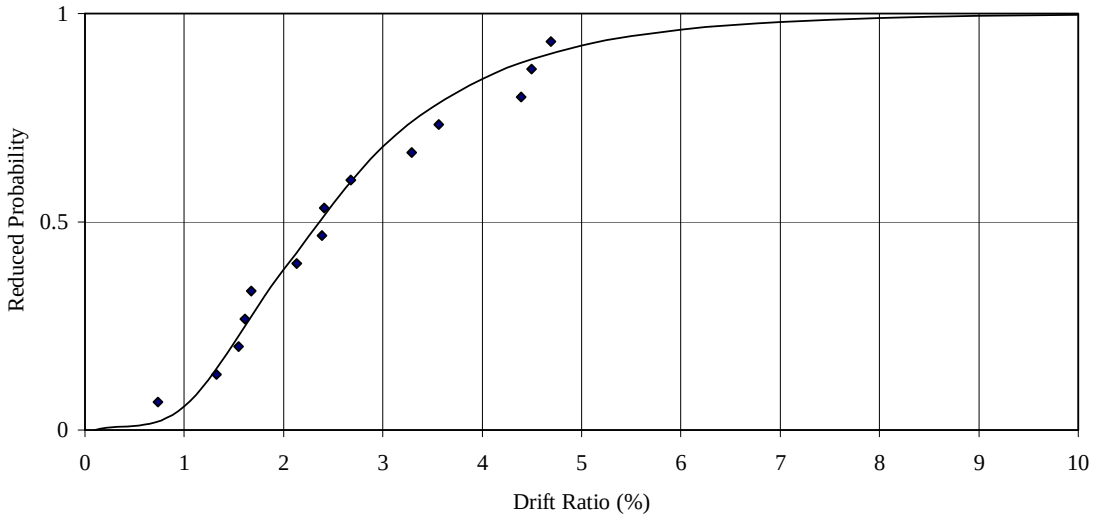

FIGURE 11 Incipient Collapse Points

Previous work done by Dooley and Bracci (2001) suggests another way to demonstrate the adequacy of a lognormal fit to certain data sets. This method utilizes the points recorded for incipient collapse in conjunction with statistical analyses. In this method the natural log of the drift value is plotted versus a z factor. The calculations as described by Dooley are shown below:

$$F(x_i) = i / (n+1)$$

$$z_i = [\ln(x_i) - \lambda\ ] / \zeta$$

$$F(x_i) = \Phi(z_i)$$

$$\text{Therefore } z_i = \Phi^{-1}[i / (n+1)]$$

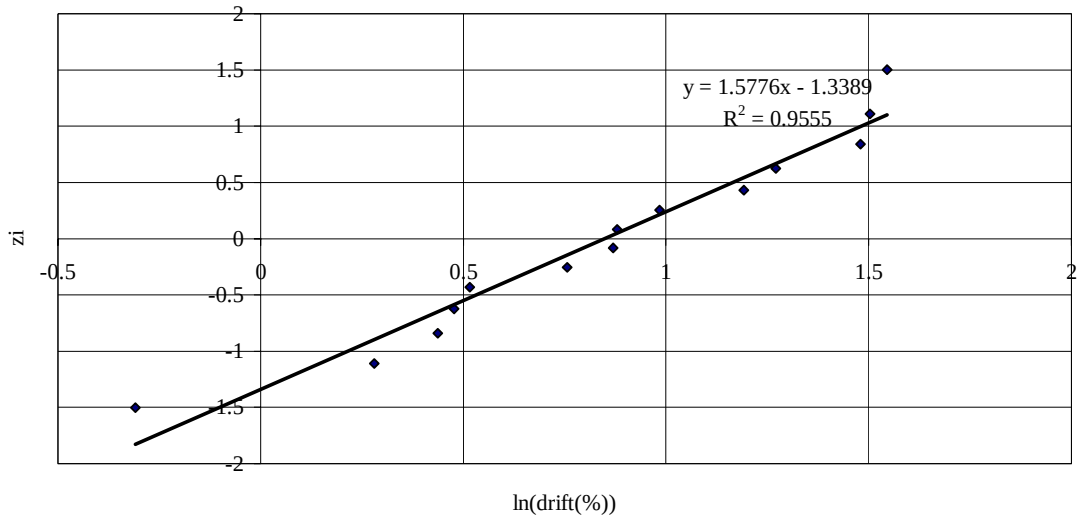

FIGURE 12 Alternate Fit Incipient Collapse Points

This value of zi is plotted versus the natural log of drift. If a log normal distribution function is adequate, then a linear trend line should be a good approximation of the recorded data points, as shown in Fig. 12. As shown, the R^2, or correlation between the original data points and the trend line, is close to one and therefore can be considered a good fit. While these results are of no particular use individually, they become pertinent when creating the required fragility curves.

TABLE 2 Capacity Factors

	FEMA-1%	FEMA-2%	FEMA-4%	IDA	Pushover-FY	Pushover-PMI
β_{ICC}	0.30	0.30	0.30	0.46	0.30	0.30
λ_{ICC}	0.00	0.69	1.39	0.87	-1.23	-0.49

As a final summary the differences between these three methods of obtaining story capacity are discussed. To do this Table 2, which displays the capacity factors

needed for the creation of a fragility curve, is utilized. The values for λ present in this chart vary greatly. The values presented for the FEMA drift limitations vary greatly from those obtained for both the incremental dynamic analyses and the pushover limit states. Additionally, the FEMA document 273 capacity requirements were created based on previously studied earthquakes. Since the research conducted in the Mid-America region is recent, it is believed that these FEMA drift limitations are more applicable to the California earthquake region.

CHAPTER V
SEISMIC DEMAND: INELASTIC TIME HISTORY DYNAMIC ANALYSES

INTRODUCTION

Inelastic time history dynamic analyses are used to find the seismic demand of a structure during earthquake ground motions. These ground motions are in the form of acceleration values at even time intervals. Ideally these ground motions would be actual earthquake records from the region where the building is located. However, actual earthquake records for the Mid-America region are not available. This is due to the fact that no large magnitude earthquakes have occurred in this region since accurate earthquake recording methods have been available. Therefore, the ground motions available for use in this research are synthetic earthquake records by Wu and Wen (2000).

USER INPUT INFORMATION

The computer program used for analysis purposes was IDASS (Kunnath, 2003). The input requirements for dynamic analyses differ from those for pushover analyses and, therefore, will be discussed. The basic geometry, static loading, hysteretic behavior, and moment curvature relationships are the same as those utilized in the pushover analyses. This type of analysis, as previously discussed, requires the use of ground motions. These ground motions must be placed into a certain format and referenced by the program. A scaling factor is used to define the peak ground acceleration.

Certain control parameters concerning the way in which the output will be expressed must also be defined before the program can read the ground motion file. The first of these is the horizontal peak ground acceleration scaling factor. The program reads the ground motion file, determines the largest acceleration value, and forces this

data point to 1.0. This alteration normalizes all of the other acceleration values in the ground motion record accordingly. These program altered accelerations are not the desired acceleration values for analysis purposes, so a scaling factor must also be defined in the program inputs to obtain the correct peak ground acceleration value. A peak ground acceleration scaling factor must also be defined for vertical accelerations to which the building is exposed. Throughout the analyses performed for this research, only longitudinal shaking damage was considered. Therefore, the vertical peak ground acceleration factor was set to zero for all analyses.

The time step that is desired for the response analysis must also be defined. The total duration of the analysis must be calculated and defined before the analysis can be run. This is done by establishing the number of acceleration points present in the ground motion record and multiplying this by the time step between acceleration points. The critical damping, equivalent linear viscous, is the final control parameter required.

Following this is a small section defining what the program will be dealing with in the ground motion record. The number of acceleration points in the ground motion file must be specified. The number designated here can be less than the actual number of data points in the acceleration file. If this occurs the program will stop running after the specified number and will not take into account any other data points. This may be useful when only looking at a specific data range in the ground motion file. However, if the number specified is greater than the actual number of data points present in the ground motion file, the program will be unable to finish its analysis and no data can be collected. In addition to the number of points present in the ground motion file, the time interval between each point must also be specified. Finally, the file name containing the ground motions, as well as the names of the output files, must be defined. The ground motion file must have a .dat extension for the program to be able to read it. The output files will automatically have an .OUT extension.

With the necessary program inputs defined, the actual analysis can be discussed. Inelastic dynamic time history analysis provides information about the behavior of the modeled structure when it is exposed to representative ground motions. As previously discussed, 19 ground motions were utilized throughout these analyses. The main point of interest in this type of analysis is the determination of the peak story drift demands for each individual story of the building during the earthquake. Since the earthquake intensities vary greatly between the records, examining the building performance for all 19 records provides a good measure of the behavior of the building under many circumstances.

In the pushover analyses, the area of interest revolved around the individual story outputs. In these analyses, the pertinent information deals with the entire building output file. The output file contains a section listing the largest drift, displacement, and story shear encountered throughout the analysis. The peak drift value listed is recorded during data collection. These values are recorded for each of the 19 earthquakes both including and neglecting the effects of p-delta. The median value of drift was calculated based on the similar earthquakes in each ground motion suite. This number was recorded and placed into chart format. This chart displays the peak percent drift value on each story for all of the similar earthquakes, in addition to the median value marked with a large box. Knowing the drift for each earthquake record and each individual story of the structure allows for the identification of the controlling story in the structure. The controlling story within the structure is the story that has the largest drift value.

With these two pieces of information, the median drift value for each story or for only the controlling story can be compared to the limit state drift values obtained from the pushover analysis. Comparing these two values allows for determination of the limit states which have been exceeded by the structure during any ground motion and whether or not the building's performance is acceptable.

GROUND MOTIONS

The ground motions used throughout this research consist of a suite of ground motions available on the web and developed by Wu and Wen (2000) for the Memphis region. This suite contains a total of 19 earthquake records. Ten of these records are 10% in 50 years probability of exceedance motions, which are relatively small amplitude earthquakes. The remaining 9 earthquake records are 2% in 50 years probability of exceedance records. Due to the smaller probability of occurrence, these earthquakes are of a significantly larger magnitude.

Fig. 13 displays two samples of the time history. The ground motions have accelerations expressed in cm/s^2 at time intervals of 0.01 seconds. Figs. 14 and 15 displays the response spectra for every record used throughout inelastic time history dynamic analyses.

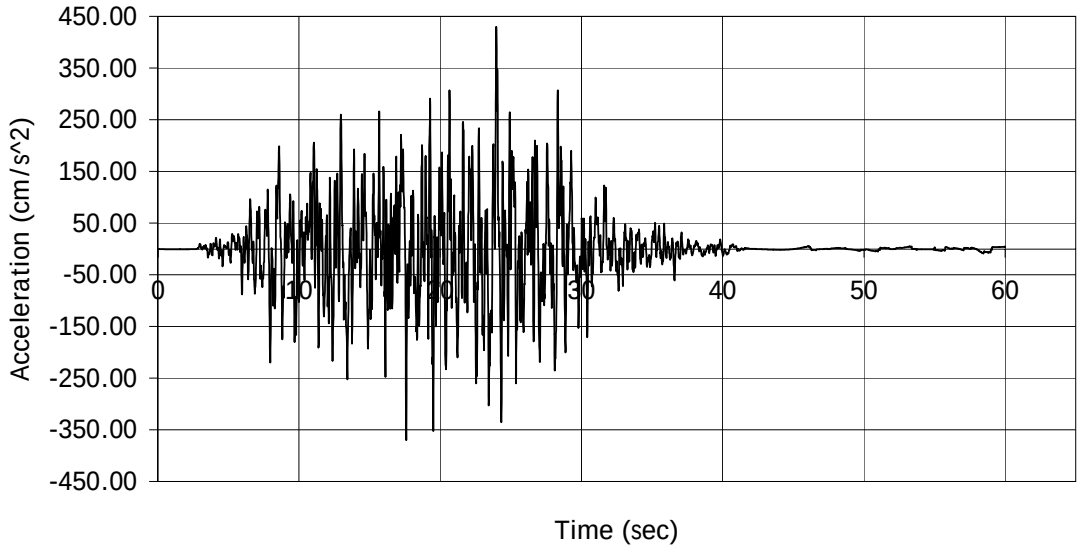

a) 2% in 50 Year Sample

FIGURE 13 Time History Samples

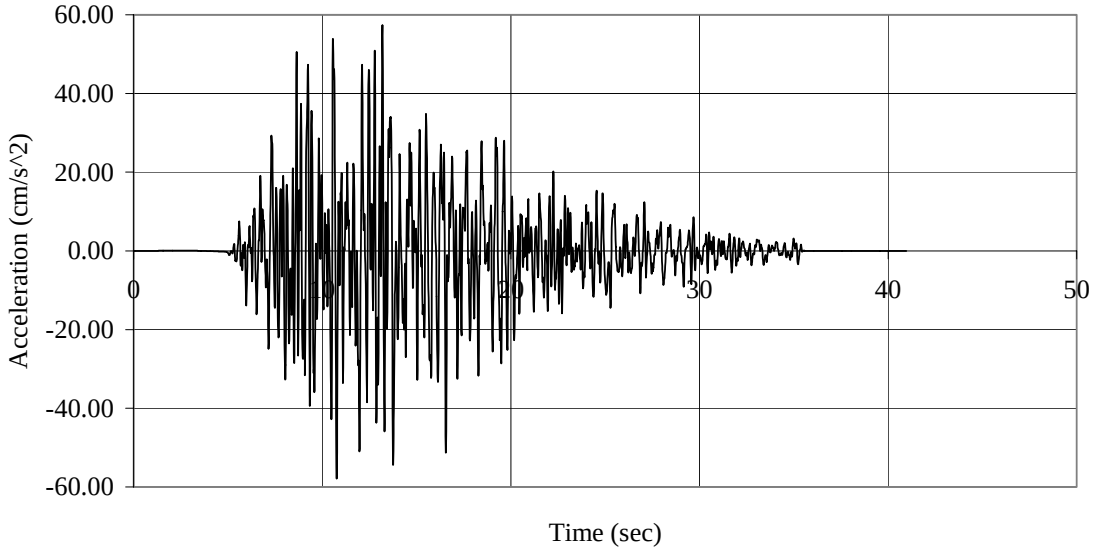

b) 10% in 50 Year Sample

FIGURE 13 (Continued)

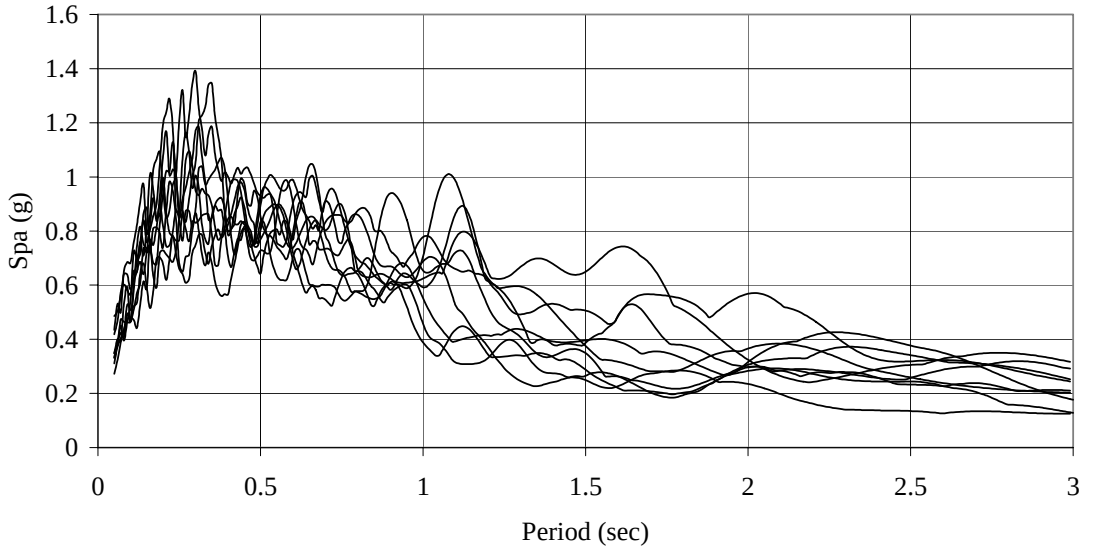

a) 2% in 50 Years Probability of Exceedance

FIGURE 14 Acceleration Response Spectra

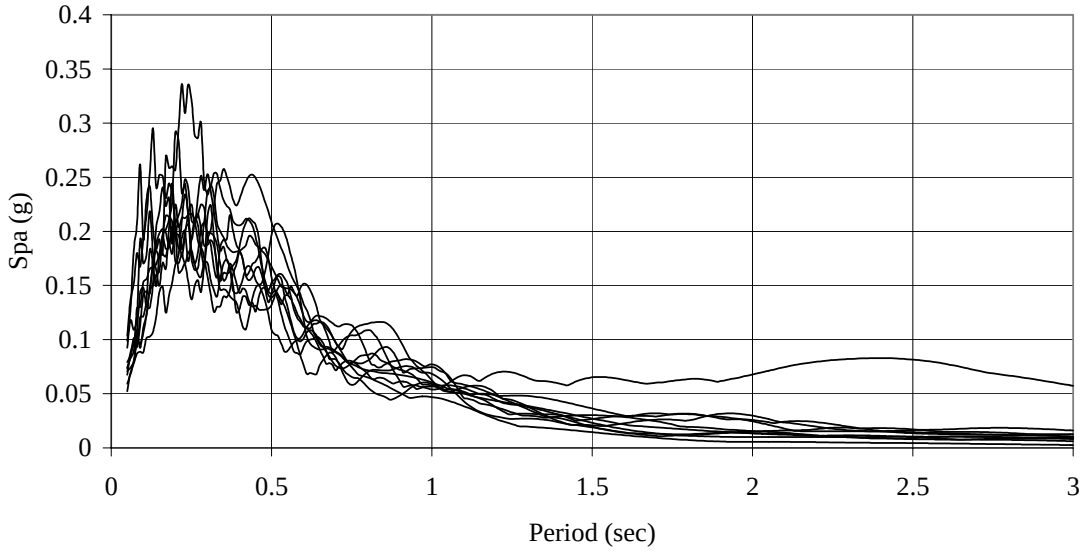

b) 10% in 50 Years Probability of Exceedance

FIGURE 14 (Continued)

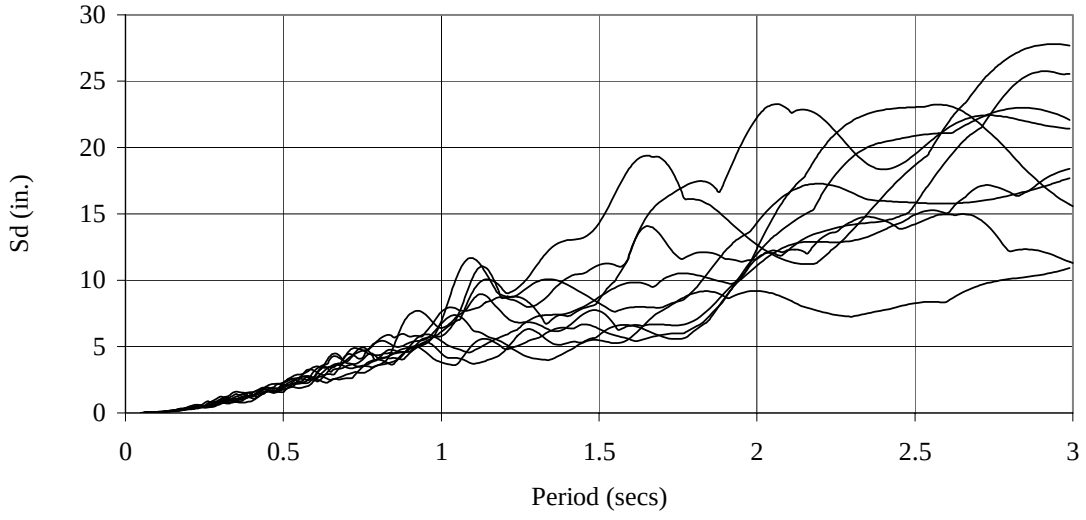

a) 2% in 50 Years Probability of Exceedance

FIGURE 15 Displacement Response Spectra

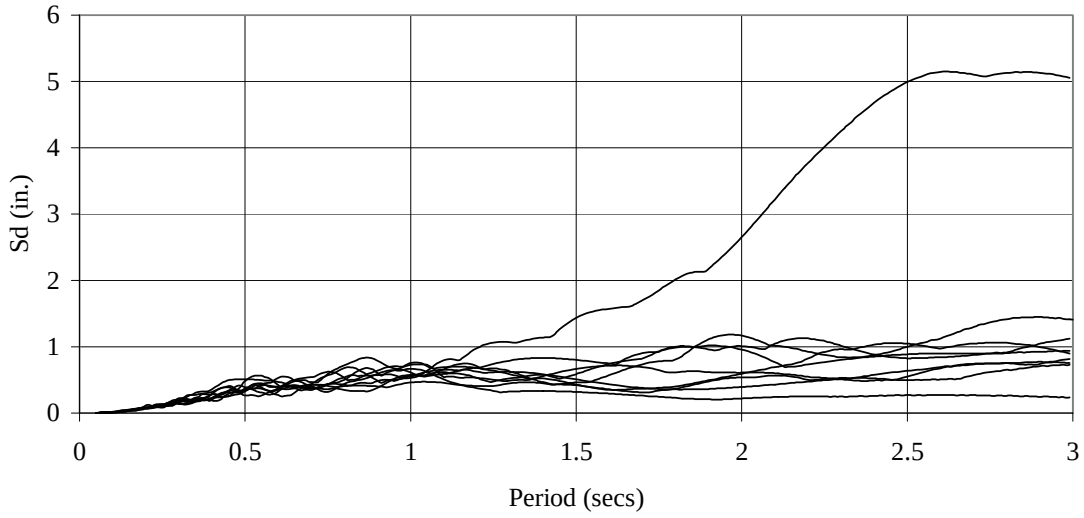

b) 10% in 50 Years Probability of Exceedance

FIGURE 15 (Continued)

All of the ground motions used for analysis are acceleration records on representative soil. The importance of using representative soil deals with the actual accelerations placed onto a building structure. Certain soil types cause amplification of the earthquake waves, thereby increasing the magnitudes of acceleration that a building would have to withstand. Therefore, ground motions with amplification could possibly cause much more damage to a structure than the same ground motion without amplification, or acceleration records on hard rock. Additionally, other soil types may have the opposite effect and reduce the acceleration demands placed onto the structure. Whether or not these ground motions are accurate and representative of an actual earthquake event in this area is unknown, since there is no comparison available. So, for the purposes of this research it was be assumed that the suite of ground motions is representative of an actual earthquake event in this region.

RESULTS

Having discerned the methods and necessary inputs for performing the inelastic time history dynamic analyses as well as the important information to be gleaned from these analyses, the actual results obtained are discussed below. Fig. 16 provides the peak story drift demand in percent of the story height obtained from the dynamic analysis for each story of the structure. Additionally, the median percent drift is identified and discussed below. The median drift values for the ten earthquake records were recorded both including and excluding the effects of p-delta.

It was found that the first story drift was the controlling story. The drift on the second story was very close to this controlling value, therefore, some attention should also be provided to the second story of the structure. The median drift value for 10% records for the first, second and third story of the structure, neglecting the effects of p-delta were 0.057, 0.052, and 0.043 respectively. Including the effects of p-delta, these drift values become 0.056, 0.054, and 0.042% drift. The 2% in 50 years probability of exceedance earthquakes showed that the first story of the structure was the controlling, or most vulnerable, story in the structure. Including the effects of p-delta the median drift values are 6.447%, 0.930%, and 0.313% for the first, second, and third stories, respectively. Excluding the effects of p-delta, the drift values are 3.812, 2.821, and 0.371% drift.

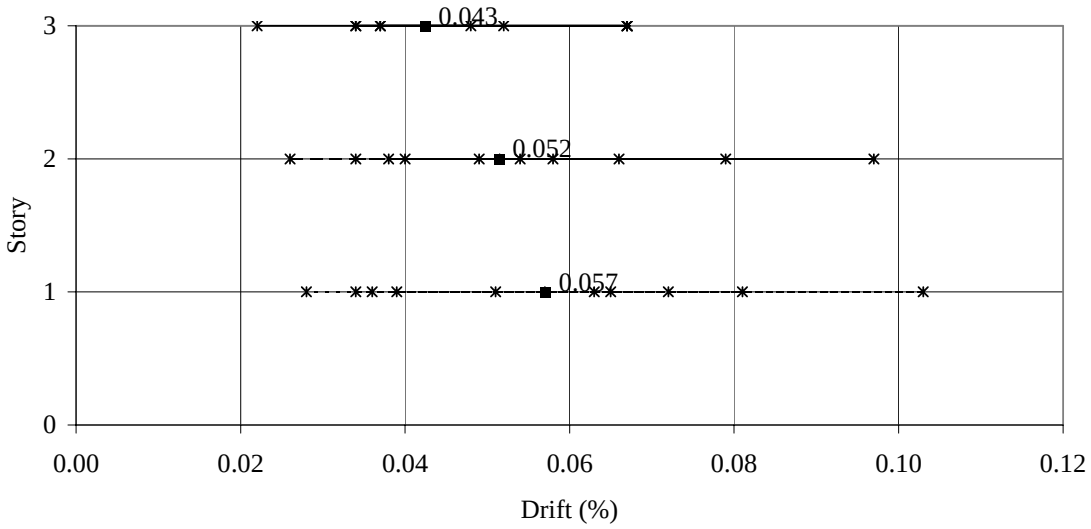

(a) 10% in 50 Ground Motions

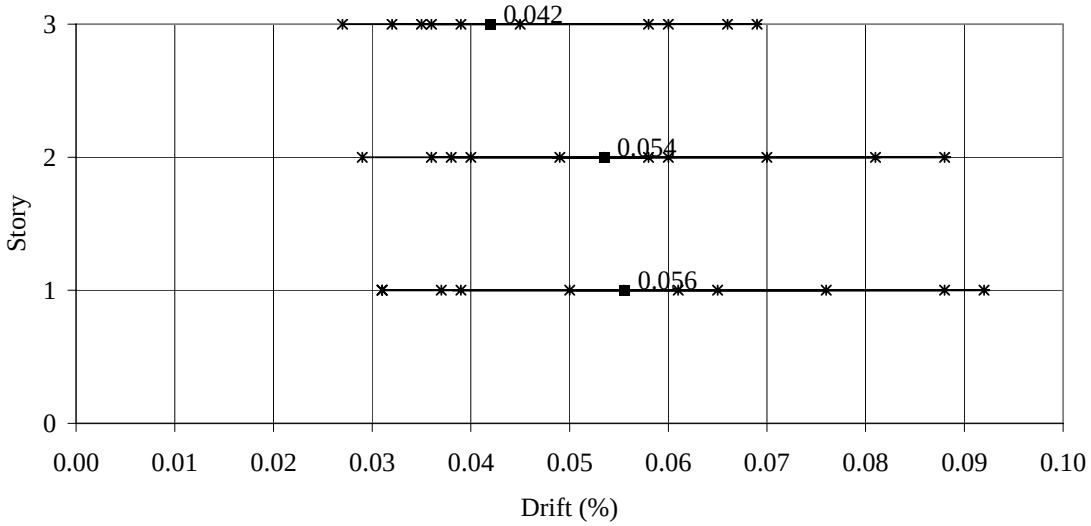

(b) 10% in 50 Years Ground Motions –With P-Delta Effects

FIGURE 16 Drift for Earthquake Records

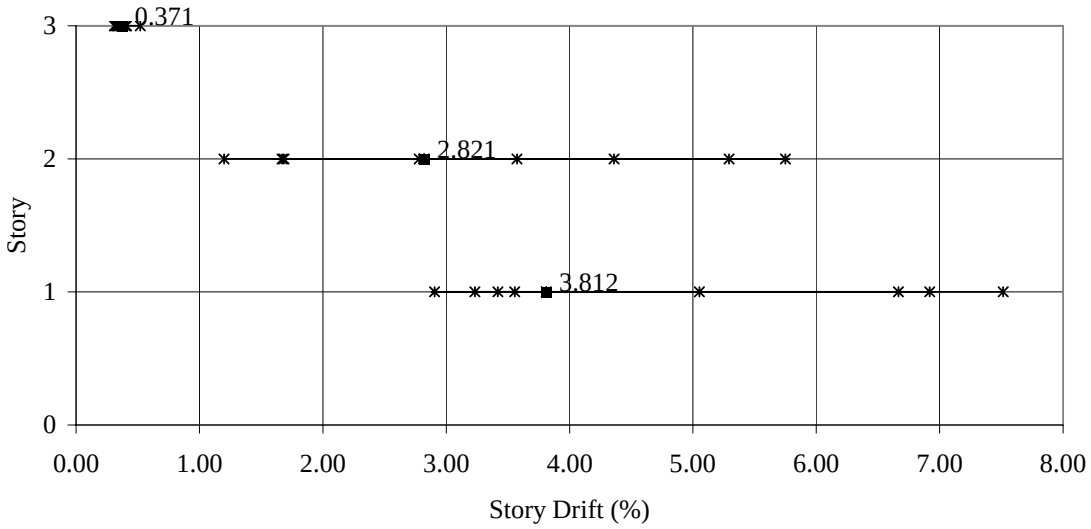

(c) 2% in 50 Years Ground Motions

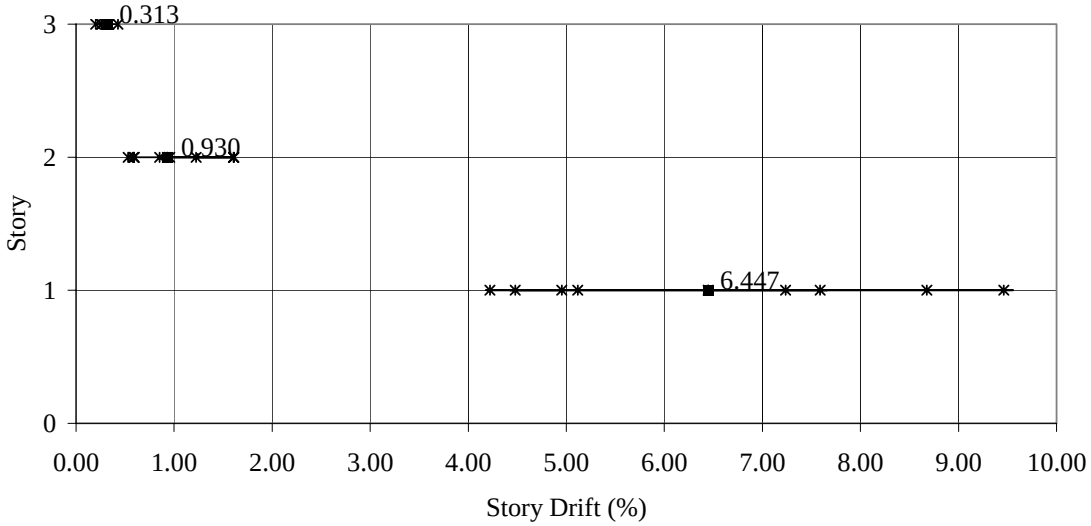

(d) 2% in 50 Years Ground Motions – With P-Delta Effects

FIGURE 16 (Continued)

Another way of presenting the seismic story drift demand is in terms of input spectral acceleration and displacement for that particular earthquake record and building fundamental period. Fig. 17 shows the peak story drift demand vs. spectral acceleration

at the fundamental building period. The figure displays the correlation between the data points and the power law trend line fit. This is a power law trend line fitted to the data points by Microsoft Excel. It should be noted that the equation for the trend line and the R^2, or correlation of this trend line to the displayed data points are displayed on the chart, shown in Fig. 17. Fig. 18 displays this same drift information vs. spectral displacement.

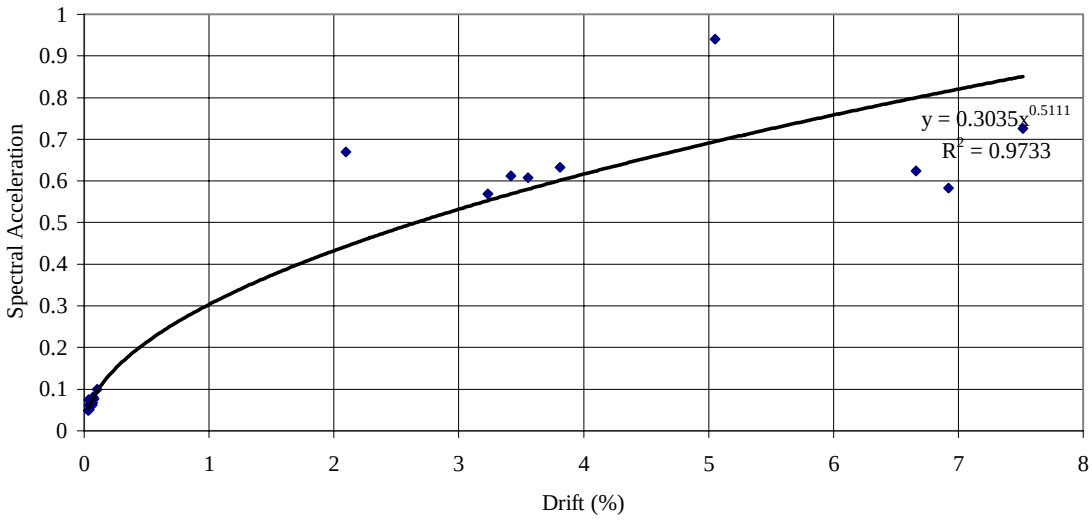

a) All Records - Without the Effects of P-Delta

FIGURE 17 Spectral Acceleration vs. Demand

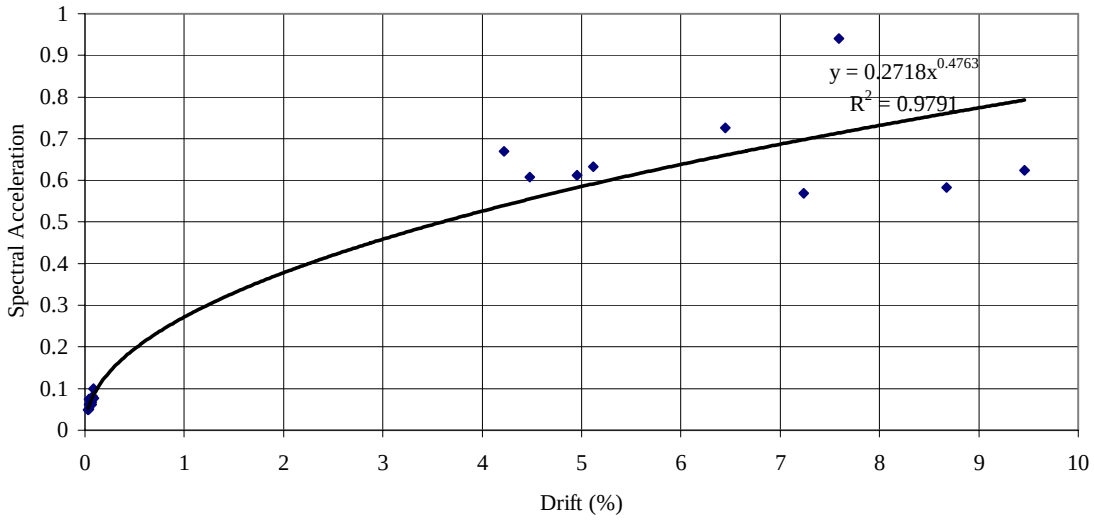

b) All Records – With the Effects of P-Delta

FIGURE 17 (Continued)

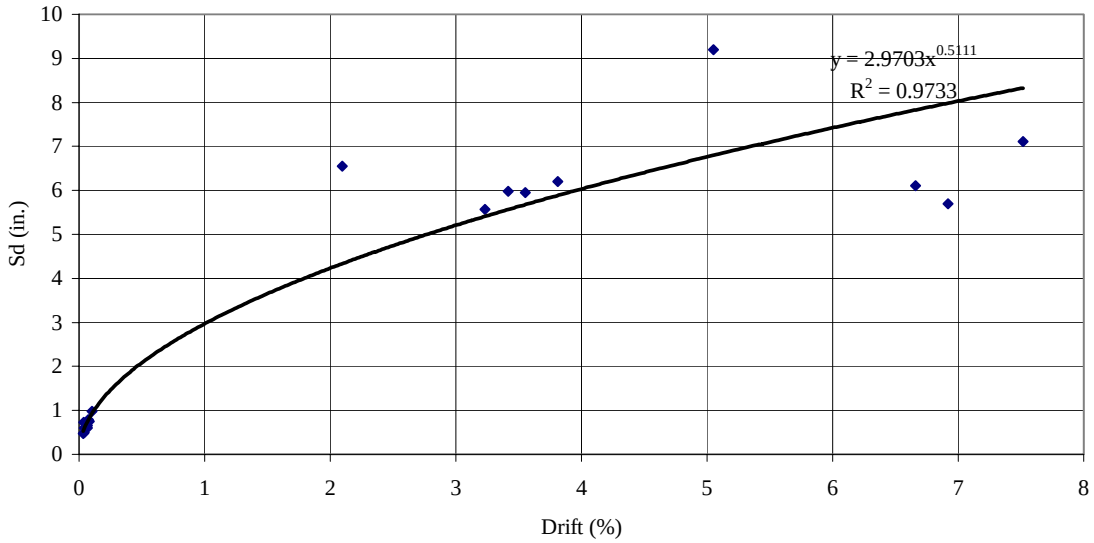

a) All Records – Without the Effects of P-Delta

FIGURE 18 Spectral Displacement vs. Demand

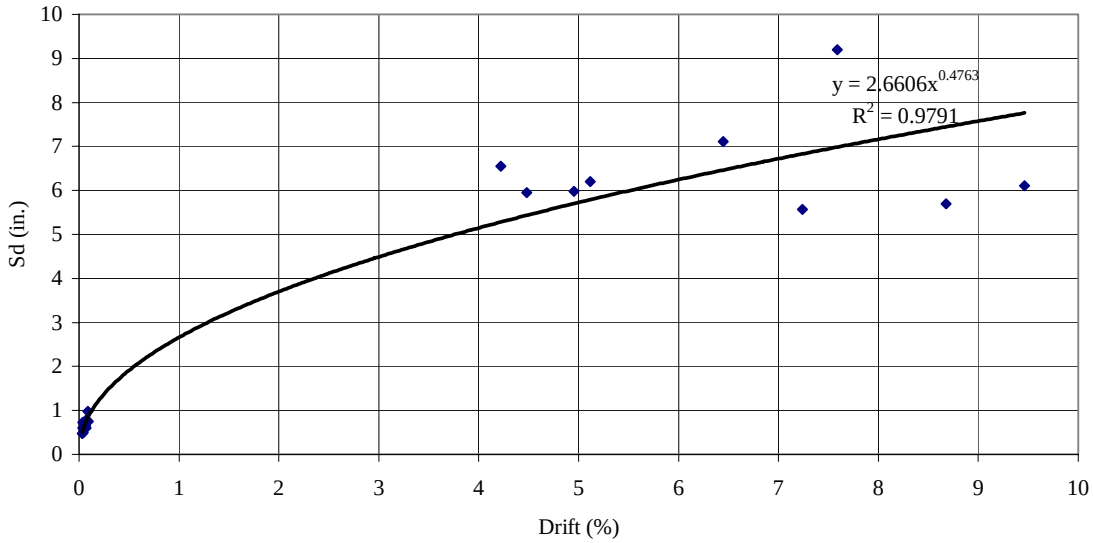

b) All Records – With the Effects of P-Delta

FIGURE 18 (Continued)

SUMMARY

The dynamic analysis of the structure during ground motion excitations provides pertinent information as to the building demand and its overall behavior. In general, the first story of the structure has the largest demands throughout all analyses. The demand for the 10% in 50 years probability of exceedance earthquake ground motions was very small. However, demand for the 2% in 50 years probability of exceedance earthquake ground motions were very large with median values greater than 4%.

TABLE 3 Power Law Equations

Excluding the Effects of P-Delta	$Spa = 0.3035\delta^{0.5111}$
Including the Effects of P-Delta	$Spa = 0.2718\delta^{0.4763}$

Table 3 displays the power law equations for the prototype structure both including and excluding the effects of p-delta. These equations are similar and have a good correlation with the data points obtained from the dynamic analyses. The fragility factors calculated from this data are $\beta_{D/Sa}$ and $\lambda_{D/Sa}$ and discussed in the following chapter. The β term is constant throughout all analyses. The λ term varies according to the power law equations defined in Table 3.

CHAPTER VI
FRAGILITY CURVES

INTRODUCTION

A fragility curve represents the probability that a limit state will be exceeded given the spectral acceleration at the fundamental period of the structure. Creating a fragility curve requires a combination of all the results from the story capacity in Chapter IV and the seismic demands discussed in Chapter V. The raw data sets obtained from these analyses were statistically analyzed to create the fragility curves. The story capacities involved with fragility curve development were obtained from the three different methods discussed in Chapter IV, including the FEMA 273 drift limits, quantitative limits from pushover analyses, and incipient collapse from incremental dynamic analyses. The seismic demand was represented by the best fit power law equation developed from the inelastic time history dynamic analyses using synthetic earthquake ground motion records described in Chapter V.

DEVELOPMENT OF FRAGILITY CURVES

The development of fragility curves involves the integration of the seismic story demands with the story capacities, in terms of statistical representation. Since the seismic demands are represented by the power law equation in Chapter V, fragility curves for a variety of capacities, or limit states, were developed. Fragility curves were created using the FEMA limit states for RC frames, 1%, 2%, and 4% drift for Immediate Occupancy, Life Safety, and Collapse Prevention, respectively. Another set of fragility curves were created for the incipient collapse limit state using incremental dynamic analyses. The final set of fragility curves used quantitative the limit states defined in pushover analyses.

The development of the desired fragility curves is achieved through the use of the following equation (Wen et al, 2004).

$$P\left(LS/S_a\right)=1-\phi\left(\frac{\lambda_{ICC}-\lambda_{D/Sa}}{\sqrt{\beta_{D/Sa}^2+\beta_{ICC}^2+\beta_C^2}}\right) \qquad \text{(EQ-2)}$$

Where: P (LS/Sa) = Probability of exceeding a limit state given spectral acceleration at the fundamental period of the building

ϕ = standard normal distribution

λ_{ICC} = ln (median (capacity drift))

$\lambda_{D/Sa}$ = ln (demand drift)-.50*$\beta^2_{D/Sa}$

$\beta_{D/Sa}$ = sqrt (ln (1+Δx^2))

β_{ICC} = sqrt (ln (1+cov^2))

βc = Modeling uncertainty

Due to the complicated nature of these terms, further discussion is required. Capacity terms are discussed first and the way in which they are calculated varies depending on the capacity analysis performed. When considering the capacity determined from the incremental dynamic analyses, the drift value utilized for the calculation of λ_{ICC} is the natural log of the median incipient collapse drift levels identified in Chapter IV. The next term to be calculated is β_{ICC}. The standard deviation and mean of the incipient collapse drift values are calculated. The standard deviation of these incipient collapse drift values is then divided by the mean drift in order to obtain the covariance of this data set and the equation listed above is used to calculate the final value. The explanation above is assuming that the capacity is determined from the incremental dynamic analyses. However, if the FEMA or pushover defined limit states were chosen, then the λ_{ICC} term would be the natural log of the specified drift limit, for example λ_{ICC} is equal to the natural log of 1 for a 1% drift limit. The β_{ICC} term when considering FEMA and pushover drift limits is held at constant 0.30.

Δx (capacity) = ln (COV) (EQ-3)

$$\Delta x(demand) = \sqrt{\frac{sum[Yi - (a + b \cdot Xi) / (a + b \cdot Xi)]^2}{n - 1}} \quad \text{(EQ-4)}$$

Sum = summation over i

yi = Calculated drift

Xi = Sa

n = sample size

a & b = power aw best fit regression coefficients

The demand variables will also be discussed in further detail. The calculation of $\lambda_{D/Sa}$ requires the determination of various drift levels corresponding to spectral acceleration values. The drift values are calculated using the power law fit, found appropriate for the demand data. Spectral acceleration is varied from 0.05 to a value of 1.0 to obtain a smooth fragility curve. These drift values are utilized to obtain the desired demand variable. The final demand term calculated is $\beta_{D/Sa}$. To calculate this term, Δx must be calculated first. Δx is found once again by utilizing the previously discussed power law equation to estimate the drift present at each record's spectral acceleration value.

The actual peak drift obtained from each dynamic analysis is divided by this estimated drift times one minus the number of points present. This value is calculated for each individual earthquake record. These numbers are then summed and the square root of this sum is defined as Δ x.

The variables concerning capacity will change based on the capacity chosen. In addition to the different types of limit states, there is also a variation among fragility curves. This variation comes from an uncertainty term in the probability equation. This uncertainty value varies between 20, 30, and 40%. Adding an uncertainty term is of importance in any such analysis because there are factors that vary in any building structure. These factors include, but are not limited to, material strength variation and differences between the designed structure and the actual structure.

RESULTS

This probability of exceedance equation is calculated for various spectral acceleration values and a fragility curve is created. The fragility curves created for this research are shown below in Fig. 19 and Fig. 20. One set of charts displayed show the fragility curves for the FEMA drift limit states in conjunction with the fragility curve created from the incremental dynamic analyses. The other charts display the fragility curves created from the pushover limit states.

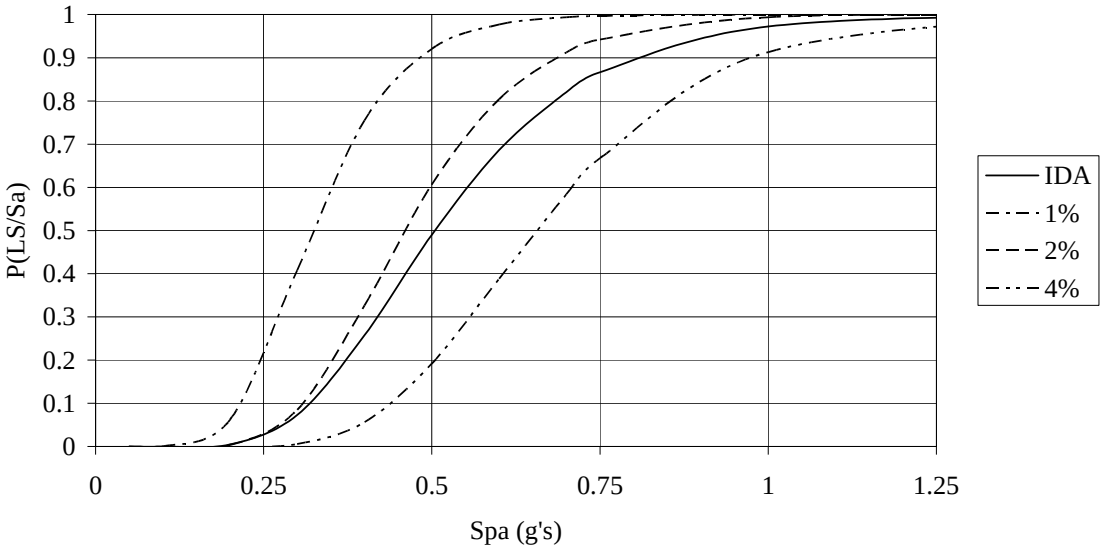

a) 20% Uncertainty – FEMA

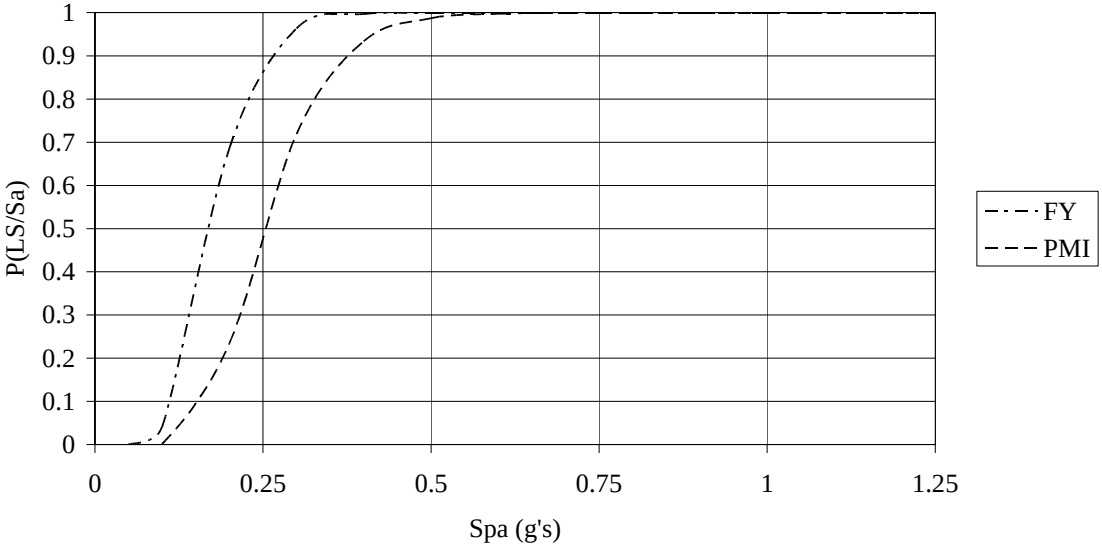

b) 20% Uncertainty – Pushover

FIGURE 19 Fragility Curves

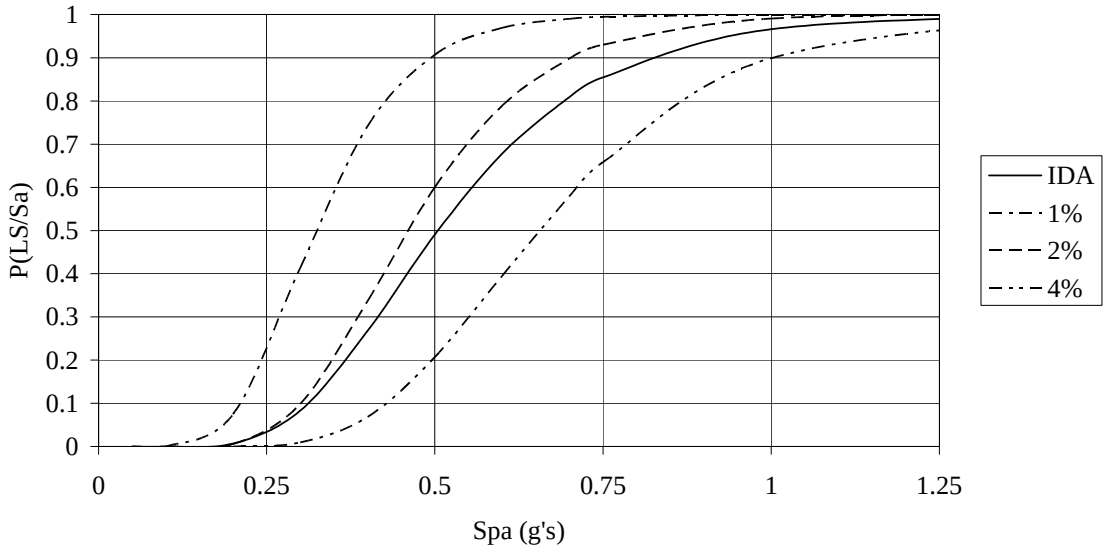

c) 30% Uncertainty - FEMA

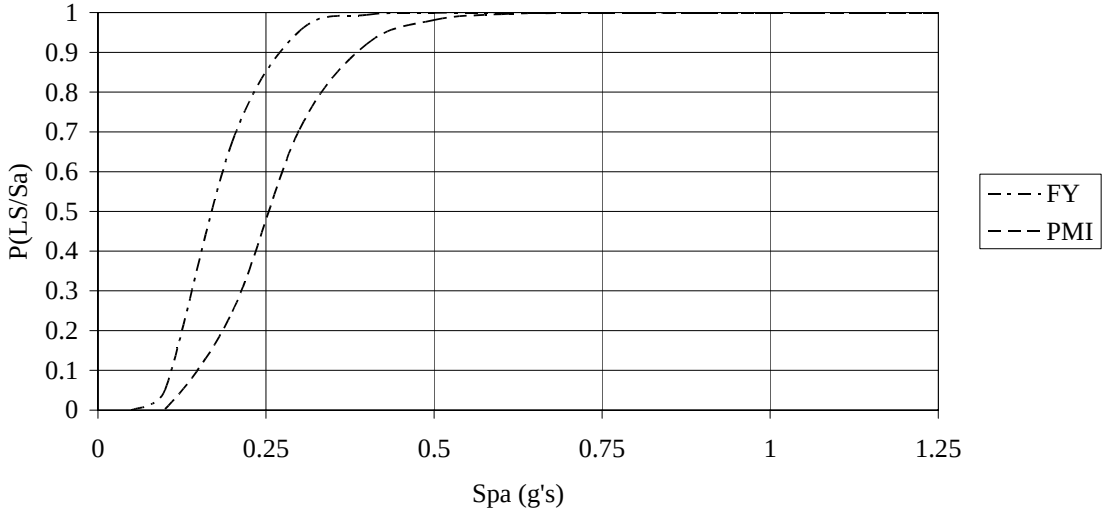

d) 30% Uncertainty - Pushover

FIGURE 19 (Continued)

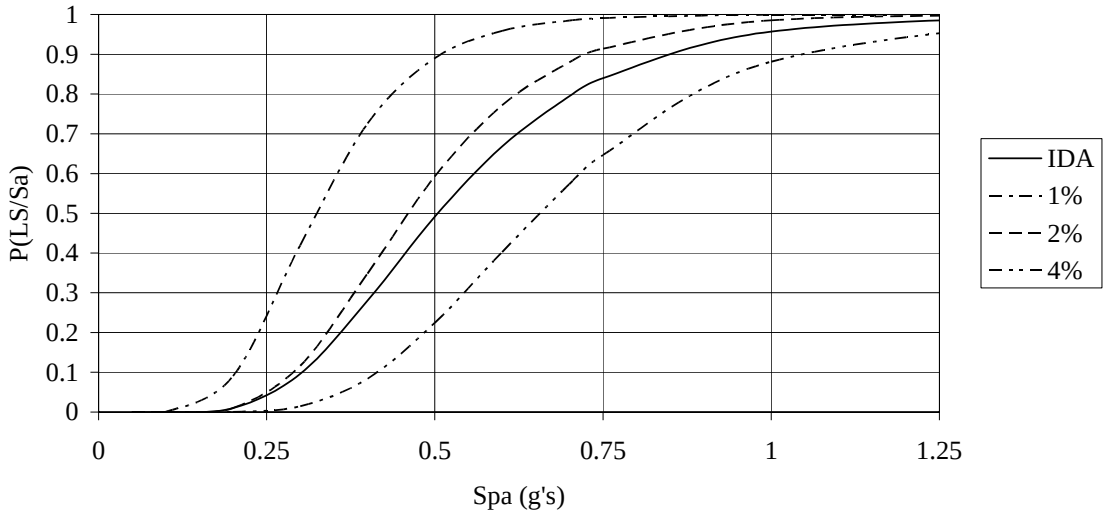

e) 40% Uncertainty - FEMA

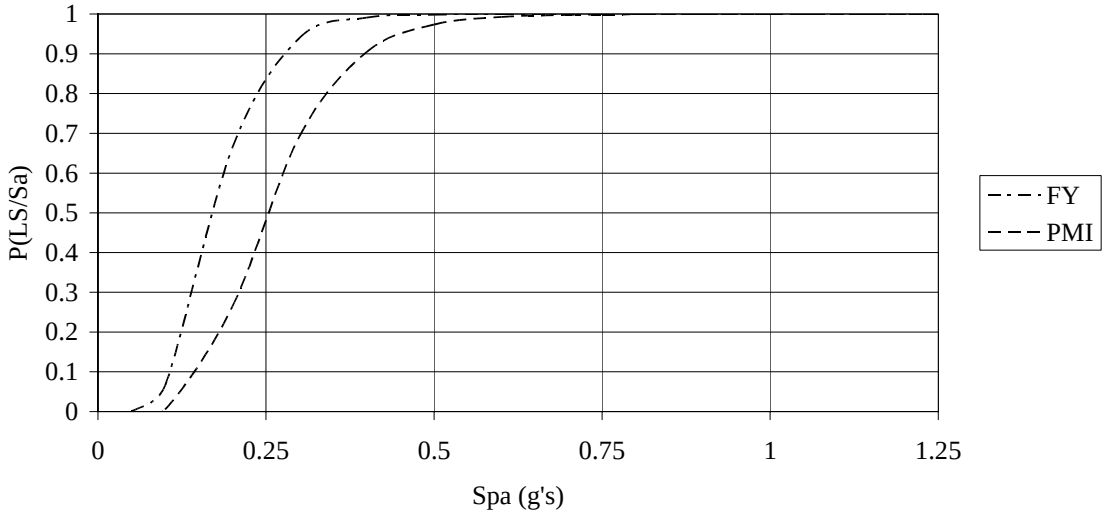

f) 40% Uncertainty – Pushover

FIGURE 19 (Continued)

Fig. 19 shows the fragility curves for the designed structure neglecting the effects of p-delta. Comparing the results between the 20, 30, and 40% uncertainty fragility curves, it can be determined that the level of modeling uncertainty is an insignificant factor in the results obtained. This is due to the high level of uncertainty present in the synthetic ground motions designed for the Memphis region. This uncertainty in ground motions far outweighs the uncertainty present in the numerical modeling and is, therefore, found to be of little importance. For this reason, all further results discussed will deal only with a 30% modeling uncertainty.

The fragility of the structure can be determined by getting the design earthquake spectral acceleration for a 2% in 50 years probability of exceedance earthquake specified in the IBC 2000 code and determining the probability of exceedance from the provided fragility curve. The spectral acceleration value calculated according to IBC 2000 is 0.74 g's. This value is calculated using the S_s and S_1 values obtained from the IBC 2000 earthquake maps. The value for S_s is 3.00 g's and S_1 is 1.00 g's, these values are multiplied by various factors to obtain the 0.74 g spectral acceleration value. The probability of exceeding the FEMA defined and incremental dynamic analysis defined limit state is 99% for the 1% drift limit state, 95% for the 2% drift limit state, 68% for the 4% drift limit state, and 85% for the incremental dynamic analysis limit state. The second charts display the fragility curves created using the pushover analysis defined limit states. The probability of exceedance of the first yield limit state is 100% and 100% for the plastic mechanism initiation limit state. The probability of exceeding the provided limit states is much larger when considering the limit states defined by the pushover analysis. This would lead to the conclusion that the pushover defined limit states are more stringent than those defined by the FEMA general reinforced concrete limit states. This is not only displayed by the use of this factor, the same conclusion can be reached by looking at the placement of the fragility curves along the spectral acceleration axis. The farther along the spectral acceleration axis that a given fragility curve is located, the less fragile the building structure is considered.

Fig. 20 displays fragility curves using the same limit states and the same originally designed prototype structure, however, these curves include the effects of p-delta. It is found that the probability of exceedance is 100% for the 1% drift limit state, 98% for the 2% drift limit state, 85% for the 4% drift limit state, and 88% for the incremental dynamic analysis fragility curves. Additionally, the first yield limit state has a 100% probability of exceedance, 100% for the plastic mechanism initiation.

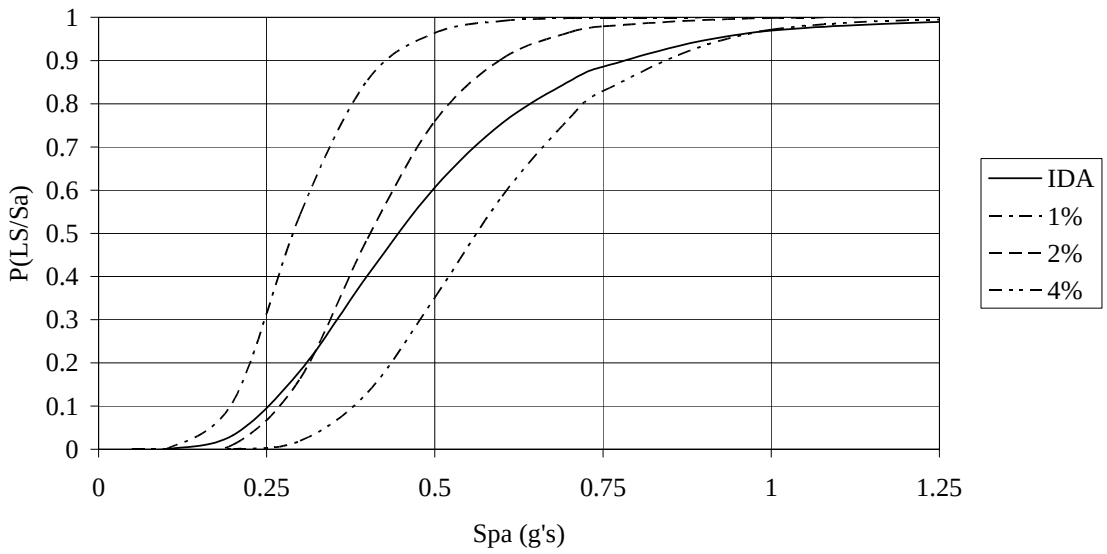

(a) 20% Uncertainty - FEMA

FIGURE 20 Fragility Curves – With the Effects of P-Delta

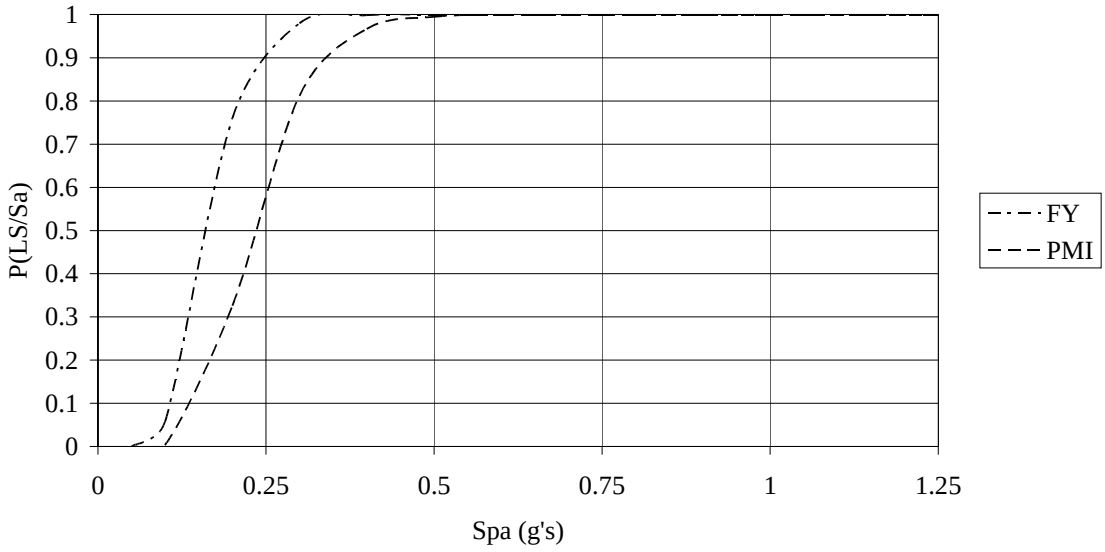

c) 20% Uncertainty – Pushover

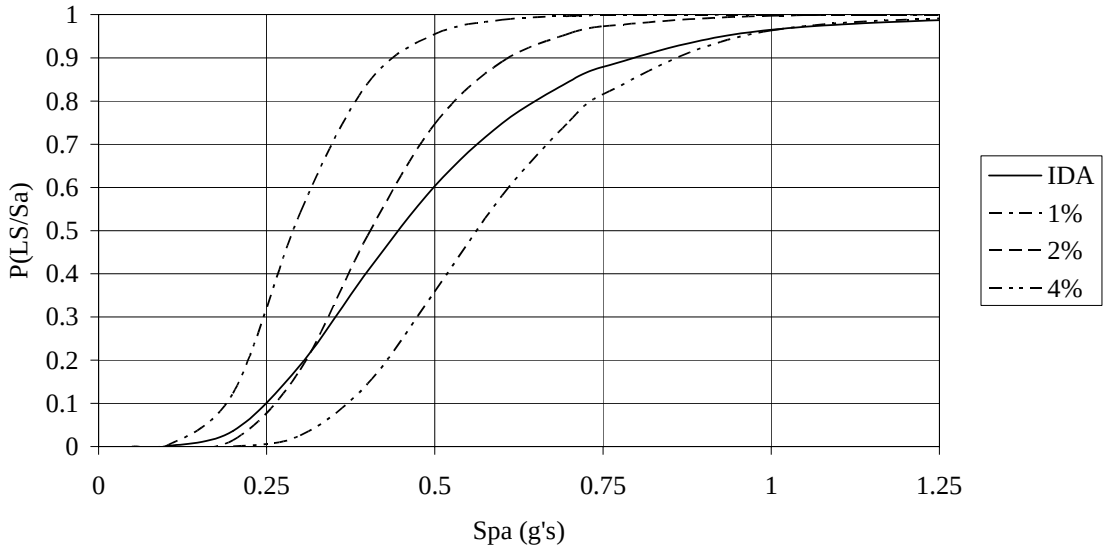

d) 30% Uncertainty - FEMA

FIGURE 20 (Continued)

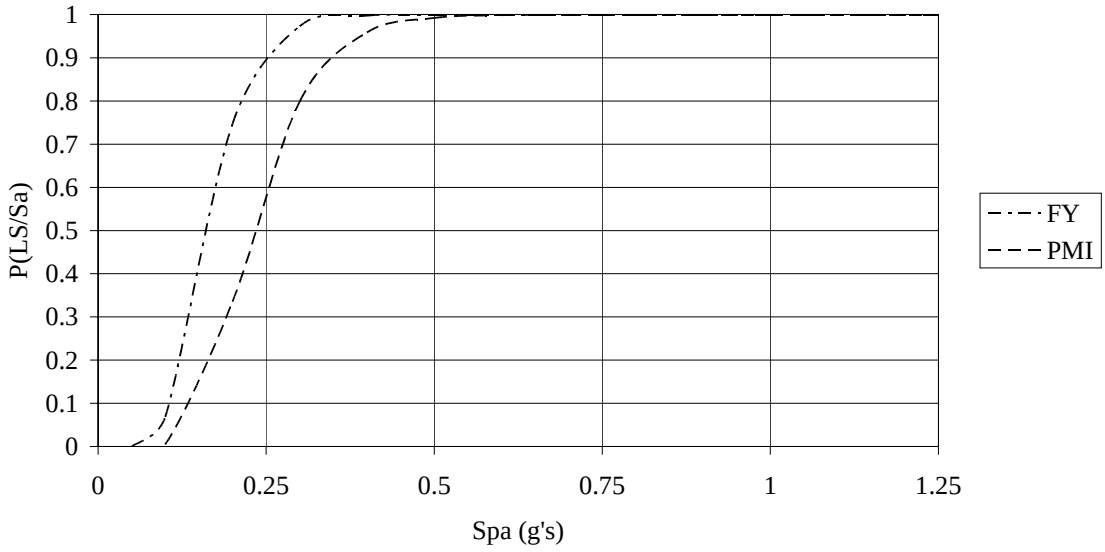

e) 30% Uncertainty – Pushover

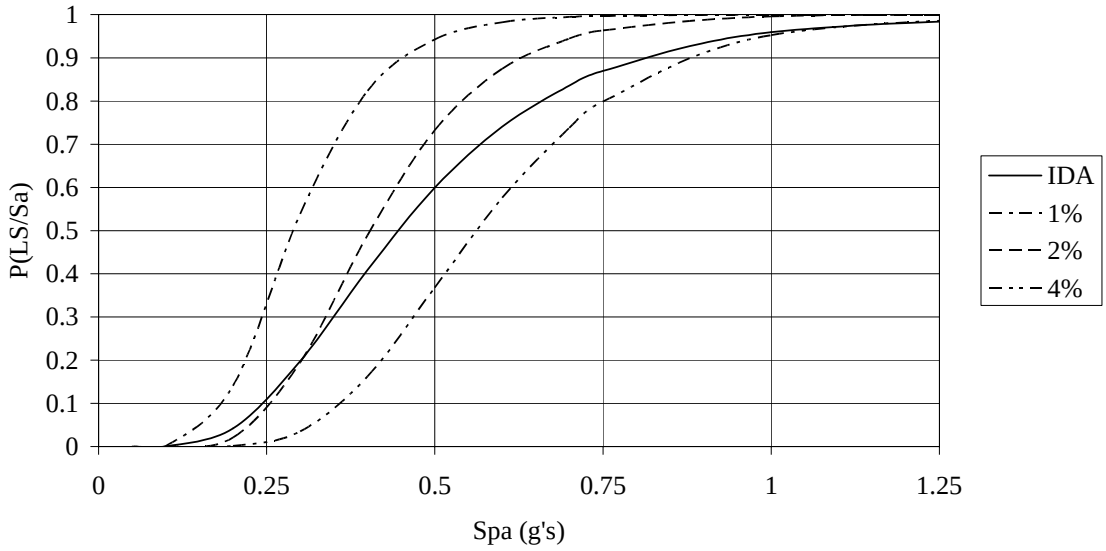

f) 40% Uncertainty - FEMA

FIGURE 20 (Continued)

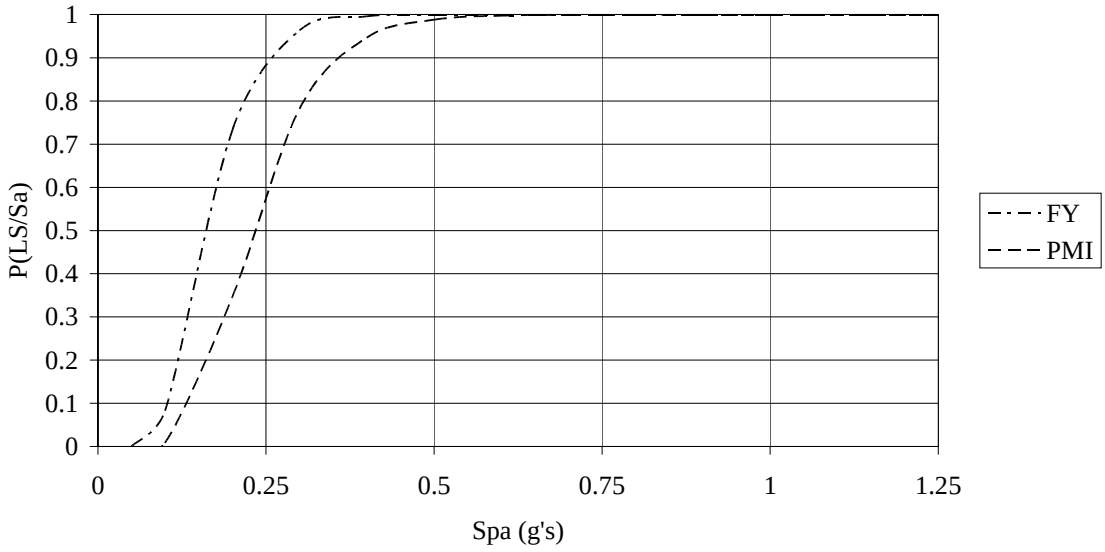

g) 40% Uncertainty - Pushover

FIGURE 20 (Continued)

Shown in Fig. 21 are fragility curves displaying the probability of exceeding a specified limit state versus the spectral displacement. This figure displays only the fragility curves considering 30% modeling uncertainty.

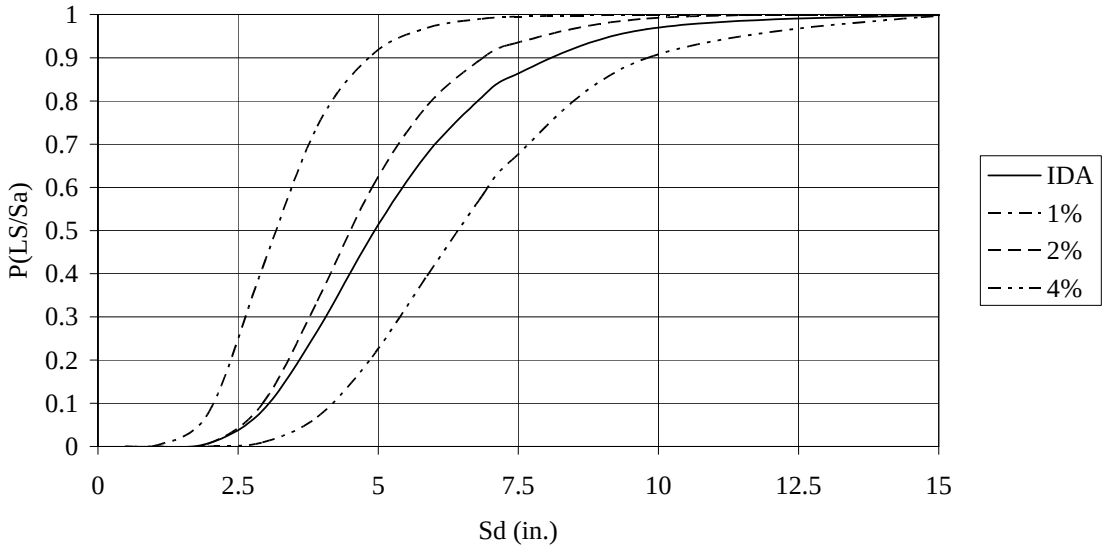

a) FEMA

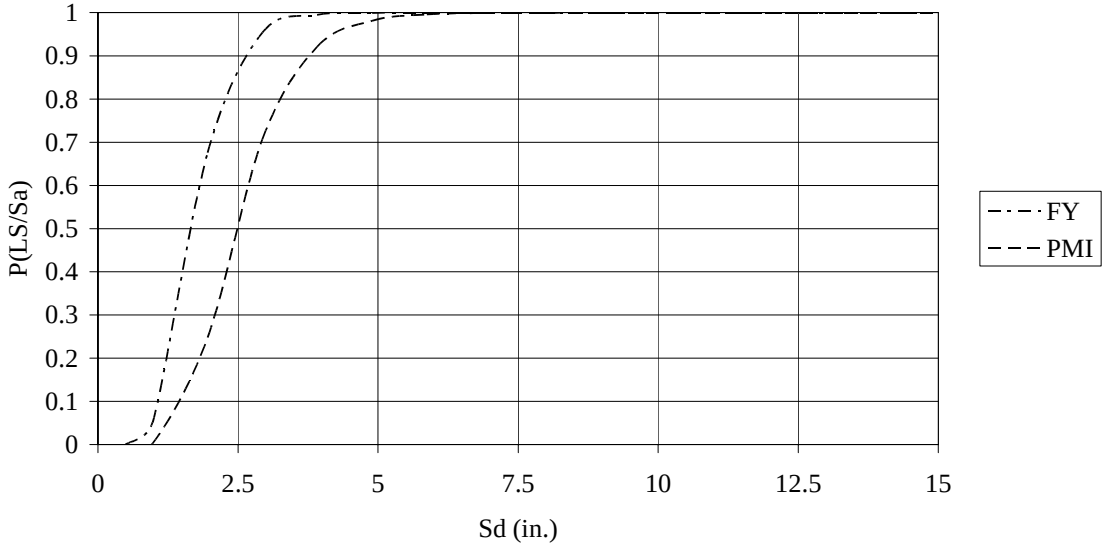

b) Pushover

FIGURE 21 Fragility Curves - Spectral Displacement

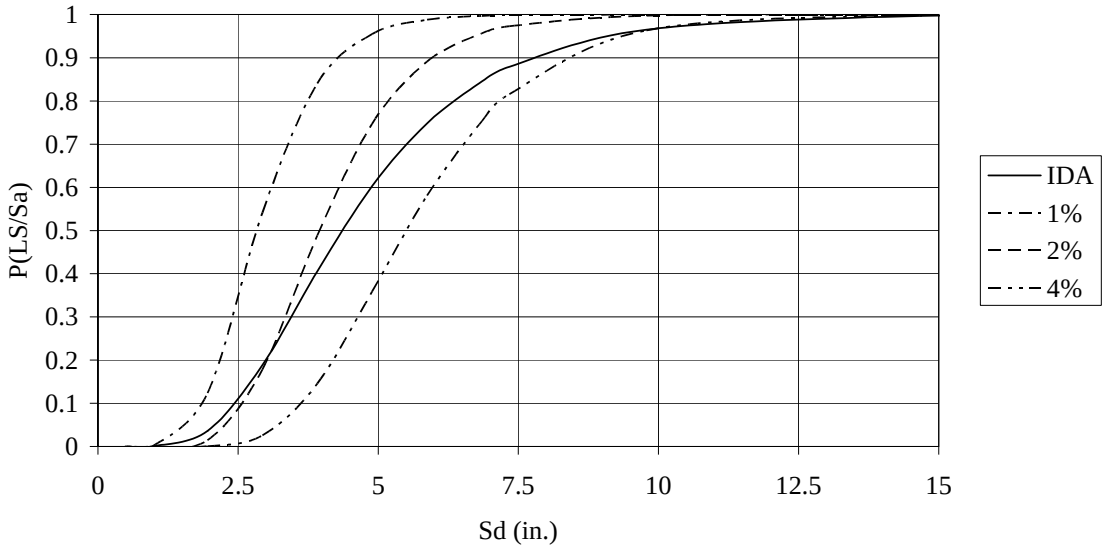

c) FEMA - Including the Effects of P-Delta

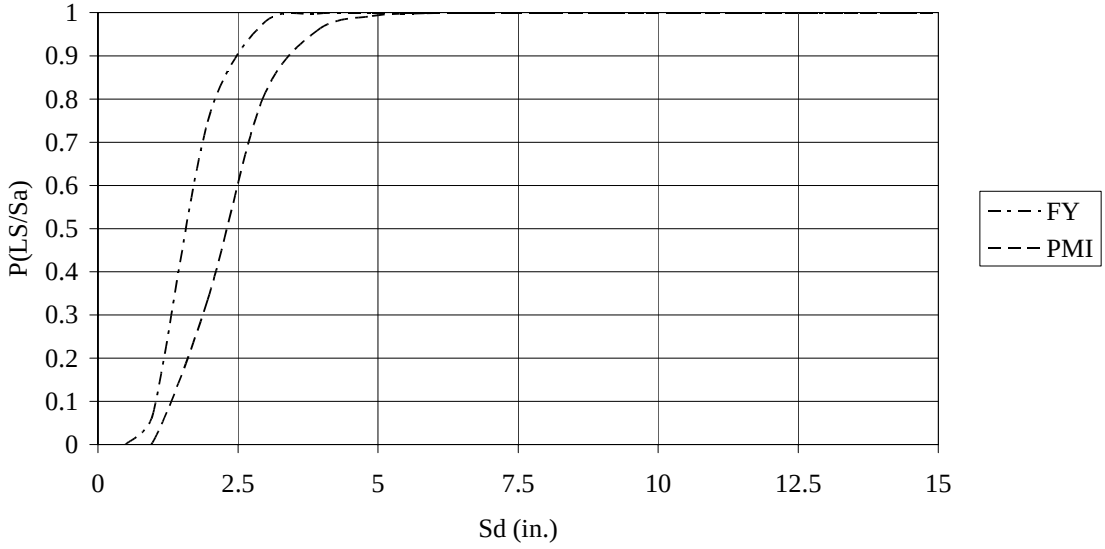

d) Pushover - Including the Effects of P-Delta

FIGURE 21 (Continued)

It can be seen by looking at the probability of exceeding the defined limit states that the prototype building is vulnerable to earthquakes of design magnitude in the New Madrid Seismic Zone. For this reason, it was decided that an attempt at retrofitting would be necessary.

CHAPTER VII
RETROFITTED STRUCTURE - 1.2 COLUMN-TO-BEAM STRENGTH RATIO

INTRODUCTION

The fragility curves for the existing RC frame structures in Mid-America show that these structures are vulnerable to significant damage potential during a strong ground motion representative of the New Madrid Seismic Zone. Of particular note regarding this type of building construction was that the columns were found to be weaker than the connecting beams. For the building design specified in Chapter III, the typical column-to-beam strength ratio was approximately 0.6. The primary conclusion from Chapter VI is that these buildings exhibit an acceptable response to small magnitude earthquakes and an unacceptable response to large magnitude earthquakes.

Based on the research done by Dooley and Bracci (2001), the column-to-beam strength ratio is a key structural parameter in controlling seismic damage. The recommendation from that work was to increase the ACI code seismic design requirements from a column-to-beam strength ratio of 1.2 to 1.8. In an effort to emphasize and evaluate structural retrofitting, fragility curves are developed based on a structural model with a column-to-beam strength ratio of 1.2 and 1.8. To change these ratios in analytical simulations, only the column strength was altered, leaving the beam strength as originally designed. This chapter is concerned with the evaluation of a retrofitted structure with a column-to-beam strength ratio of 1.2 and Chapter VIII is presents the results for a column-to-beam strength ratio of 1.8.

Fig. 22 shows the column moment-curvature relationship for the various column-to-beam strength ratios tested in this research. This figure demonstrates that both the

moment and curvature capacity of the column sections increase as the column-to-beam strength ratio is increased.

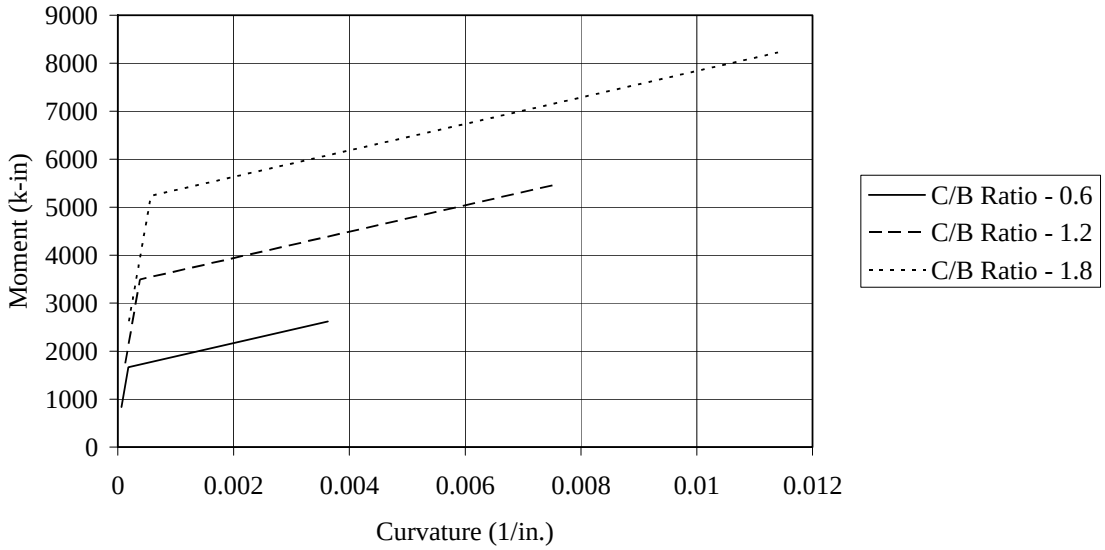

FIGURE 22 Column Moment vs. Curvature

STORY CAPACITIES

All capacity measures utilized in the analysis of the originally designed structure were replicated here to observe the differences between the original and retrofitted structural model. The drift limitations, specified in FEMA document 273 are the same values as previously discussed which are 1% for Immediate Occupancy, 2% for Life Safety, and 4% for Collapse Prevention, and they are intended for well designed structure or retrofitted structures. Pushover analyses were run as another method to determine the story capacity of the structure by quantitative techniques. The results from these pushover analyses are displayed in Figs. 23 and 24. These figures display the entire pushover results obtained, both including and excluding the effects of p-delta. The pushover limit states obtained excluding the effects of p-delta are 0.6% drift for first yield and 2.0% drift for plastic mechanism initiation. Including the effects of p-delta,

the drift limit for first yield is 0.6% and 1.4% for plastic mechanism initiation. No limit state value was found for the strength degradation limit state because the structure did not undergo a large amount of strength loss throughout loading even when the effects of p-delta were considered.

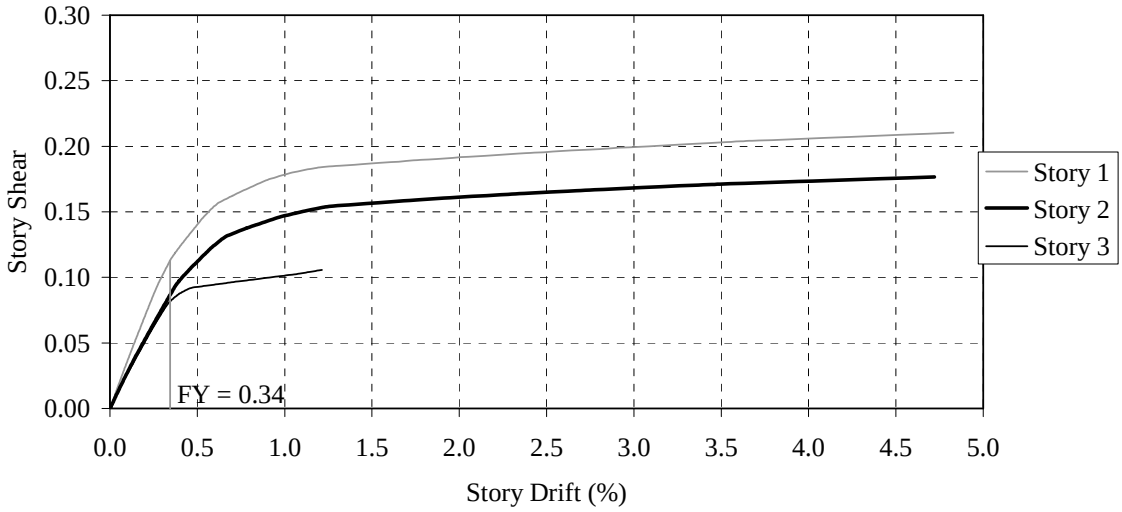

(a) Force Control – Inverted Triangular Distribution

FIGURE 23 Pushover Results – C/B Ratio 1.2

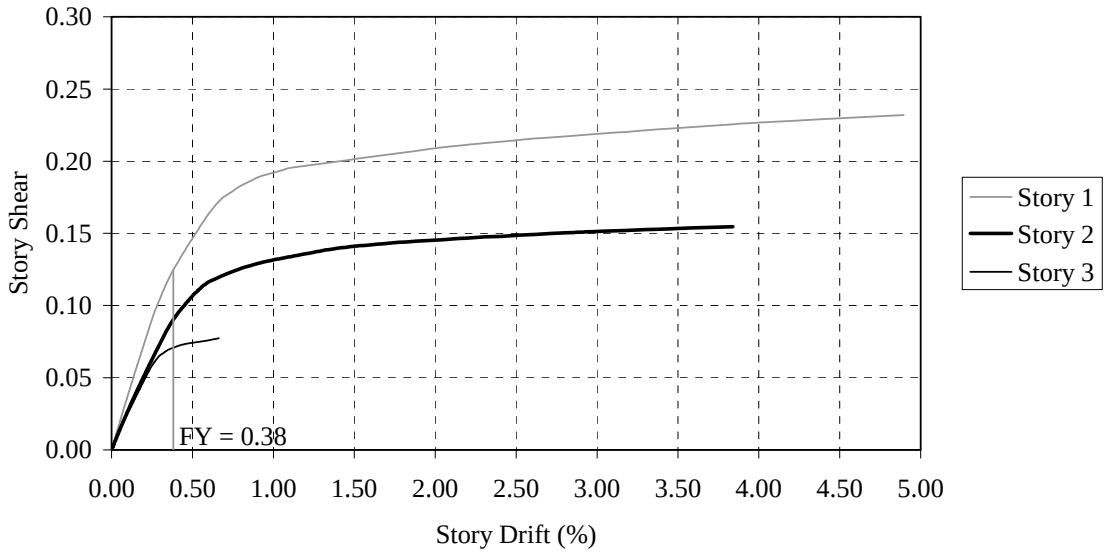

(b) Force Control Uniform Distribution

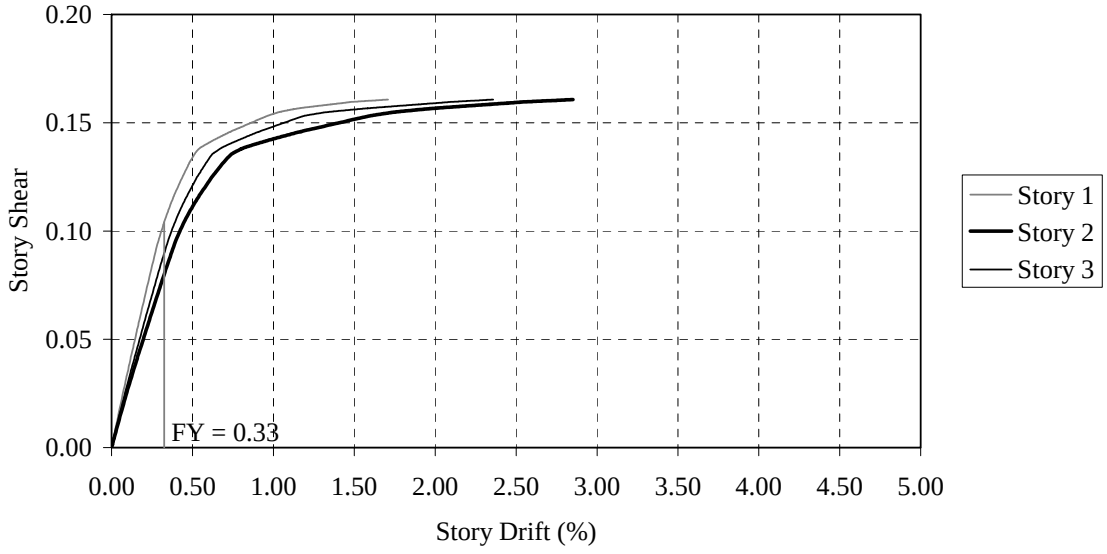

(c) Displacement Control – 10% on 3rd Story

FIGURE 23 (Continued)

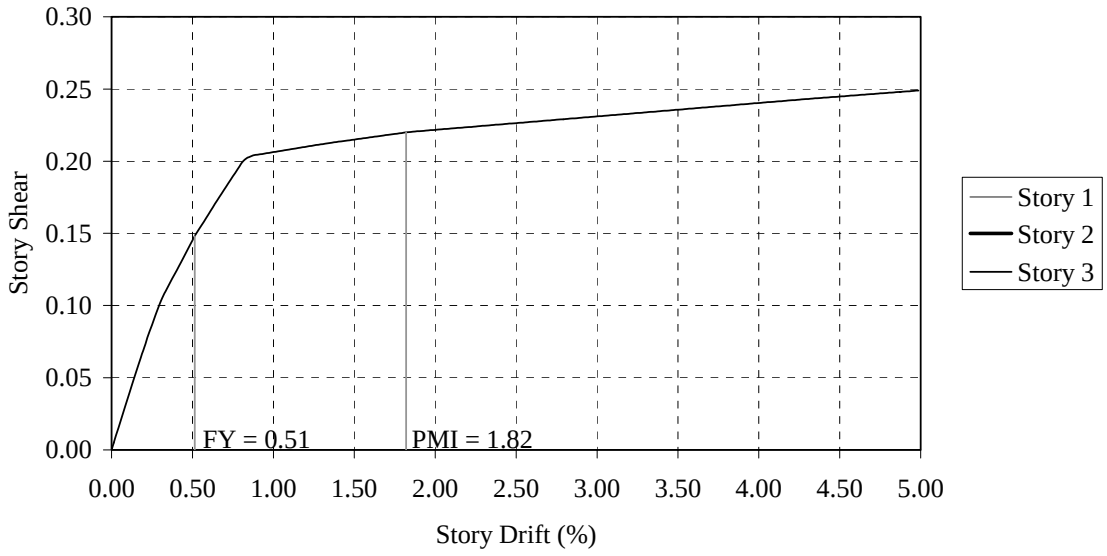

(d) Displacement Control – 10% on 3rd Story and 0% on 2nd Story

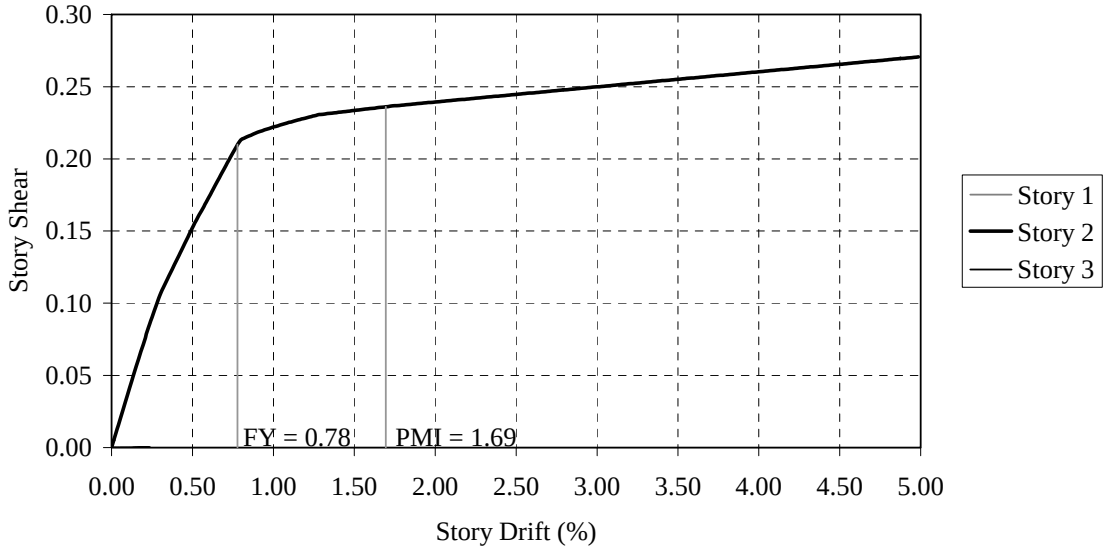

(e) Displacement Control – 10% on 2nd Story and 0% on 1st Story

FIGURE 23 (Continued)

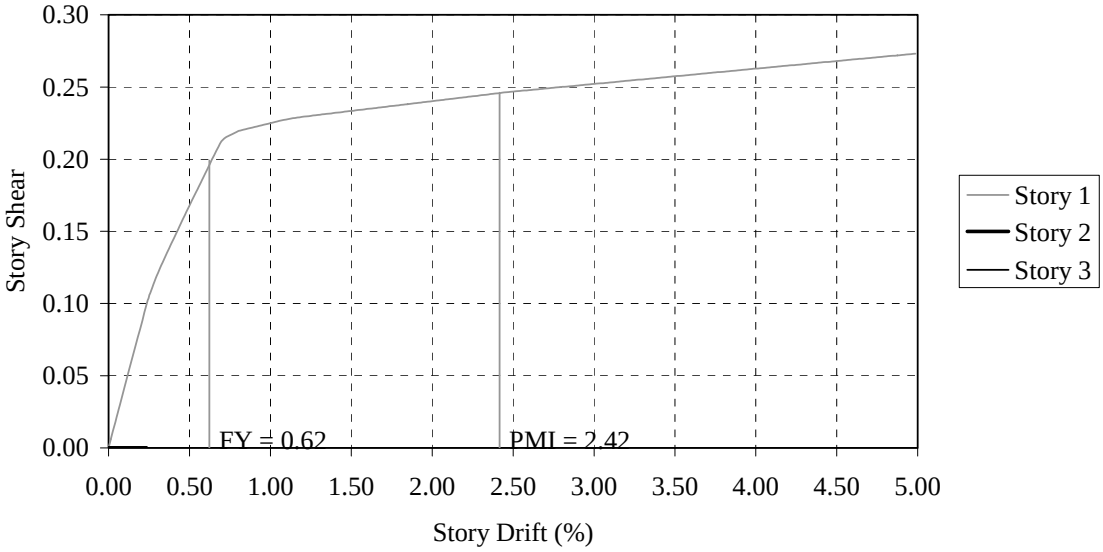

(f) Displacement Control – 10% on 1st Story

FIGURE 23 (Continued)

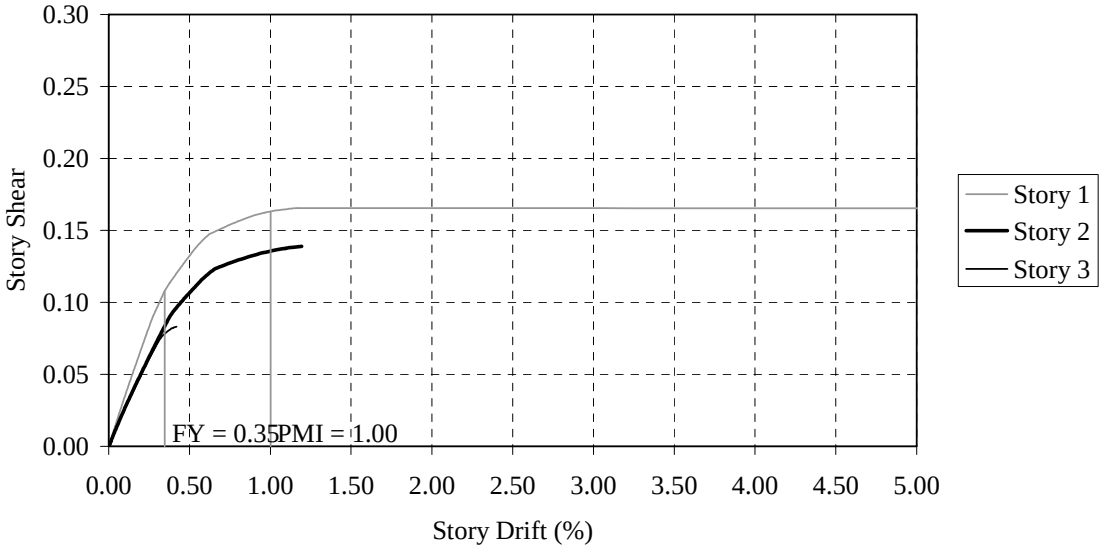

a) Force Control – Inverted Triangular Distribution

FIGURE 24 Pushover Results – With the Effects of P-Delta – C/B Ratio 1.2

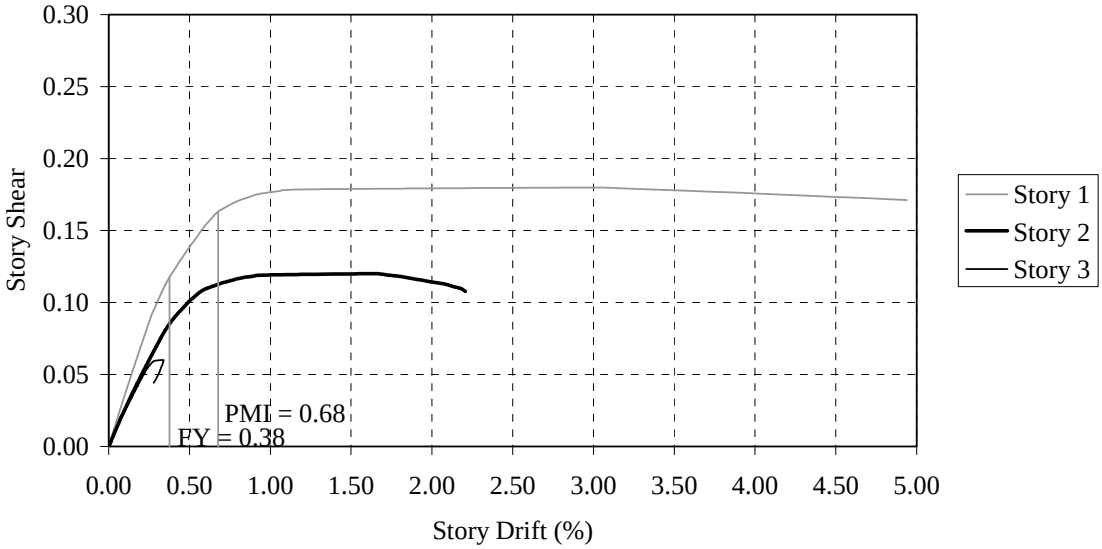

b) Force Control – Uniform Distribution

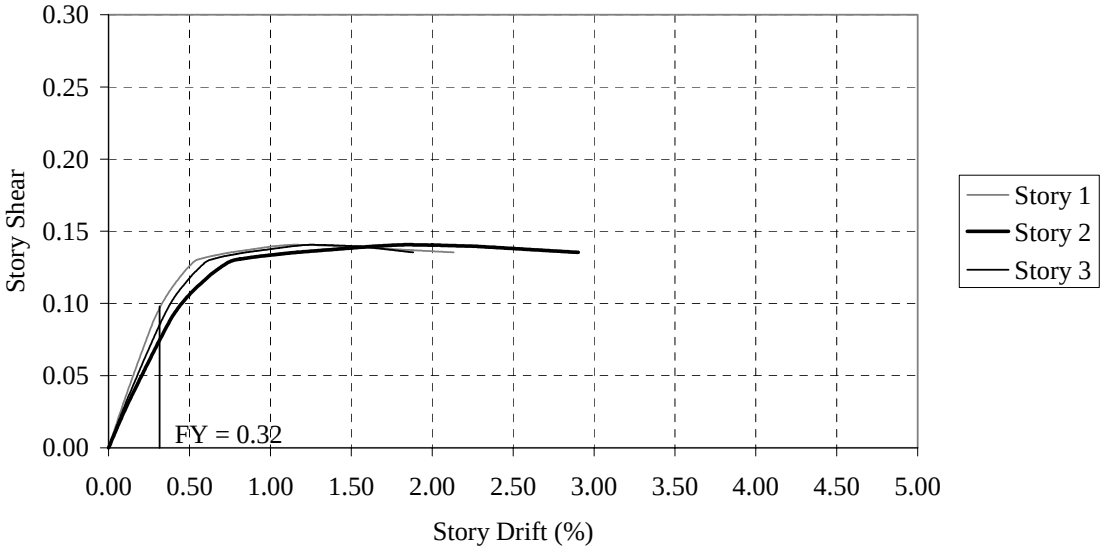

c) Displacement Control – 10% on 3rd Story

FIGURE 24 (Continued)

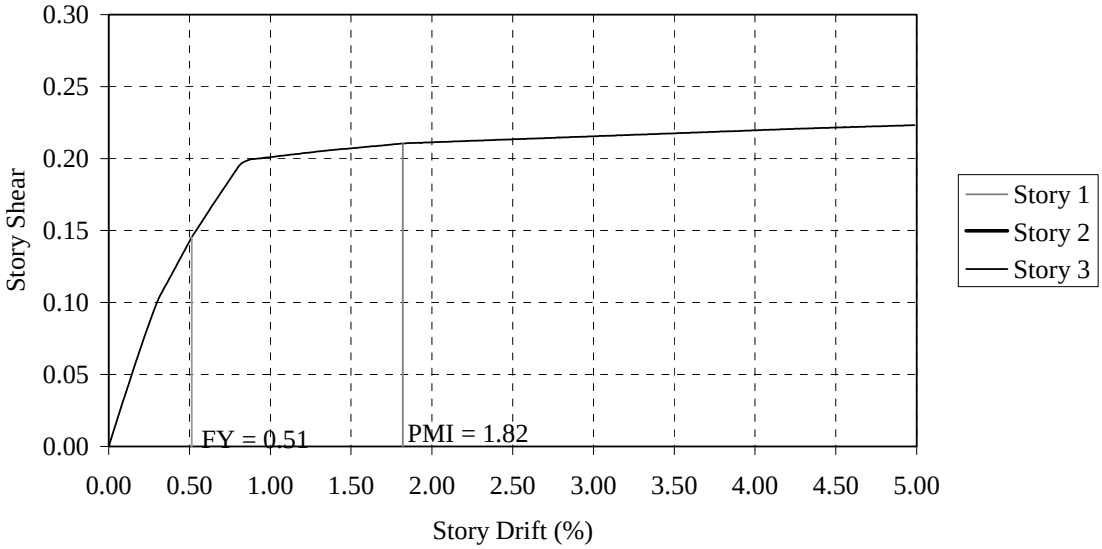

d) Displacement Control – 10% on 3rd Story and 0% on 2nd Story

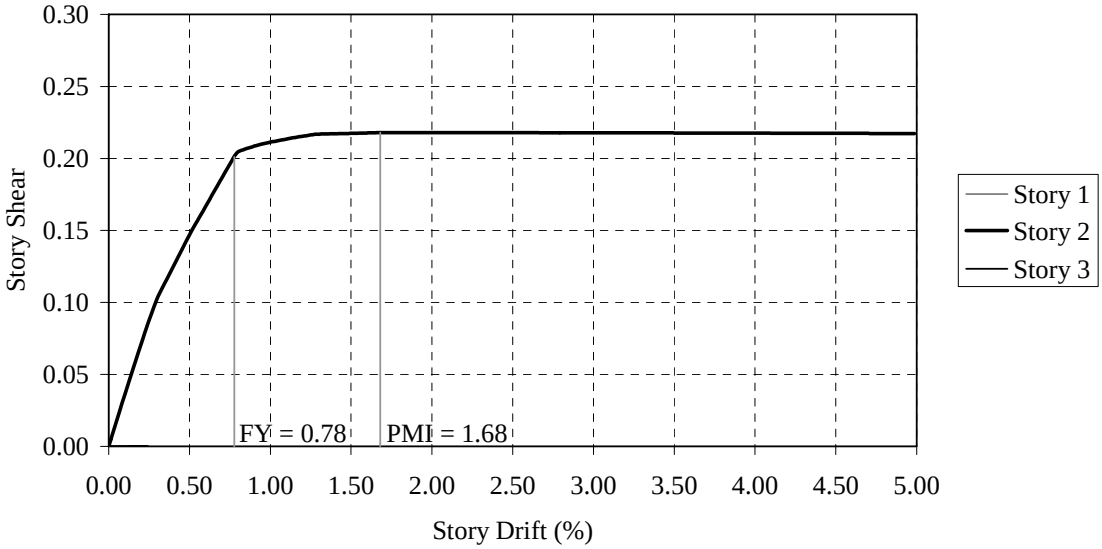

e) Displacement Control – 10% on 2nd Story and 0% on 1st Story

FIGURE 24 (Continued)

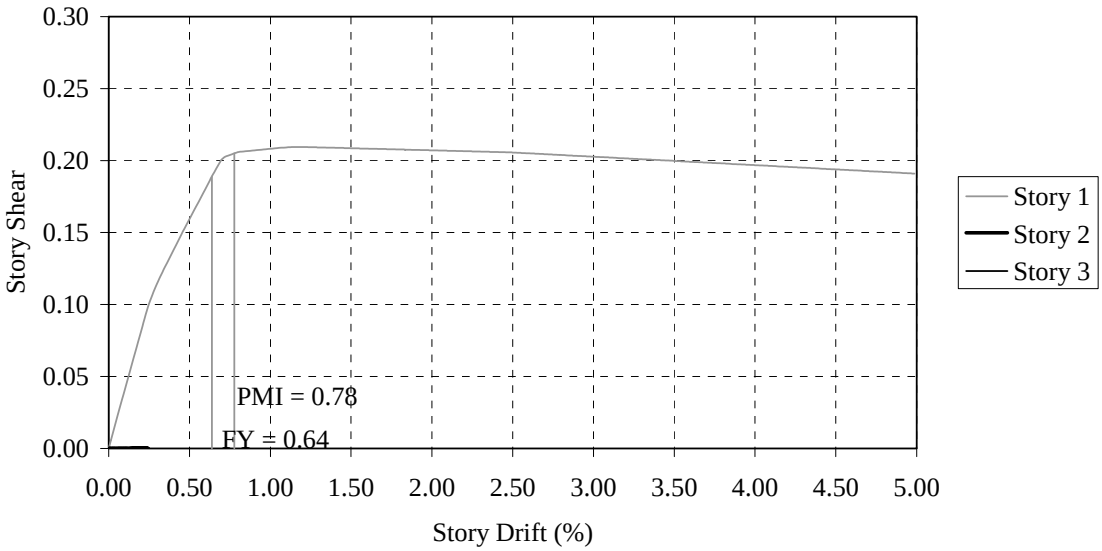

f) Displacement Control – 10% on 1st Story

FIGURE 24 (Continued)

Fig. 25 displays the pertinent yielding points for the retrofitted structure. The pushover charts displayed in Fig. 23 and 24 show that the behavior of the structure is no longer solely dominated by the first story. Therefore, Fig. 25 will display the mechanisms for each individual story in the structure.

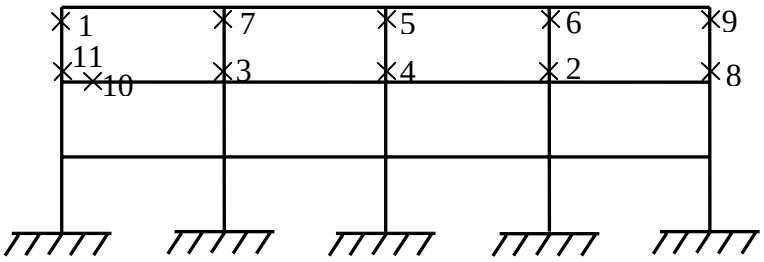

a) 10% on 3rd Story and 0% on 2nd Story - Yielding Points

FIGURE 25 Yielding Points - 1.2 Column-to-beam Strength Ratio

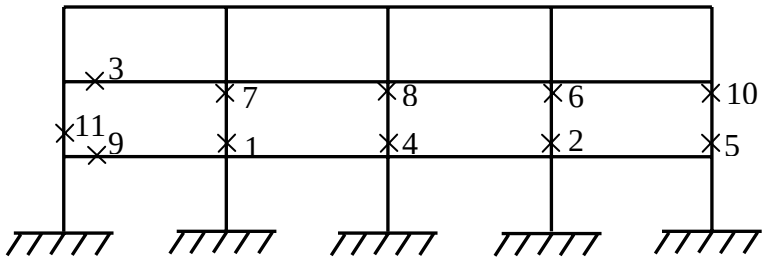

b) 10% on 2nd Story and 1st Story - Yielding Points

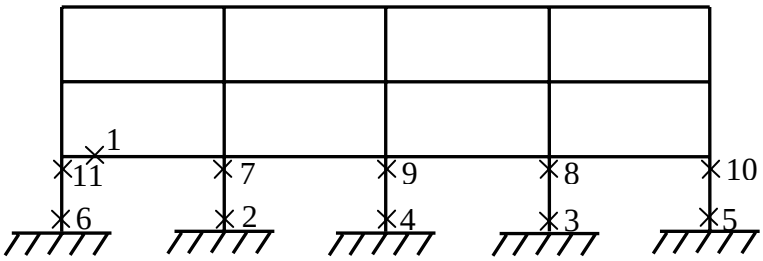

c) 10% on 1st Story - Yielding Points

FIGURE 25 (Continued)

The final type of analyses utilized in this research to determine the incipient collapse story capacity of the building structure was by incremental dynamic analyses. Charts displaying the correlation between these incipient collapse values and a lognormal distribution are displayed in Fig. 26. Fig. 26 once again shows a good correlation between the data obtained from analyses and a lognormal distribution. Fig. 26 displays all of the records on one chart only, since this is the information needed for calculation of the fragility curve. In the previous incremental dynamic analysis chapter another method of demonstrating the lognormal correlation was shown. Table 4 displays the β and λ capacity terms for the retrofitted structure with a column-to-beam strength ratio of 1.2.

TABLE 4 Capacity Factors - 1.2 Column-to-beam Strength Ratio

	FEMA-1%	FEMA-2%	FEMA-4%	Pushover-FY	Pushover-PMI	IDA
β_{ICC}	0.30	0.30	0.30	0.30	0.30	0.42
λ_{ICC}	0	0.69	1.39	-0.44	0.69	0.79

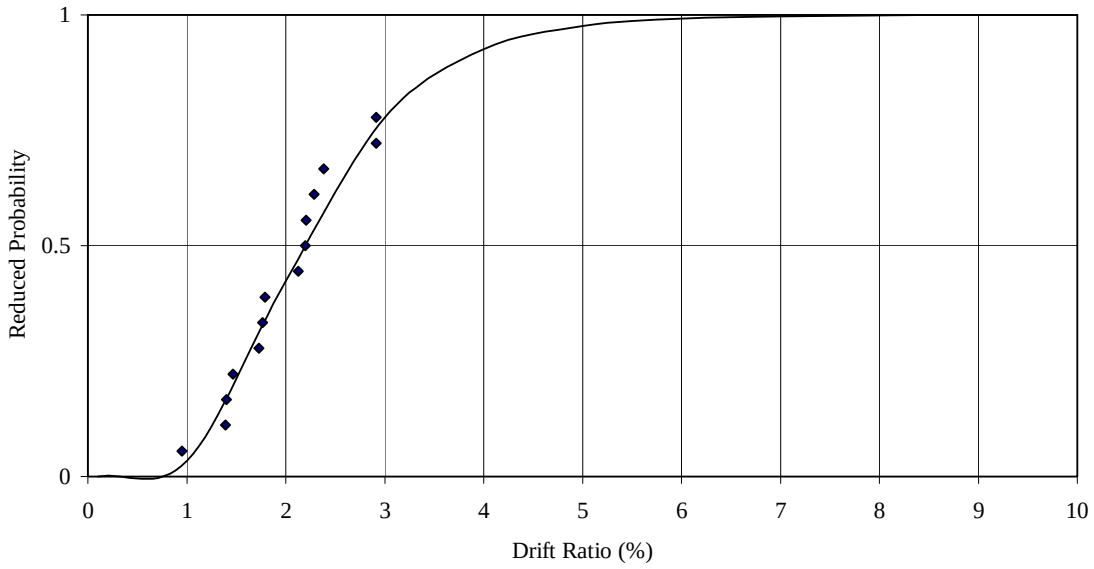

FIGURE 26 Incipient Collapse Points - 1.2 Column-to-beam Strength Ratio

SEISMIC DEMAND

To determine the seismic demand, non-linear time history dynamic analyses were utilized for the suite of ground motions including both 10% in 50 years probability of exceedance records and 2% in 50 years probability of exceedance records. Shown in Fig. 27 are the median drift values caused by each of these 19 ground motions. Shown in

Fig. 28 is the data correlating spectral acceleration and drift. The power law fit and corresponding equation are displayed in Fig. 28 and are necessary to create the previously discussed fragility curves.

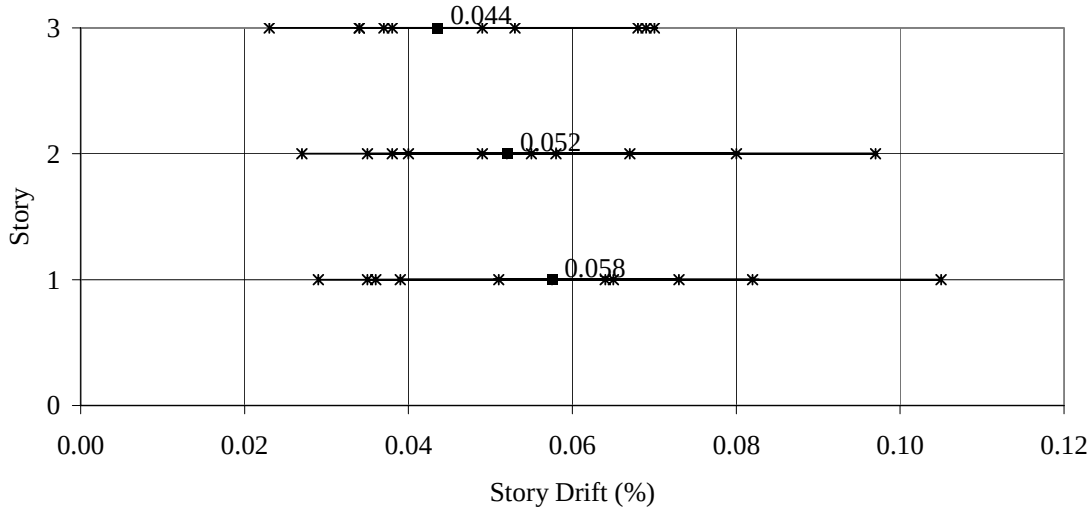

a) 10% in 50 Years Probability of Exceedance Earthquakes

FIGURE 27 Median Drift Values – C/B Ratio 1.2

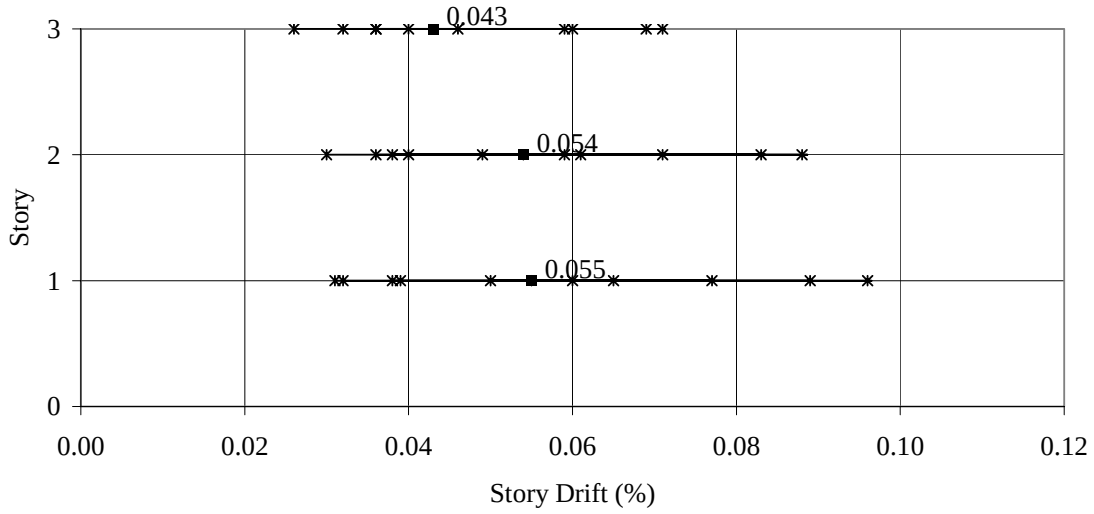

b) 10% in 50 Years Probability of Exceedance Earthquakes – With the Effects of P-Delta

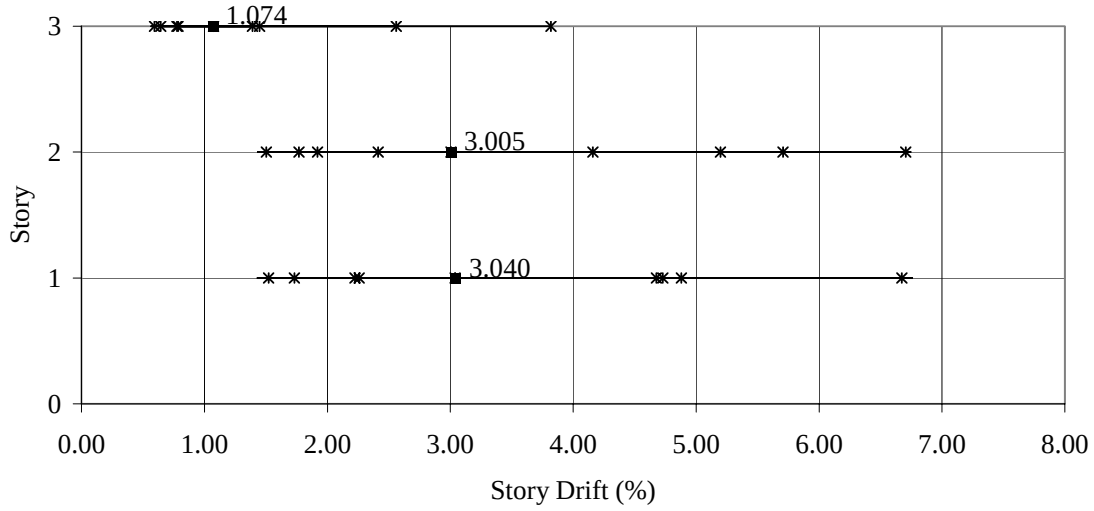

c) 2% in 50 Years Probability of Exceedance Earthquakes

FIGURE 27 (Continued)

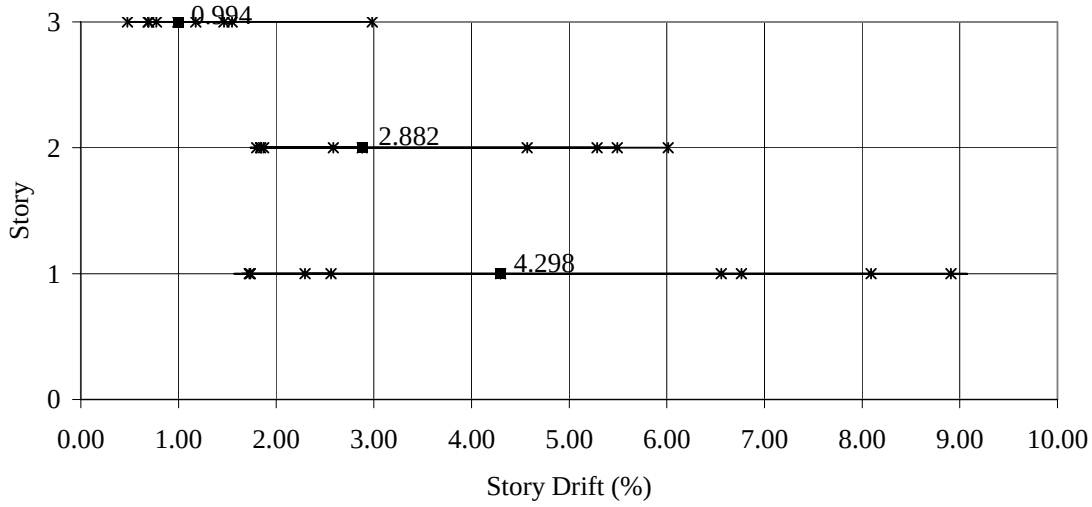

(d) 2% in 50 Years Probability of Exceedance Earthquakes – With the Effects of P-Delta

FIGURE 27 (Continued)

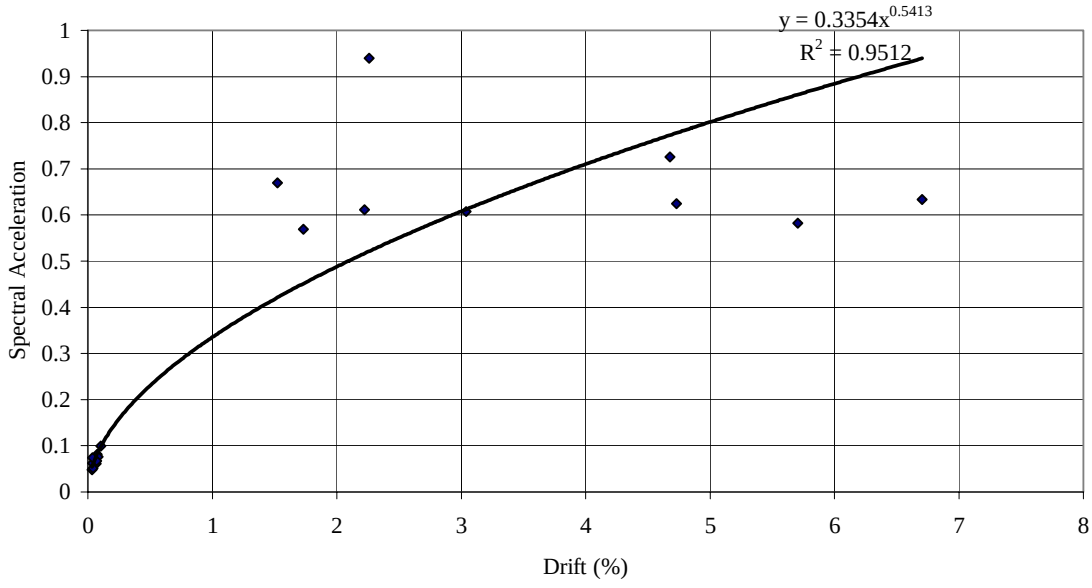

FIGURE 28 Spectral Acceleration vs. Drift – C/B Ratio 1.2

FRAGILITY CURVES

All of these analyses combine to create the required fragility curves. The types and methods of fragility curves created are discussed in the previous chapters. Fig. 29 displays the fragility curves obtained, neglecting the effects of p-delta. Once again the basis for comparisons between these limit states is the probability of exceedance at a spectral acceleration value of 0.74 g's. The probability of exceeding a limit state corresponding to a 1% drift is 93% for a drift level of 2% the probability of exceedance is 74%, for a 4% drift limitation the probability of exceedance is 42%, and for the incremental dynamic analysis the probability of exceedance is 69%. Shown in Fig. 30 are the same charts including the effects of p-delta. The probability of exceedance corresponding to the later figure is 96% for the 1% drift limit state, 85% for the 2% drift limit state, 54% for the 4% drift limit, and 73% for the incremental dynamic analysis. Fig. 29 also shows the fragility curves created by using the story capacities provided by both the pushover analyses and the incremental dynamic analyses. Excluding the effects of p-delta the probability of exceedance for first yield is 93% and 73% for plastic mechanism initiation. Including the effects of p-delta the probability of exceedance is 96% for first yield and 92% for plastic mechanism initiation.

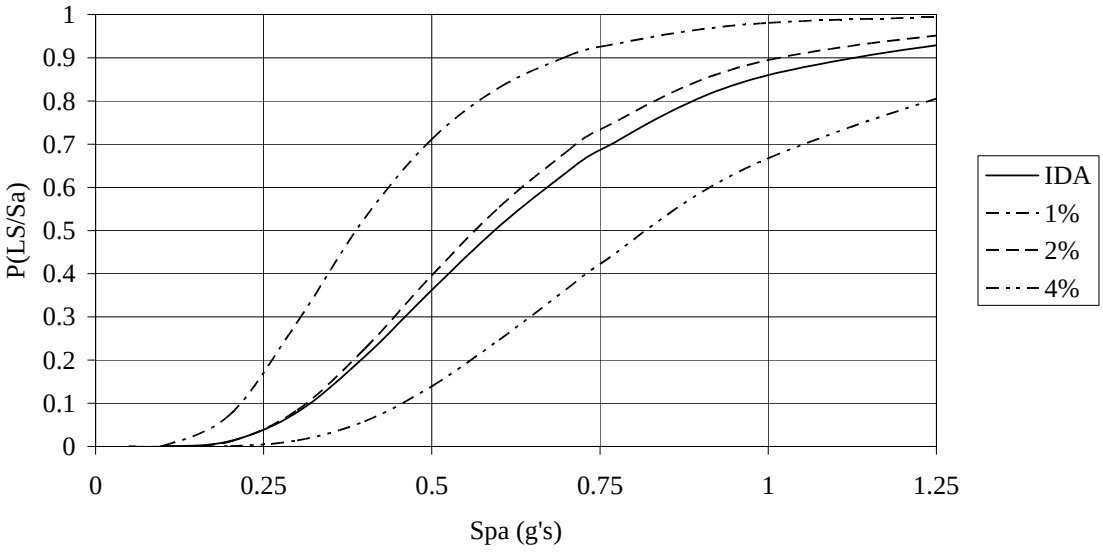

a) FEMA

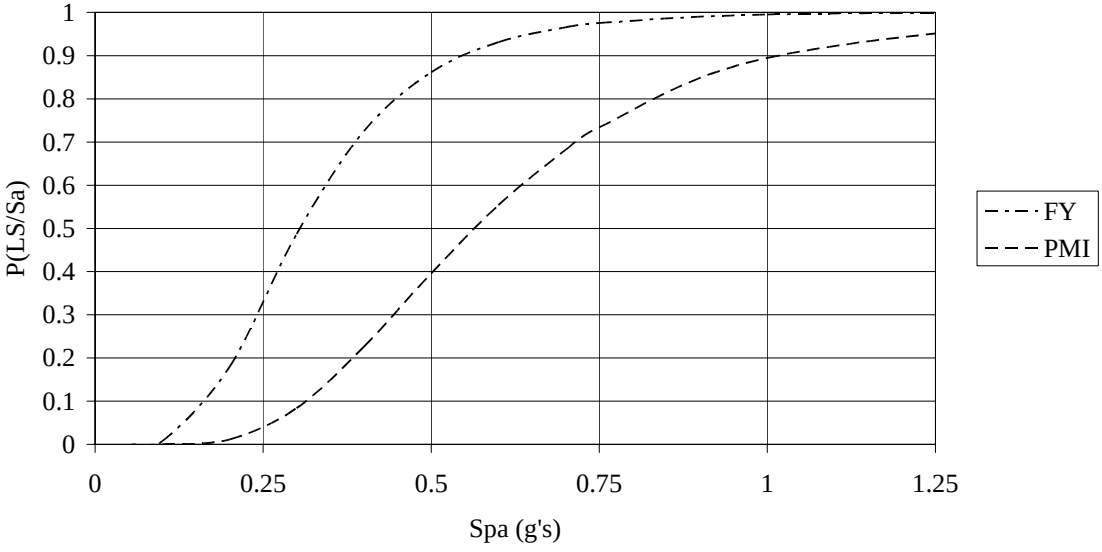

b) Pushover

FIGURE 29 Fragility Curves – C/B Ratio 1.2

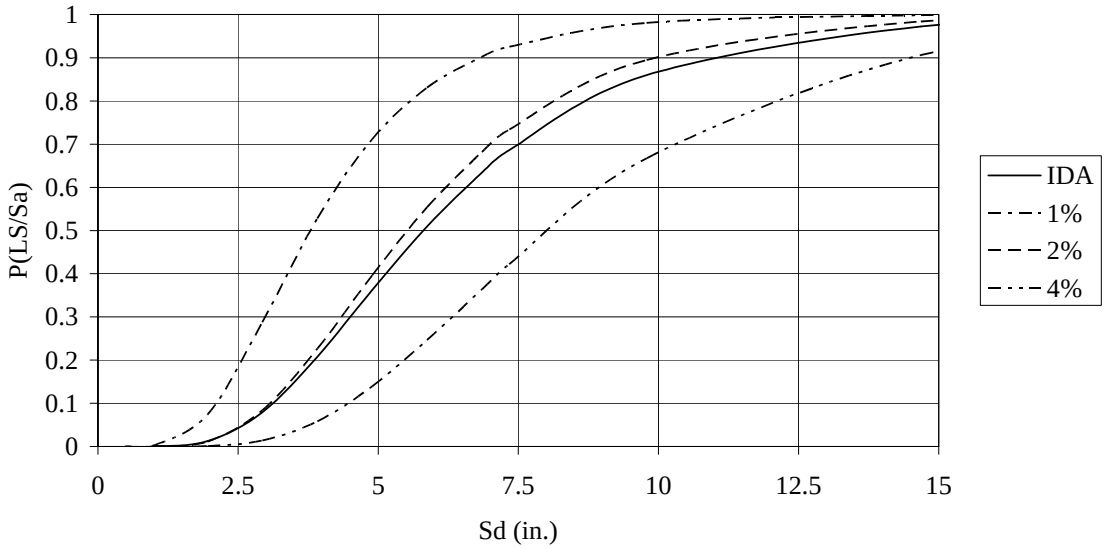

c) FEMA -Spectral Displacement

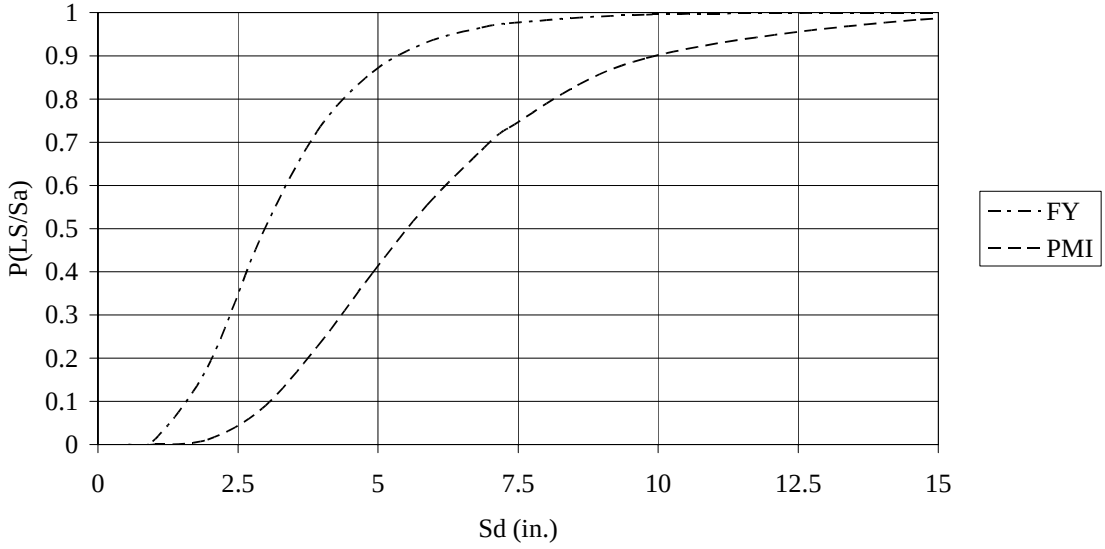

d) Pushover - Spectral Displacement

FIGURE 29 (Continued)

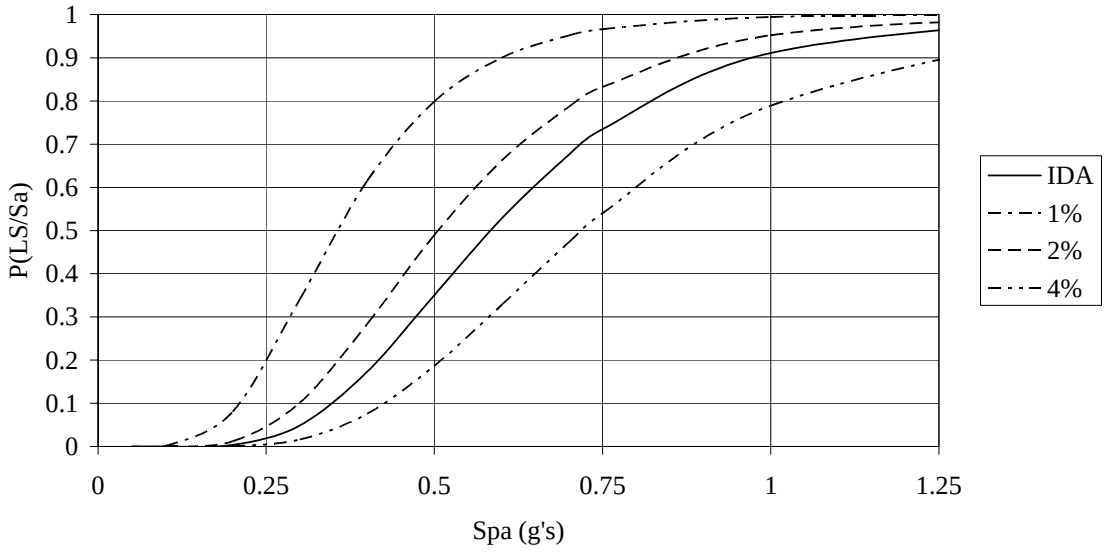

a) FEMA

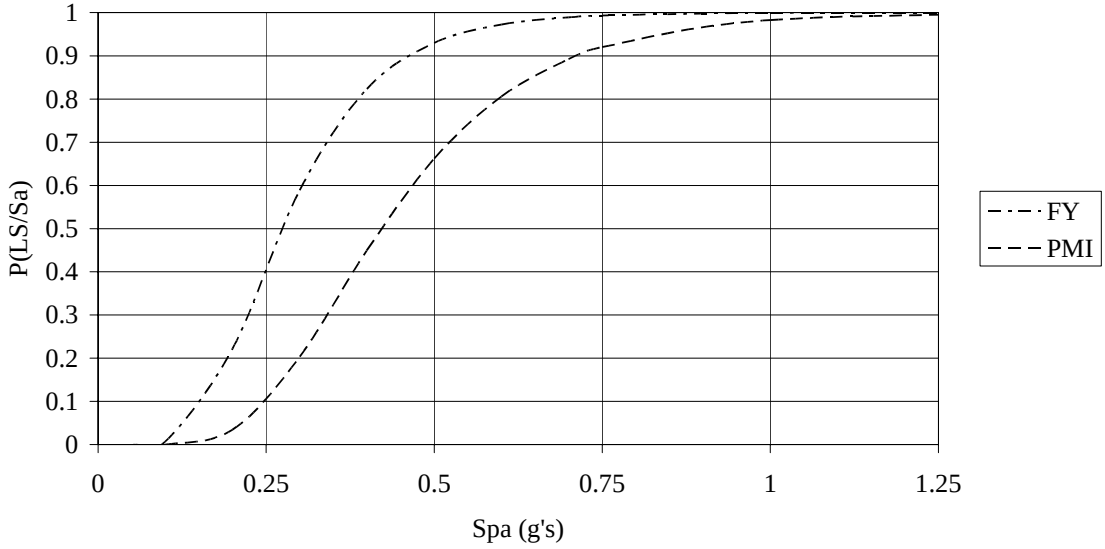

b) Pushover

FIGURE 30 Fragility Curves – With the Effects of P-Delta – C/B Ratio 1.2

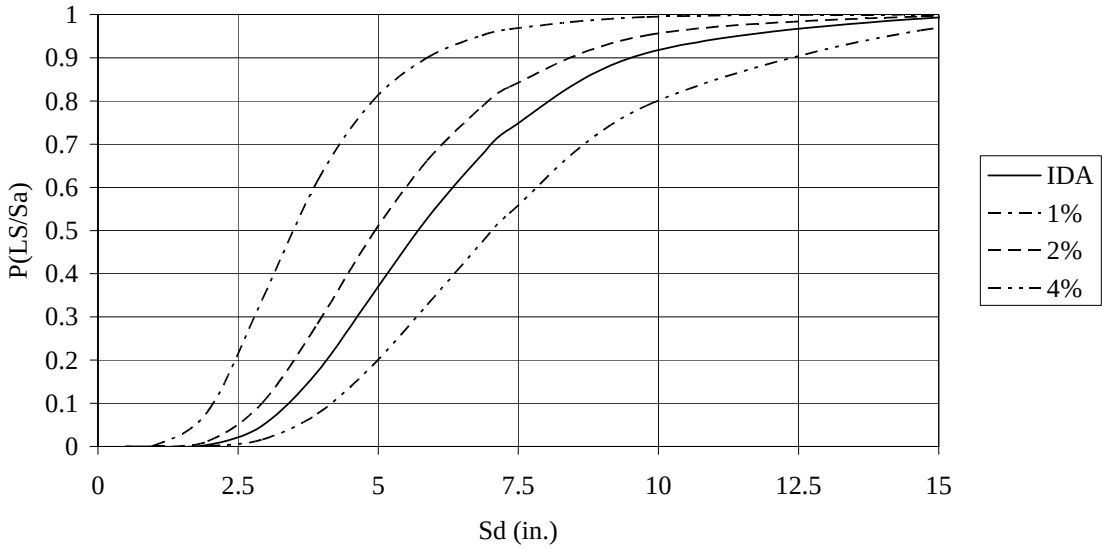

c) FEMA - Spectral Displacement

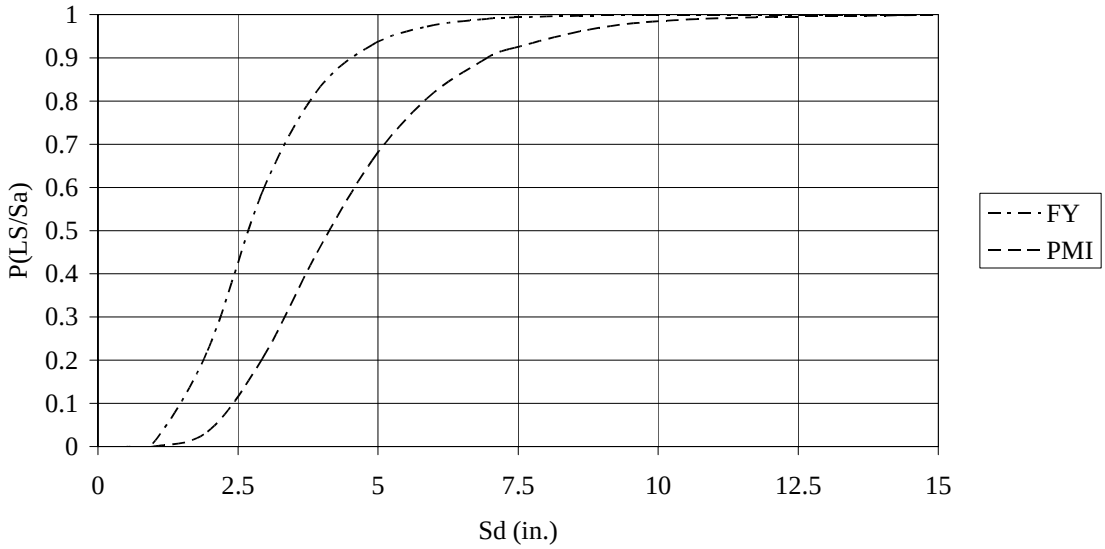

d) Pushover - Spectral Displacement

FIGURE 30 (Continued)

SUMMARY

This building performed better than the prototype structure as shown by the decreased probability of limit state exceedance, when neglecting the effects of p-delta. Including the effects of p-delta the probability of exceeding the defined limit states is similar to the originally designed building structure. It should be noted that the final FEMA limit state showed a large reduction in probability of exceedance. This means that the building would exceed the immediate occupancy and life safety limit but would have a lower probability of collapsing, making repair of the structure feasible. The decrease in probability of exceedance when neglecting the effects of p-delta means that under the design earthquake for the New Madrid region the structural damage occurring in this type of structure should be considerably less than that of the original structure. Therefore, this retrofit would improve the behavior of the modeled structure.

It should be noted that the limit state of strength degradation was not found to occur at any story of the structure under any loading condition. This means that under every loading condition the structure was found to survive and obtain some excess load resistance before collapse could occur.

The behavior of this retrofitted structure is superior to the behavior of the originally designed structure. Based on the research performed by Dooley and Bracci (2001) better performance can be obtained from a retrofit if the column-to-beam strength ratio is increased from the 1.2 value specified in the ACI code provisions to 1.8. The following chapter will investigate the feasibility of this further retrofit.

CHAPTER VIII
RETROFITTED STRUCTURE - 1.8 COLUMN-TO-BEAM STRENGTH RATIO

INTRODUCTION

As discussed in Chapter VI, the fragility curves for the prototype structure depicted the vulnerability of older reinforced concrete frame structures to earthquake ground motions representative of the New Madrid seismic zone. The 1.2 column-to-beam strength ratio discussed in the previous chapter is the column-to-beam strength ratio currently required by the ACI building code provisions. The research done by Dooley and Bracci (Dooley 2001) suggests that structures with a 1.8 column-to-beam strength ratio perform better than structures following the ACI building code provisions minimum requirements. For this reason, it was decided that the originally designed structure would once again be altered to have a column-to-beam strength ratio of 1.8. As in the previous chapter the column-to-beam strength was altered by changing the strength of the columns while leaving the strength of the beams as originally designed.

STORY CAPACITIES

The FEMA limit states were again utilized to define one set of story capacities. These FEMA limit states are 1%, 2%, and 4% for Immediate Occupancy, Life Safety, and Collapse Prevention. Incipient collapse capacity was also defined using the incremental dynamic analyses, shown in Fig. 31.

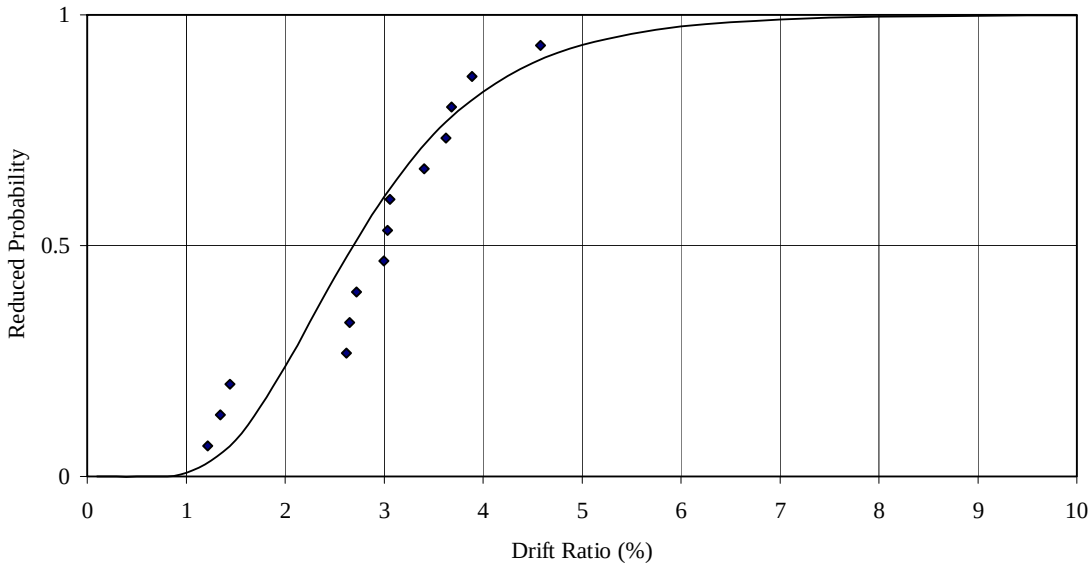

a) Lognormal Fit

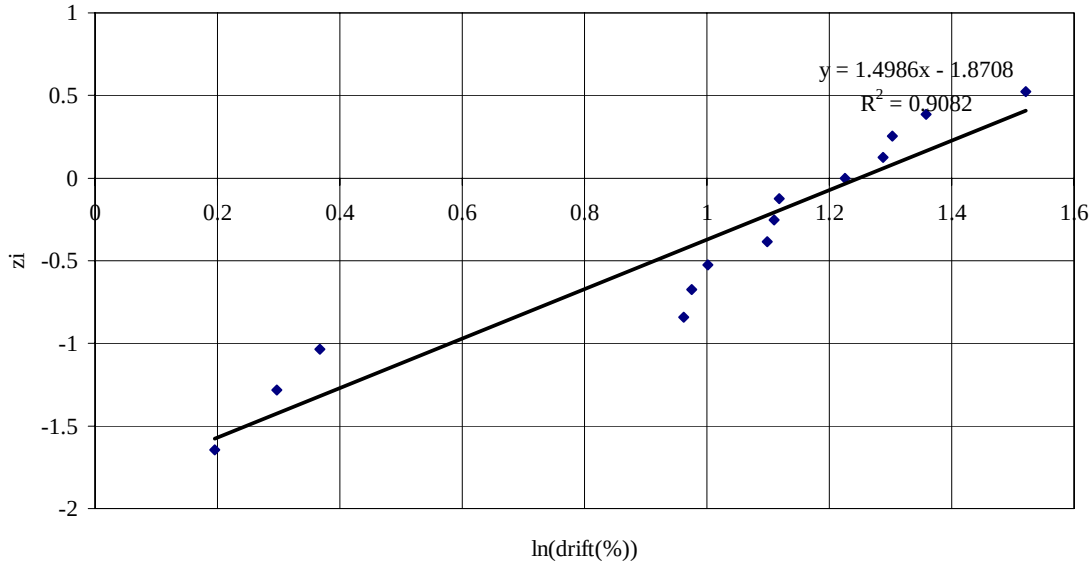

b) Log Graphs

FIGURE 31 Incipient Collapse Points - 1.8 Column-to-beam Strength Ratio

The pushover analyses were used in order to obtain first yield and plastic mechanism initiation. These pushover analyses were run, both including and neglecting the effects of p-delta. Excluding the effects of p-delta the limit state for first yield was found to be 0.6% drift. For plastic mechanism initiation the limit state was found to be 4.5% drift. This value was obtained from only two of the pushover analyses. As already discussed only the pushover analyses forcing a mechanism into an individual story are utilized for determining the limit states, in this case only two of these runs was found to reach plastic mechanism initiation. This third run does not form a mechanism when loaded and therefore does not reach this second limit state. This means that the lateral load resistance of the structure is substantially greater. Including the effects of p-delta we find that the first yield limit state is defined as 0.6% drift and that the plastic mechanism initiation limit state is 2.7% drift. This second limit state is obtained from only two of the pushover runs. The remaining two pushover analyses vary greatly in the plastic mechanism initiation value when including the effects of p-delta. The run that lowers the drift limit value is the pushover analysis that places all of the lateral loading onto the first story of the structure and has a plastic mechanism initiation value of 1.1% drift. This means that the first story of the structure is still substantially weaker than the other stories of the structure. This is only found in the p-delta analyses because of the added moment that must be resisted by the first story of a structure once these effects are added. The results obtained from the pushover analyses are displayed in Figs. 32 and 33. These figures display results both including and excluding the effects of p-delta.

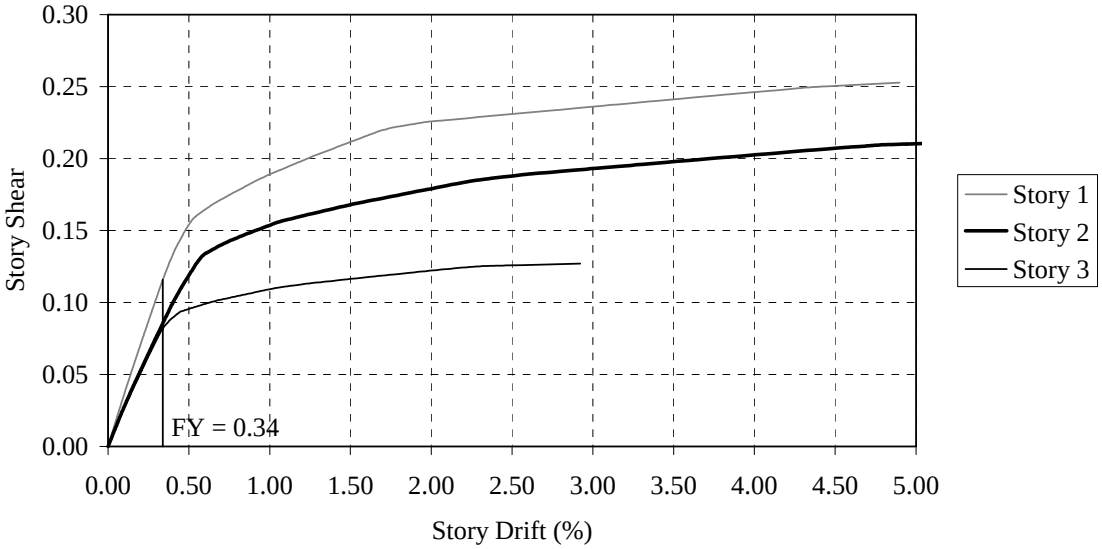

a) Force Control – Inverted Triangular Distribution

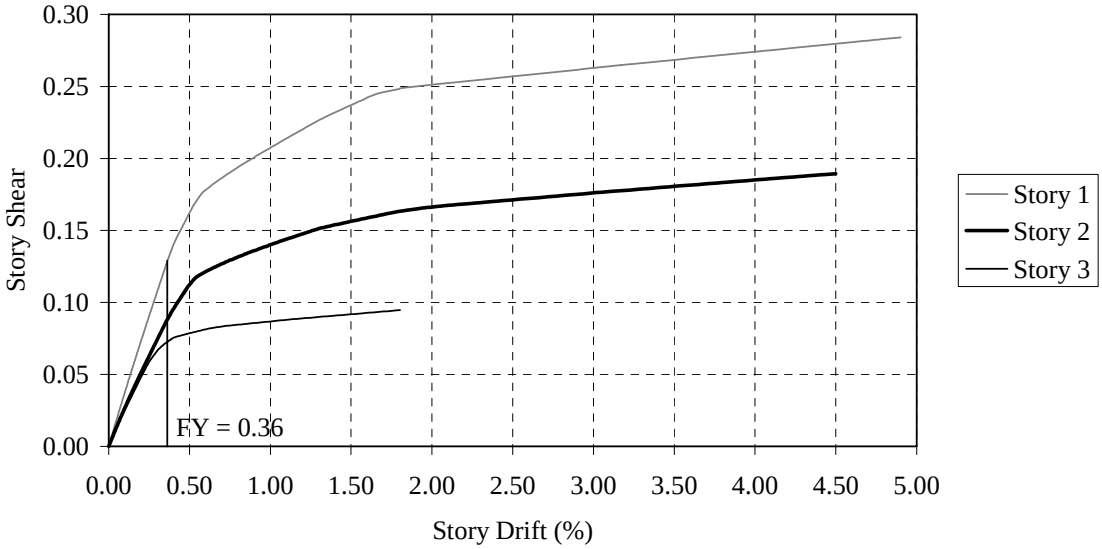

b) Force Control – Uniform Distribution

FIGURE 32 Pushover Results – C/B Ratio 1.8

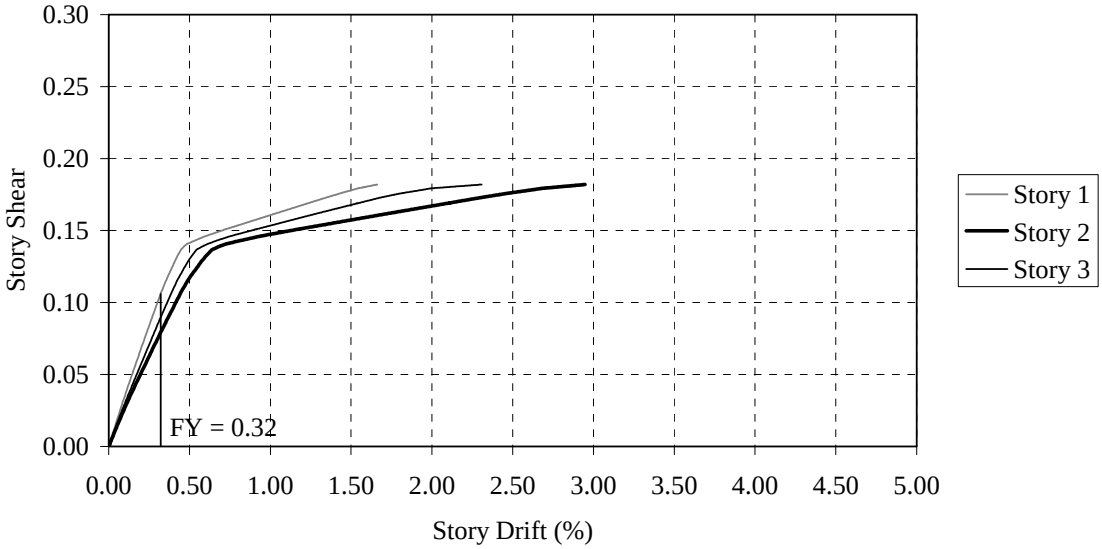

c) Displacement Control – 10% on 3rd Story

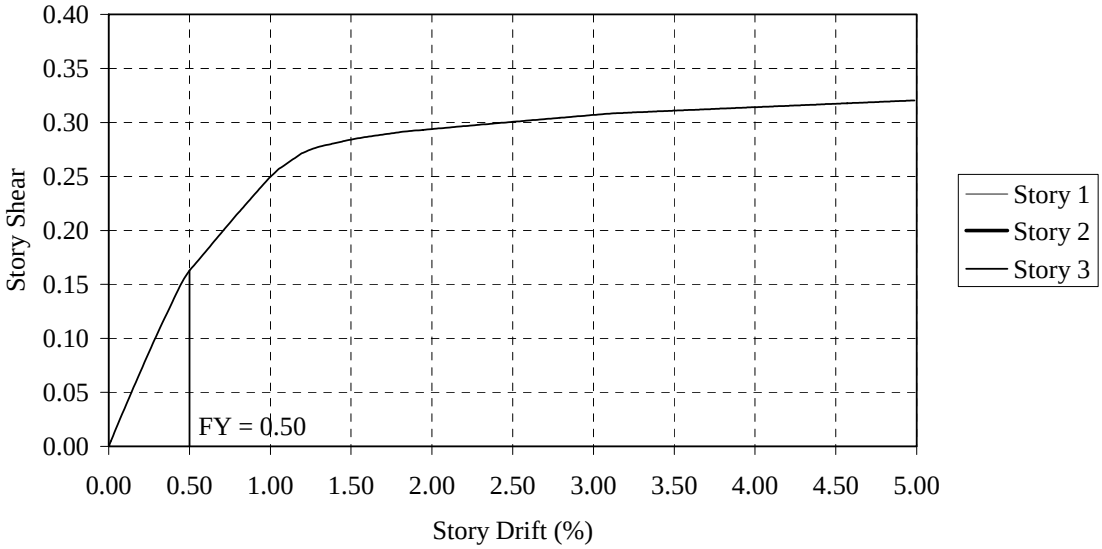

d) Displacement Control – 10% on 3rd Story and 0% on 2nd Story

FIGURE 32 (Continued)

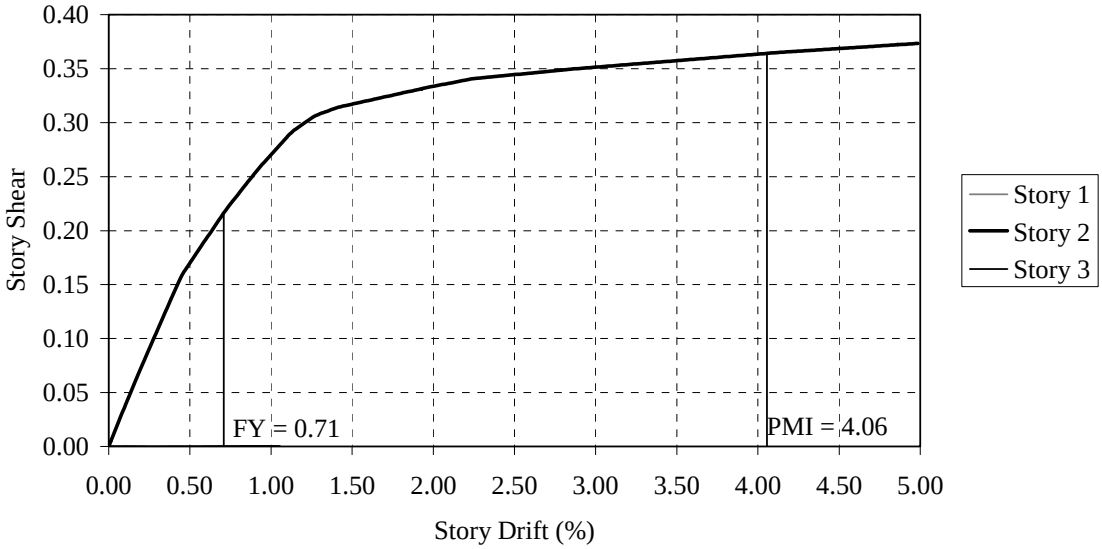

e) Displacement Control – 10% on 2nd Story and 0% on 1st Story

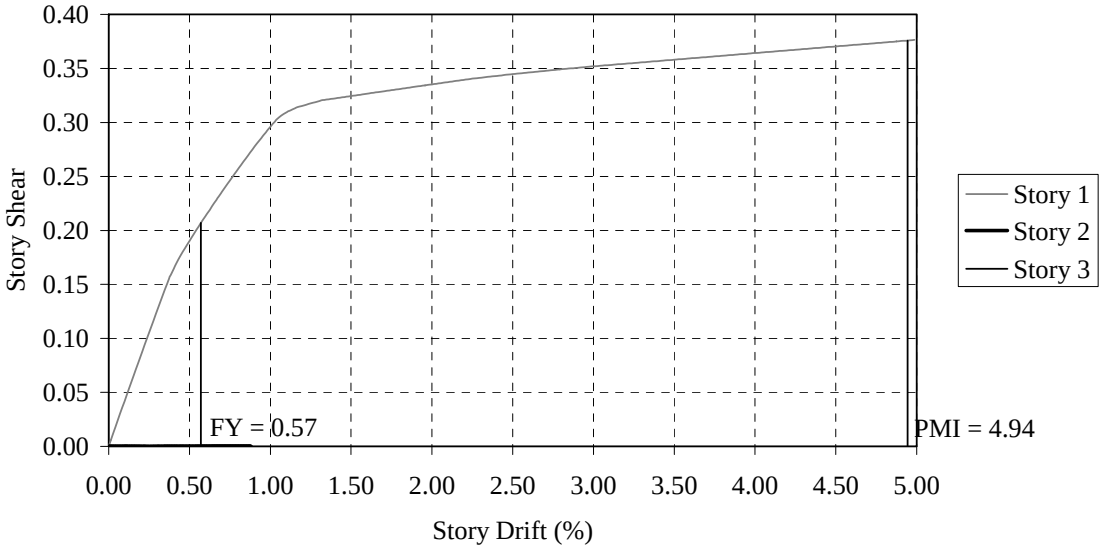

f) Displacement Control – 10% on 1st Story

FIGURE 32 (Continued)

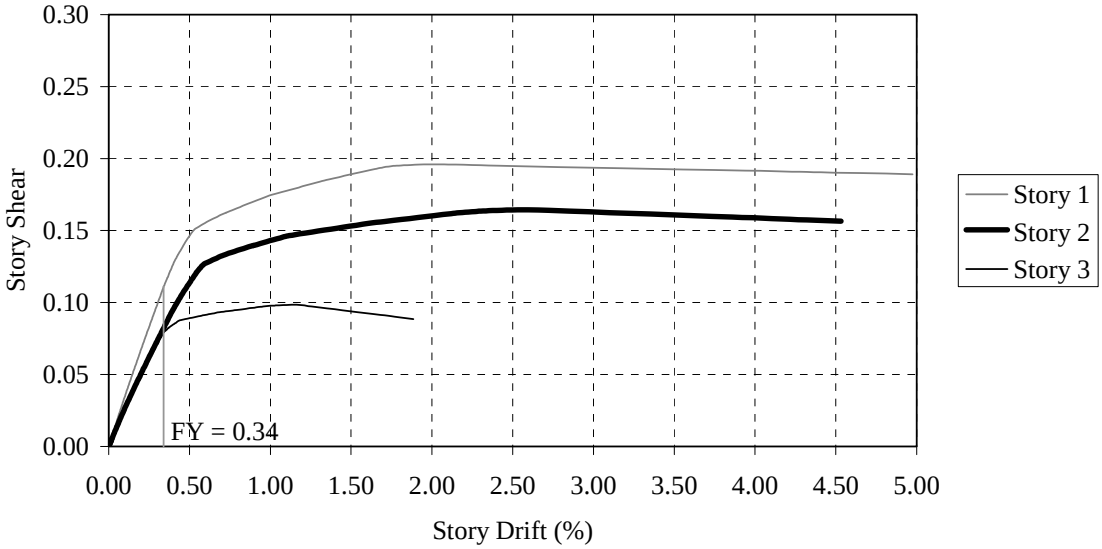

a) Force Control – Inverted Triangular Distribution – With the Effects of P-Delta

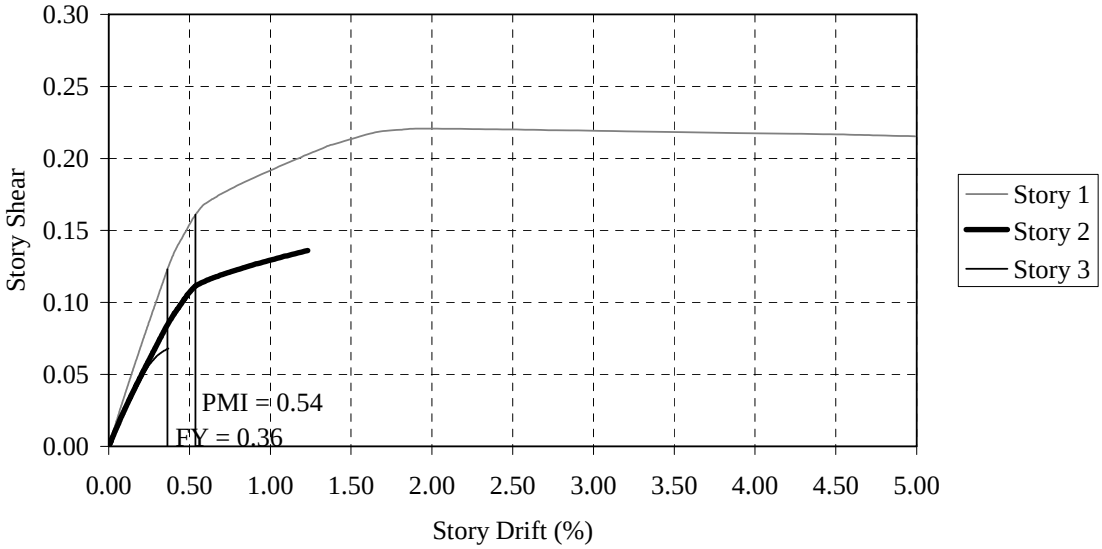

b) Force Control – Uniform Distribution – With the Effects of P-Delta

FIGURE 33 Pushover Results – C/B Ratio 1.8 – With the Effects of P-Delta

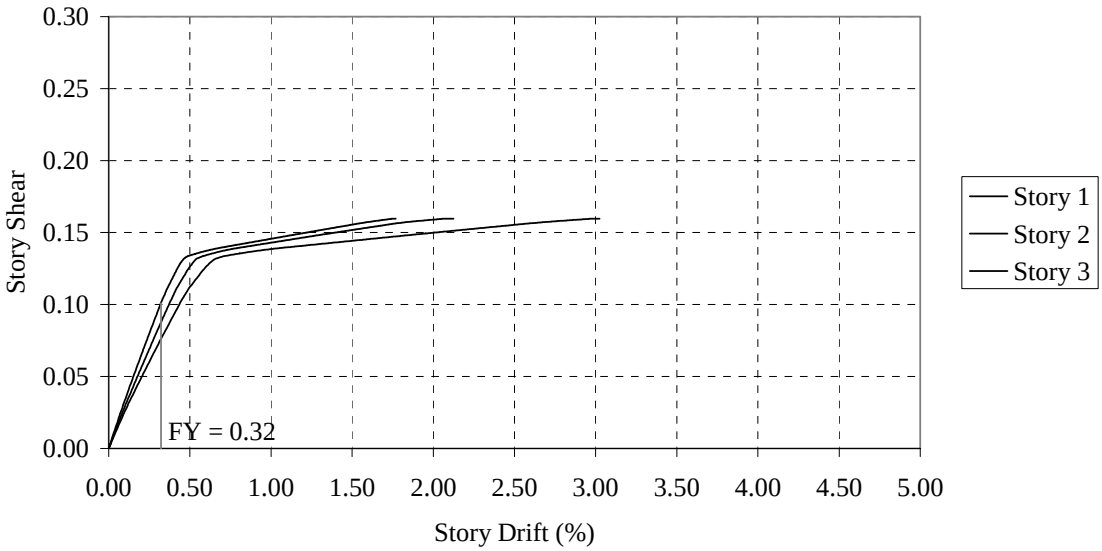

c) Displacement Control – 10% on 3rd Story – With the Effects of P-Delta

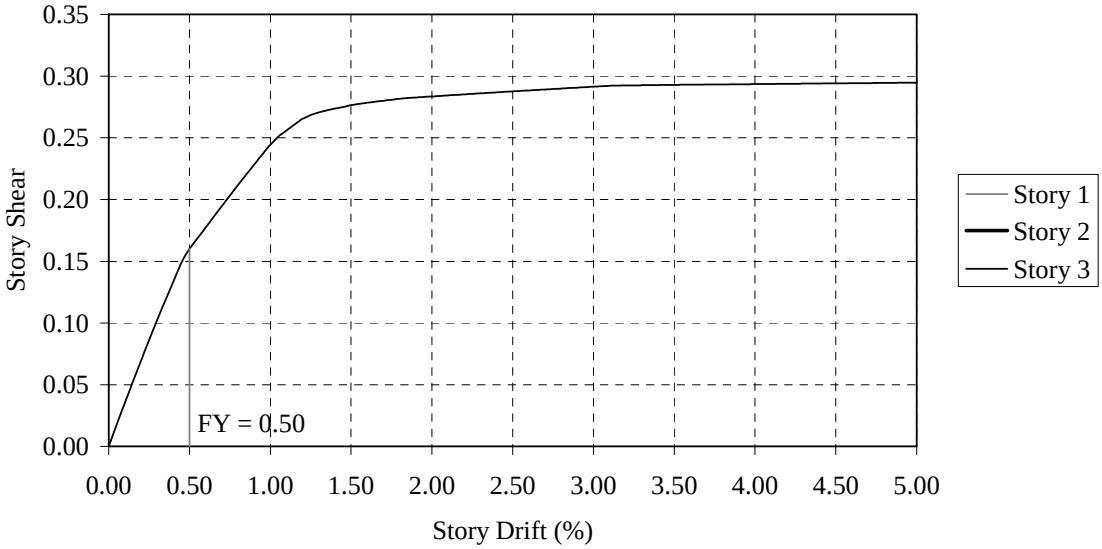

d) Displacement Control – 10% on 3rd Story and 0% on 2nd Story – With the Effects of P-Delta

FIGURE 33 (Continued)

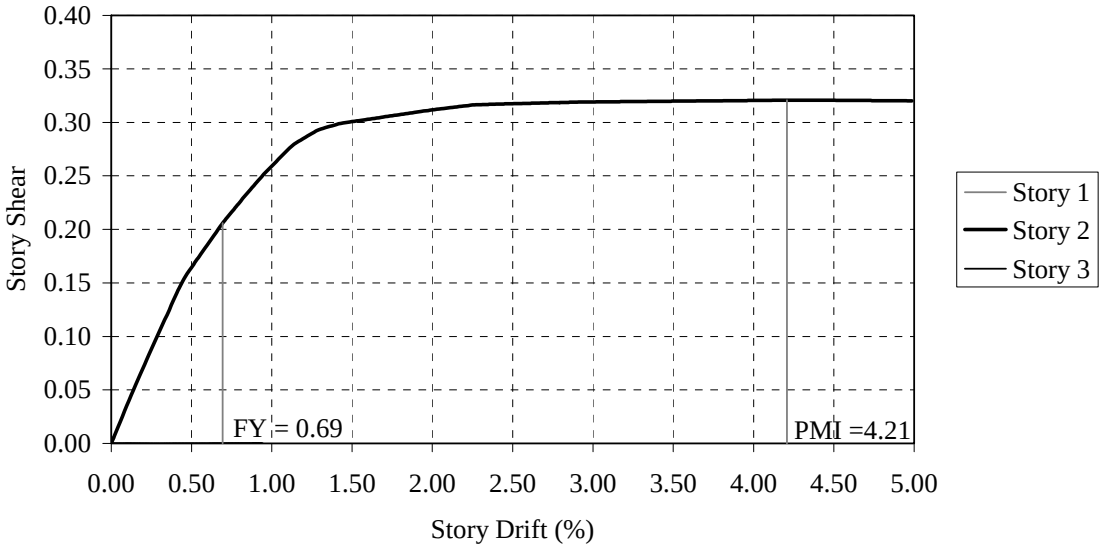

e) Displacement Control – 10% on 2nd Story and 0% on 1st Story – With the Effects of P-Delta

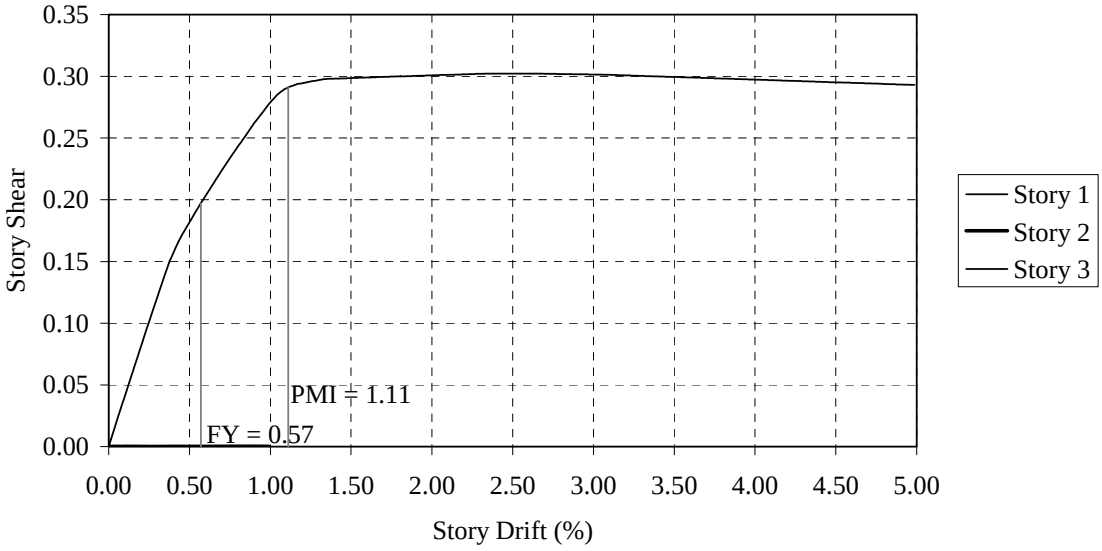

f) Displacement Control – 10% on1st Story – With the Effects of P-Delta

FIGURE 33 (Continued)

TABLE 5 Capacity Factors - 1.8 Column-to-beam Strength Ratio

	FEMA-1%	FEMA-2%	FEMA-4%	Pushover-FY	Pushover-PMI	IDA
β_{ICC}	0.30	0.30	0.30	0.30	0.30	0.34
λ_{ICC}	0	0.69	1.39	-0.51	1.50	1.10

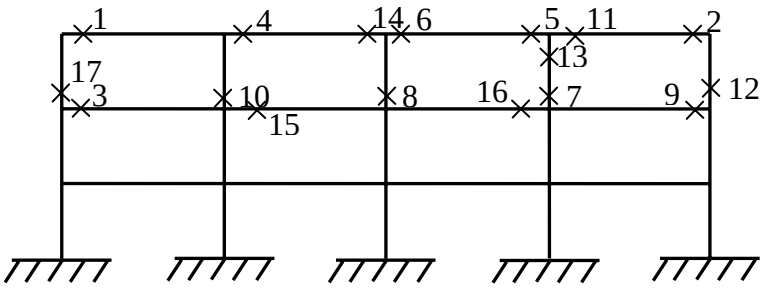

a) 10% on 3rd Story and 0% on 2nd Story - Yielding Points

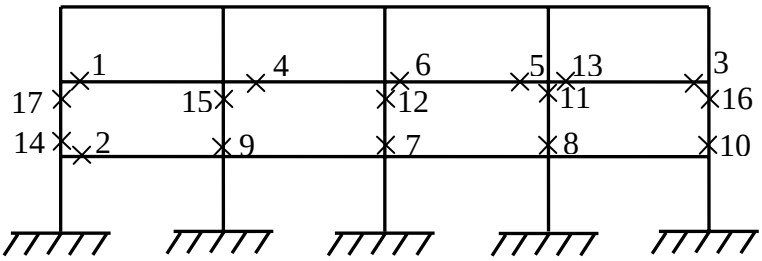

b) 10% on 2nd Story and 0% on 1st Story - Yielding Points

FIGURE 34 Yielding Points - 1.8 Column-to-beam Strength Ratio

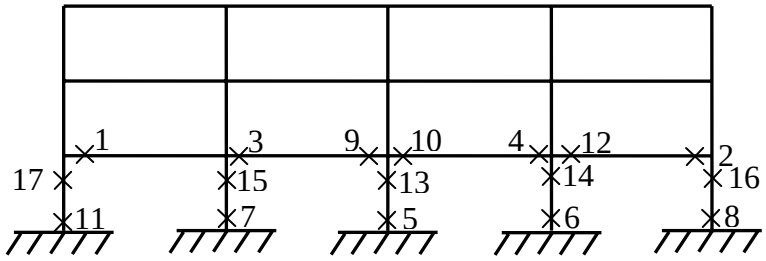

c) 10% on 1st Story - Yield Points

FIGURE 34 (Continued)

Shown in Fig. 34 are the yielding points for the retrofitted structure with a 1.8 column-to-beam strength ratio. This figure shows more members yielding throughout the structure before a failure mechanism occurs. Many of the members shown to yield are beam members, the behavior desired in a lateral load resisting situation.

SEISMIC DEMAND

The seismic demand was determined by using both the 2% in 50 years probability of exceedance ground motion records and the 10% in 50 years probability of exceedance ground motion records in conjunction with non-linear time history dynamic analyses. These analyses utilize the 19 ground motion records to estimate the drift that these ground motions will cause on the designed building. These drift values are displayed in Fig. 35. Also displayed in these figures are the median drift values necessary to create the required fragility curves.

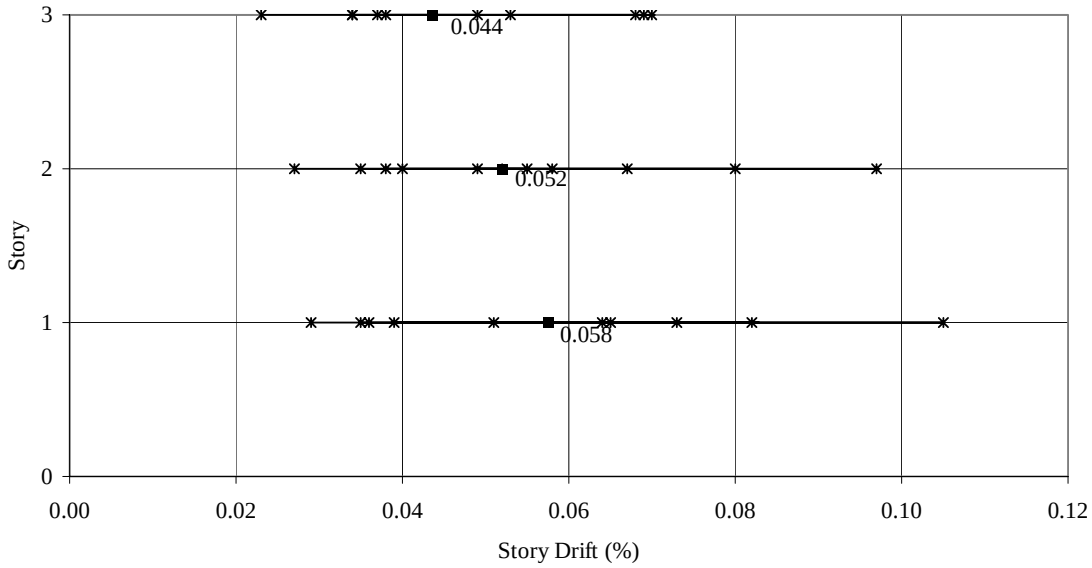

a) 10% in 50 Years Probability of Exceedance– C/B Ratio 1.8

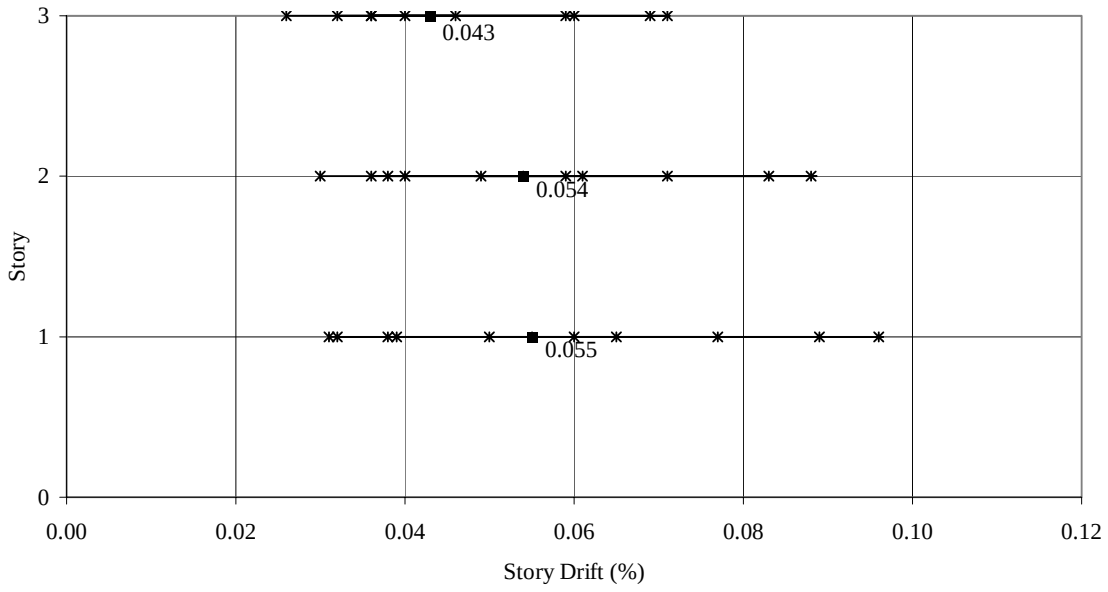

b) 10% in 50 Years Probability of Exceedance– With the Effects of P-Delta - C/B Ratio 1.8

FIGURE 35 Median Drift Values – C/B Ratio 1.8

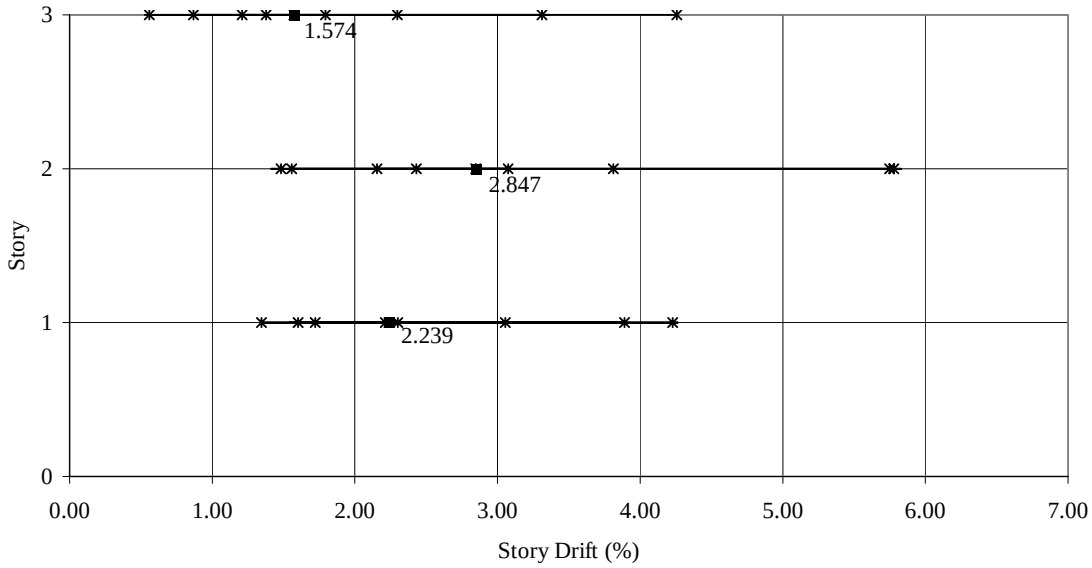

c) 2% in 50 Years Probability of Exceedance

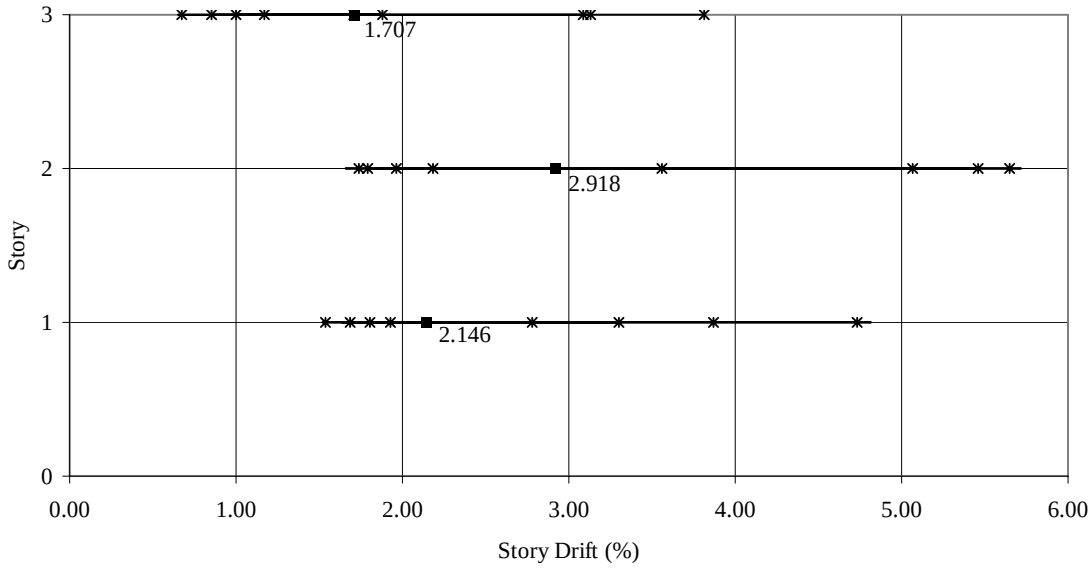

d) 2% in 50 Years Probability of Exceedance– With the Effects of P-Delta

FIGURE 35 (Continued)

FRAGILITY CURVES

With all of the necessary inputs obtained, the results are combined to create the fragility curves desired. These fragility curves were calculated following the same procedures already outlined and utilized for the previous two buildings. The same fragility curves were created and are displayed in Fig. 36 and Fig. 37

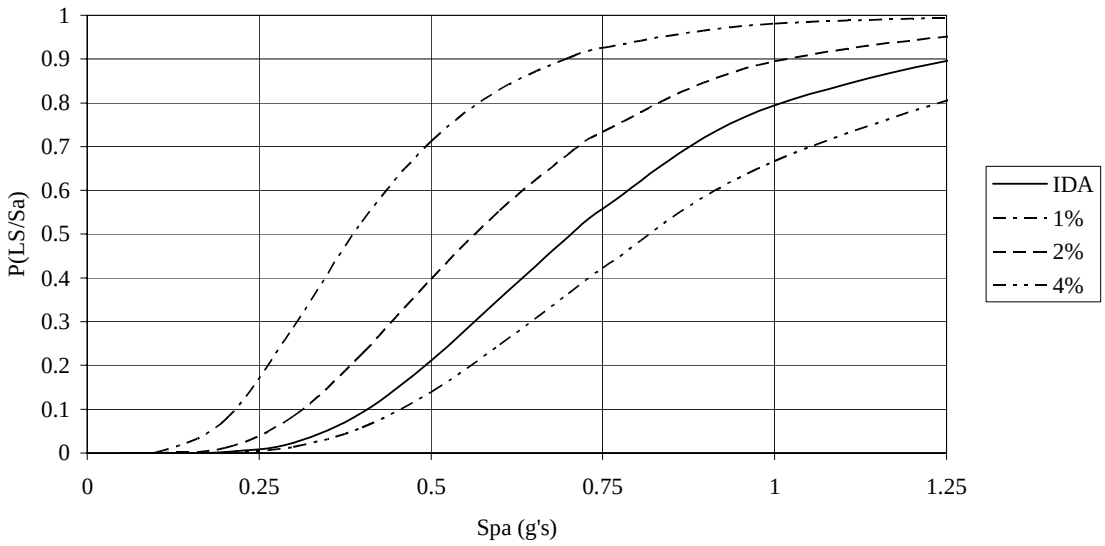

(a) FEMA

FIGURE 36 Fragility Curves – C/B Ratio 1.8

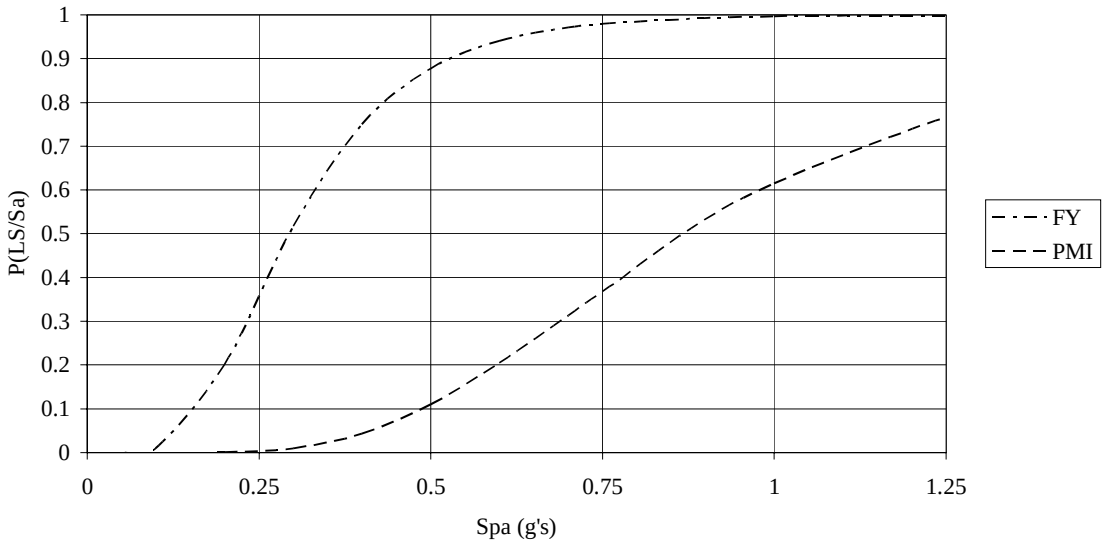

(b) Pushover

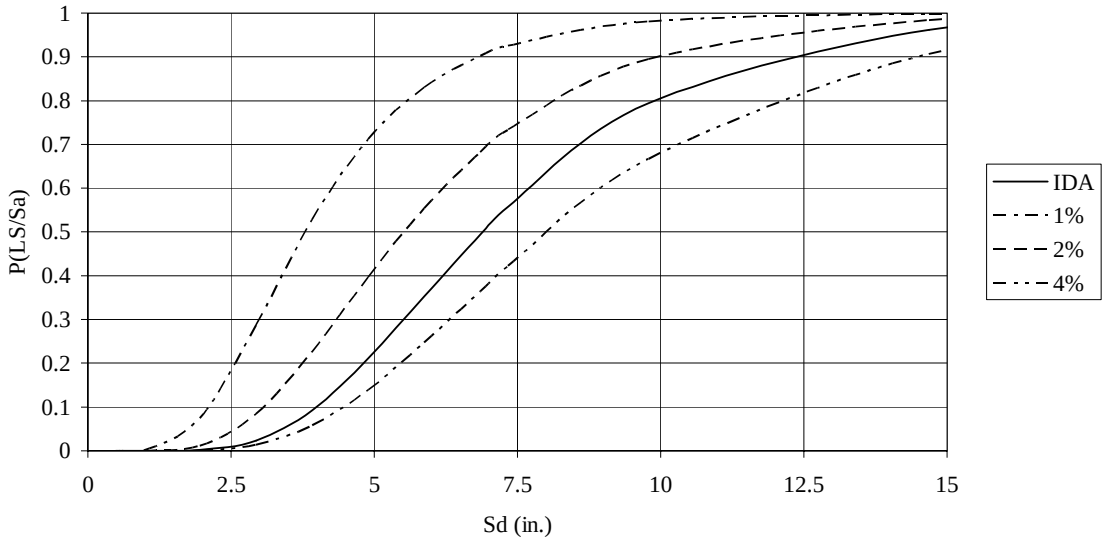

c) FEMA - Spectral Displacement

FIGURE 36 (Continued)

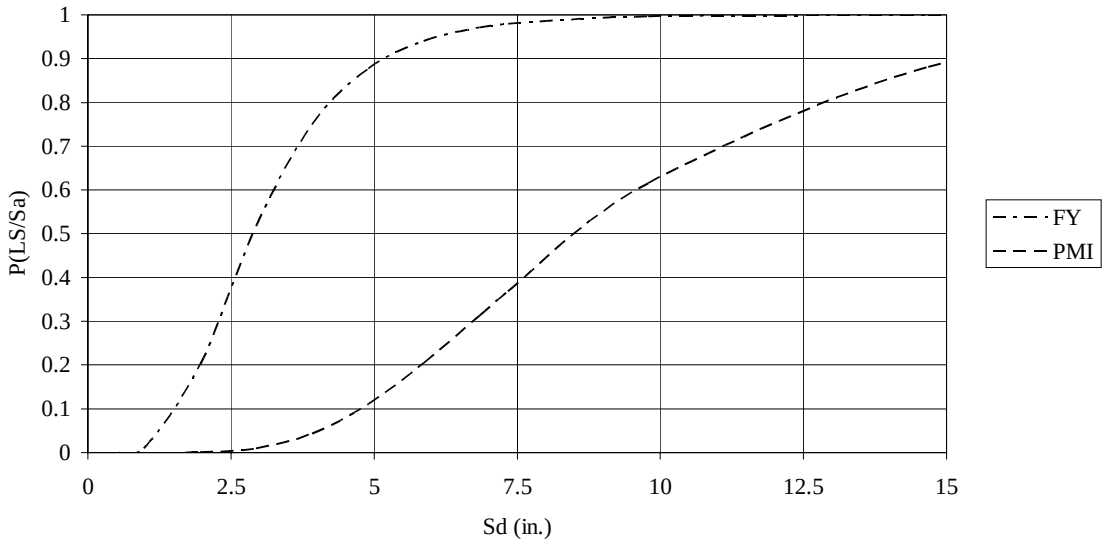

d) Pushover - Spectral Displacement

FIGURE 36 (Continued)

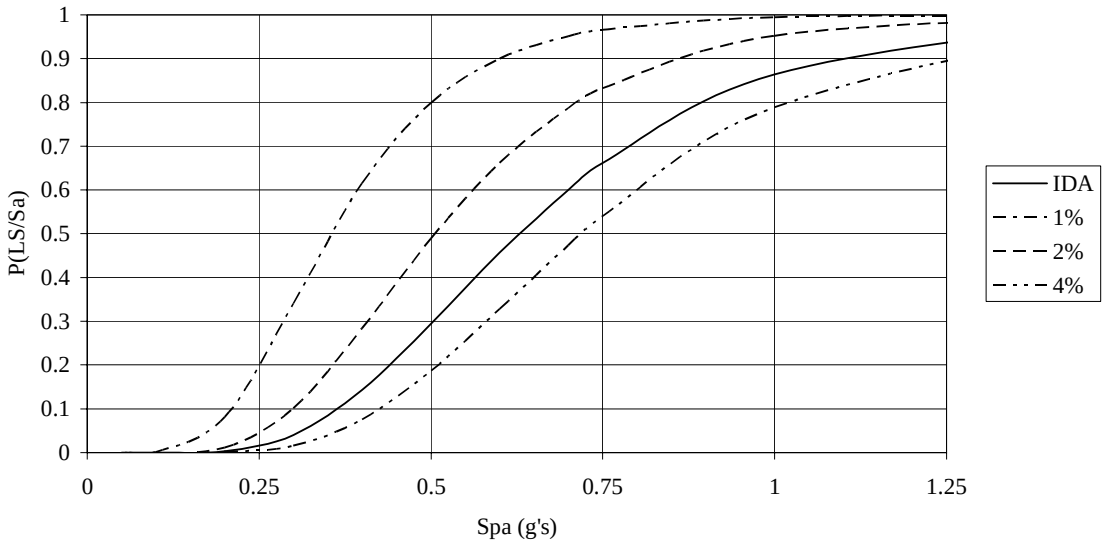

(a) FEMA

FIGURE 37 Fragility Curves – With the Effects of P-Delta – C/B Ratio 1.8

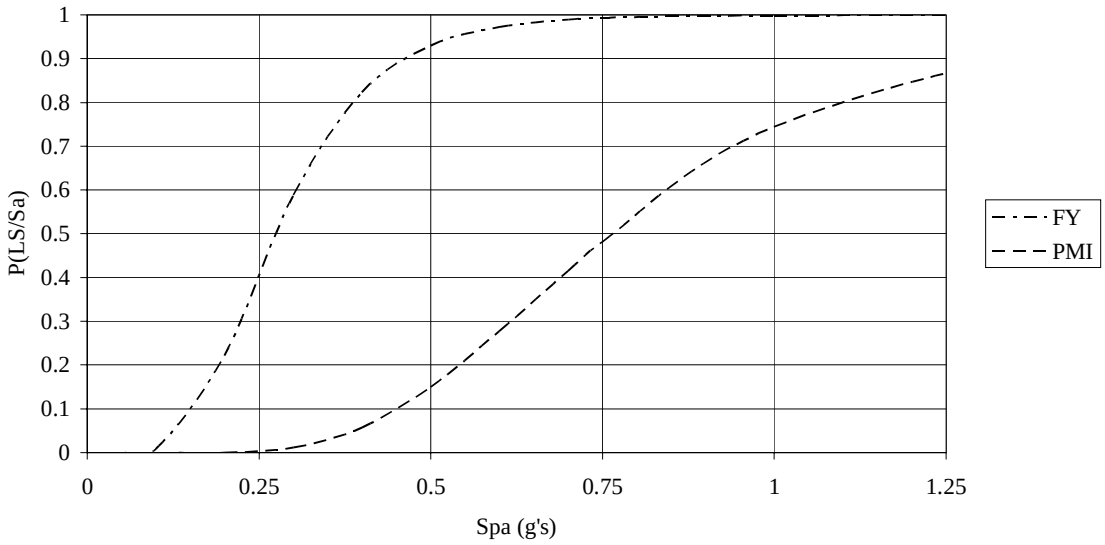

(b) Pushover

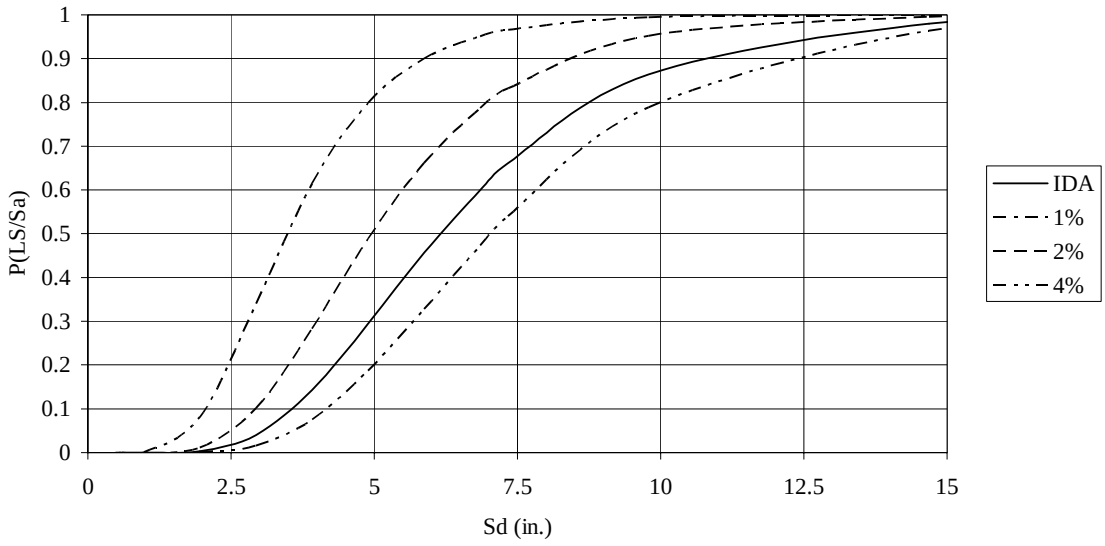

c) FEMA - Spectral Displacement

FIGURE 37 (Continued)

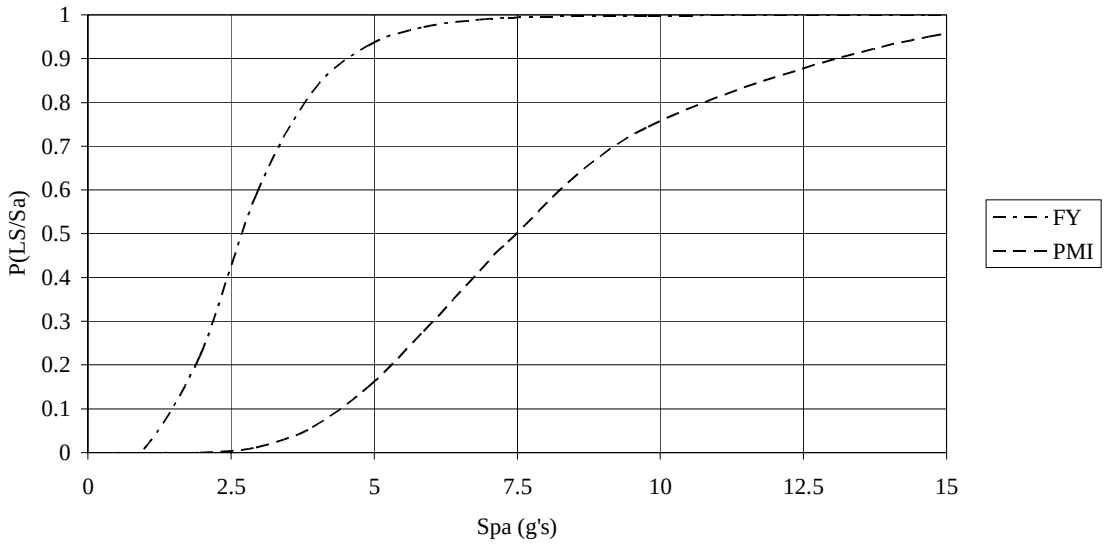

d) Pushover - Spectral Displacement

FIGURE 37 (Continued)

SUMMARY

These fragility curves can be compared using the spectral acceleration value for Memphis in the IBC 2000 code provisions, 0.74 g's. This value of spectral acceleration is then found on the fragility curves and the probability of the designed building exceeding the required limit state is determined. The fragility curves created using the FEMA limit states as the story capacity are shown with the fragility curve created using the incremental dynamic analyses as story capacity. The probability of exceedance for the 1% drift limit is 93%, for the 2% drift limit it is 73%, for the 4% drift limit it is 42%, and finally for the incremental dynamic analysis story capacity it is 56%. Also shown in Fig. 36 are the fragility curves created using the pushover analysis results as the story capacity. For the graphs the probability of exceedance for first yield is 98%, for plastic mechanism initiation it is 37%. Shown in Fig. 37 are the same fragility curves created from analyses including the effects of p-delta. The probability of exceedance for the

first set of fragility curves is 97% for a 1% drift limit, 83% for a 2% drift limit, 54% for a 4% drift limit, and 66% for the drift limit corresponding to the results obtained from the incremental dynamic analyses. Finally, the probability of exceedance for first yield is 99%, for plastic mechanism initiation it is 48%.

As can be seen from these results the probability of exceedance obtained from the FEMA limit state fragility curves have a closer correlation to the probability of exceedance obtained from the pushover limit state fragility curves than any other column-to-beam strength ratio. For this reason it is believed that the FEMA limit states suggested in document 273 are good indicators of the fragility of a well designed stable structure. Additionally, it can be seen by comparing the probability of exceedance obtained from all three of the building structures that the structure with a 1.8 column-to-beam strength ratio shows less vulnerability to the ground motions present in the New Madrid seismic zone.

In addition to the probabilities of exceedance determined at a spectral acceleration value of 0.74, the shape of the fragility curve should also be noted. When looking at the shape of the fragility curve one can easily ascertain that the shape of the fragility curve becomes more satisfactory as the column-to-beam strength ratio is increased. This should be mentioned because the spectral acceleration values compared in this research are for the extreme design earthquake in the New Madrid Seismic Zone. Other portions of the New Madrid Seismic Zone do not have design spectral acceleration values of such great magnitude. Therefore, more improvement would be seen in the probability of exceeding a defined limit state should a smaller spectral acceleration value be feasible.

CHAPTER IX
CONCLUSIONS AND FUTURE WORK

SUMMARY

In summary, much knowledge has been gained from the research performed for this thesis. The behavior of older reinforced concrete frame structures located in the Mid-America region, exposed to lateral loads was studied. This study began with the design of a representative prototype structure, followed by the analysis of that structure, and the creation of fragility curves for the prototype structure. The behavior of this structure was analyzed under both small and large lateral, or earthquake, loads. It was found that this structure could withstand small magnitude earthquakes adequately, however, large magnitude earthquakes posed a threat. The threat present with the occurrence of large magnitude earthquake events would most likely cause collapse of the structure. This threat led to a retrofit of the prototype structure. This retrofit was then analyzed to determine if the retrofitted prototype structure would be capable of resisting large lateral loads with a smaller threat of collapse. The retrofit was put into place by strengthening the column members in the prototype structure, recommended by Dooley and Bracci (2001), thereby increasing the column-to-beam strength ratio. Two different retrofits were tested in order to obtain the most effective option. It was found that with a column-to-beam strength ratio of 1.2 the buildings performance was significantly improved. The second retrofit option involved increasing the column-to-beam strength ratio to a value of 1.8. More improvement in behavior was once again found with this retrofit. Therefore, it is suggested here that while the originally designed older reinforced concrete frame structure was not deemed adequate, increasing the column-to-beam strength ratio to a value of 1.8 provided the most adequate structural performance. Below is a discussion of the individual structural performance throughout the analysis process the led to the conclusion discussed above.

When performing pushover analyses on the originally designed prototype structure, it was found that limit states occurred at small drift values. This means that only a small amount of drift of the structure would cause exceedance. In addition, almost all of the damage was confined to the columns in one story of the structure. When looking at the force control analyses in conjunction with the 10% on 3rd story displacement control analysis it is found that the first story is critical and will control the behavior of the entire structure. This is the exact opposite of the desired pushover analysis behavior, marking the possibilities of a building not suited to withstand lateral loading typical of earthquakes.

The dynamic analyses show that the drift values obtained from the individual 2% in 50 years probability of exceedance ground motion records are large. The incremental dynamic analyses indicate that most of the records form an incipient collapse point. The records that did not form incipient collapse points were the 10% in 50 years probability of exceedance typically records of small magnitude earthquakes. For comparison amongst the buildings tested, the probability of the designed structure exceeding a defined limit state at a spectral acceleration value of 0.74 was compared. This spectral acceleration value is determined through the IBC 2000 building code provisions, and considered an extreme spectral acceleration value for this portion of the country. When considering the originally designed structure it is found that all of the limit states have a high probability of exceedance.

Based on the work of Dooley and Bracci (2001), a retrofit of the gravity load designed structure was conducted by column strengthening only. The purpose of this effort was to determine whether or not strengthening the columns of a structure designed for gravity loads only would allow this structure to be less seismically vulnerable.

The first retrofit attempted was to change the column-to-beam strength ratio to 1.2, instead of the original structures 0.6 column-to-beam strength ratio value. The

pushover analyses showed numerous characteristics representing better behavior of the structure under lateral loading. The first of these is that the limit state values of first yield and plastic mechanism initiation were larger than those obtained in the original structure. This shows that more drift can be withstood before limit states and performance of the structure becomes an issue. Additionally, it should be noted that the strength degradation limit state was not found to exist in these pushover analyses. This means that the structure under lateral loading, including the effects of p-delta, was not found to degrade to a level that would be considered failure of the structure, or that the story shear in the building was not found to drop by 20% throughout analyses. Additionally, the yielding, or damage, of members in the structure was more evenly dispersed than in the original building structure. All of these characteristics indicate that this retrofitted structure, with a column-to-beam strength ratio of 1.2, has larger deformable capacity than the originally designed prototype structure. Additionally, the dynamic time history analyses of the retrofitted structure were found to provide smaller drift demand values for the individual earthquake records. In order to fully grasp the level to which this building exceeds the performance of the prototype structure, fragility curves were compared. The fragility curves for this structure were located further to the right side of the chart, meaning that there is a lower probability of exceedance given any spectral acceleration value. Once again the probability of limit state exceedance at a spectral acceleration value of 0.74 g's was used to determine the adequacy of the building behavior. These probabilities of exceedance are discussed in the following section.

Desiring even better performance from the retrofit of the structure, the column-to-beam strength ratio was again increased. For the second retrofit analysis the column-to-beam strength ratio was raised to a value of 1.8. The pushover analyses at this column-to-beam strength ratio displayed many desirable characteristics. The first of these is that the limit state values were much larger than in any other analysis, suggesting that the structure can withstand higher lateral loading values. In addition to

this, under these loading conditions, the plastic mechanism initiation limit state value was not found to exist in most of the pushover analyses. This shows that some of the pushover analyses are actually forming no failure mechanisms, another positive trait. In addition to this, the damage caused by these pushover forces and displacements throughout the structure is almost completely even, meaning that the damage is dispersed evenly throughout all stories of the structure. Additionally, in these analyses the yielding of individual members is concentrated on the beams members. This is desirable because when columns are the main structural member yielding, only one floor of columns must yield in order to form a story mechanism. If the beams are the primary yielding structural member, then all of the beams in the structure must yield before a beam side sway mechanism is considered to occur. From looking at these pushover analyses it can be determined that this structure resists lateral loads much more adequately than the originally designed structure. The incremental dynamic analyses are also promising in that all earthquake records do not reach an incipient collapse value. The dynamic analyses also provide positive information. The peak drifts obtained from the earthquakes records are much smaller than those found in the original structure. Finally, the fragility curves for this structure can be compared. These fragility curves are located further to the right of the chart than any other building analyzed in this research, meaning that this structure has the least probability of failure. The probability of exceeding defined limit states are discussed in the following section. These results lead to the conclusion that the originally designed structure with a retrofit increasing the column-to-beam strength ratio to 1.8 performs better than the other building options.

CONCLUSIONS

The fragility curves created throughout this research provide a vast amount of information concerning the behavior of older reinforced concrete frame structures located in Mid-America, historically an area of low to moderate seismic risk. In addition to providing information regarding the originally designed structure, these analyses have

provided information pertaining to the possible retrofit of this type of structure and the results that can be expected from such a retrofit.

TABLE 6 Power Law Equations – Seismic Demand Comparison

Mc/Mb=0.6		
	Excluding the Effects of P-Delta	Spa = 0.3035δ^0.5111
	Including the Effects of P-Delta	Spa = 0.2718δ^0.4763
Mc/Mb=1.2		
	Excluding the Effects of P-Delta	Spa = 0.3354δ^0.5413
	Including the Effects of P-Delta	Spa = 0.3154δ^0.5101
Mc/Mb=1.8		
	Excluding the Effects of P-Delta	Spa = 0.3496δ^0.5580
	Including the Effects of P-Delta	Spa = 0.3428δ^0.5506

Table 6 shows the power law equations for each of the three buildings analyzed both excluding and including the effects of p-delta. This power law equation is necessary for determining the $\lambda_{D/Sa}$ term present in the probability of exceedance equation. The power law coefficients are similar among all of the structures tested. However, some variation was found to exist. This variation in power law coefficients accounts for some of the differences in $\lambda_{D/Sa}$ throughout the various structures, thereby impacting the probability of exceeding a given limit state.

Table 7 displays the fragility coefficients needed to determine the probability of a structure exceeding a defined limit state. These terms include $\beta_{D/Sa}$, β_{ICC}, β_C, and λ_{ICC}. The β_C term is assumed to be a constant of 0.30 throughout all analyses, as discussed in Chapter IV. $\beta_{D/Sa}$ is constant within the analyses performed for an individual structure. This is the case because only one analysis was performed to determine the demand of each structure. β_{ICC} is the same for each of the three structures when considering the FEMA defined drift limit states and the quantitative pushover analysis defined limits. λ_{ICC} is found to vary throughout all analyses. However, both of these terms are found

TABLE 7 Fragility Coefficients

Mc/Mb=0.6		λ_{ICC}	$\beta_{D/Sa}$	β_{ICC}	β_C
	FEMA-1%	0	0.50	0.30	0.30
	FEMA-2%	0.69	0.50	0.30	0.30
	FEMA-4%	1.39	0.50	0.30	0.30
	FY	-1.23	0.50	0.30	0.30
	PMI	-0.49	0.50	0.30	0.30
	IDA	0.87	0.50	0.46	0.30
Mc/Mb=1.2					
	FEMA-1%	0	0.73	0.30	0.30
	FEMA-2%	0.69	0.73	0.30	0.30
	FEMA-4%	1.39	0.73	0.30	0.30
	FY	-0.45	0.73	0.30	0.30
	PMI	0.69	0.73	0.30	0.30
	IDA	0.79	0.73	0.42	0.30
Mc/Mb=1.8					
	FEMA-1%	0	0.51	0.30	0.30
	FEMA-2%	0.69	0.51	0.30	0.30
	FEMA-4%	1.39	0.51	0.30	0.30
	FY	-0.51	0.51	0.30	0.30
	PMI	1.50	0.51	0.30	0.30
	IDA	1.10	0.51	0.34	0.30

to vary when considering the limit states defined by the incremental dynamic analyses. Additionally, the terms for the FEMA defined limit states in conjunction with the terms for the incremental dynamic analyses and pushover defined limit states correlate more as the building structure becomes more stable. This leads to the belief that the FEMA defined limit states are representative of a well designed structure and are not so representative of older reinforced concrete frame structure located in Mid-America.

Table 8 discusses the probability of each of the three designed structures exceeding the previously defined limit states. The probability of exceeding the defined limit states decreases as the column-to-beam strength ratio of the structure is increased from 0.6, the value for the originally designed prototype structure, to 1.2, the value suggested as a minimum by ACI 318. This improved performance is found again when the column-to-beam strength is raised to 1.8 for the limit states corresponding to 4% drift, IDA, and PMI. The probability of exceedance between the initially retrofitted structure and the 1.8 column-to-beam strength ratio retrofit is basically nonexistent for the FEMA defined limit states. However, improvement is found when considering the limit states defined by the pushover and incremental dynamic analyses.

TABLE 8 Probability of Exceedance

Mc/Mb=0.6			Including P-Delta	
	1%	99%	1%	100%
	2%	93%	2%	97%
	4%	66%	4%	82%
	IDA	85%	IDA	88%
	FY	100%	FY	100%
	PMI	100%	PMI	100%
Mc/Mb=1.2				
	1%	93%	1%	96%
	2%	74%	2%	85%
	4%	42%	4%	54%
	IDA	69%	IDA	73%
	FY	93%	FY	96%
	PMI	73%	PMI	92%
Mc/Mb=1.8				
	1%	93%	1%	97%
	2%	73%	2%	83%
	4%	42%	4%	54%
	IDA	56%	IDA	66%
	FY	98%	FY	99%
	PMI	37%	PMI	48%

FUTURE WORK

The research performed for this thesis provides much information about older reinforced concrete frame structures, but future work is still needed. The methods used for creating the fragility curves were based on an assumption of a power law fit to the demand data. This power law fit can only be assumed to be accurate when good correlation is found throughout the center portion of the data set. For this research synthetic ground motions were utilized and no data points were found in the central portion of the chart declaring the power law adequate. Therefore, these analyses would need to be refined as more accurate ground motions are identified. This improvement in ground motion definition would also decrease the uncertainty present when calculating the probability of exceedance. It is believed that the research presented herein provides a good beginning evaluation of the vulnerability of older reinforced concrete frame structures. There is room for improvement in the analysis process with the creation of more accurate computer simulations and ground motions.

REFERENCES

Aycardi, L .E., Mander, J. B., and Reinhorn, A. M. (1994). "Seismic Resistance of Reinforced Concrete Frame Structures Designed Only for Gravity Loads: Experimental Performance of Sub Assemblages," *ACI Structural Journal*, ACI, 91(5), 552-563.

Bracci, J. M., Reinhorn, A. M., and Mander, J.B. (1995). "Seismic Resistance of Reinforced Concrete Frame Structures Designed for Gravity Loads: Performance of Structural System," *ACI Structural Journal*, ACI, 92(5), 597-609.

Building Code Requirements for Structural Concrete (ACI 318-71) and Commentary (ACI 318R-71), American Concrete Institute, Farmington Hills, MI.

Building Code Requirements for Structural Concrete (ACI 318-83) and Commentary (ACI 318R-83), American Concrete Institute, Farmington Hills, MI.

Building Code Requirements for Structural Concrete (ACI 318-99) and Commentary (ACI 318R-99), American Concrete Institute, Farmington Hills, MI.

Building Code Requirements for Structural Concrete (ACI 318-02) and Commentary (ACI 318R-02), American Concrete Institute, Farmington Hills, MI.

Cornell, C. A. and D. Vamvatsikos. (2002). "Incremental Dynamic Analysis." *Earthquake Engineering and Structural Dynamics, 31*, 491-514.

Dooley, K. L. (2001). "Effect of Column-to-Beam Strength Ratio on Earthquake Resistance of RC Moment Frames Using Probabilistic Performance-Based Design Methodologies," M.S. Thesis, Texas A&M University.

Dooley, K.L. and J. Bracci. (2001). "Seismic Evaluation of Column-to-Beam Strength Ratios in Reinforced Concrete Frames." *ACI Structural Journal*, 98 (6), 843-851.

El-Attar, A. G, White, R. N., and Gergely, P. (1997). "Behavior of Gravity Load Designed Reinforced Concrete Buildings Subjected to Earthquakes," *ACI Structural Journal*, ACI, 94(2), 133-145.

International Code Council. (2000). *International Building Code*. Falls Church, VA.

Federal Emergency Management Agency. (1997). *NEHRP Guidelines for the Seismic Rehabilitation of Buildings.* Washington D.C.

Nordenson, G. J. P. (1993). "Seismic Codes," *Monograph 2 Mitigation of Damage to the Built Environment,* Central United States Earthquake Consortium. Memphis Tennessee, 89-114.

Nuttli, O. W. (1987). *The Effects of Earthquakes in the Central United States*, Central United States Earthquake Consortium. Marion, Illinois.

Olshansky, R. B. (1993). "Selling Seismic Building Codes in the Central United States," *Proceedings of the 1993 National Earthquake Conference*, 1, 694-658.

PCACOL, version 2.20. (1992) Portland Cement Association.

Pessiki, S.P., Conley, C.H., Gergely, P., White, R.N. (1990). "Seismic Behavior of Lightly Reinforced Concrete Column and Beam-Column Joint Details," *Technical Report NCEER-90-00014*, State University of New York at Buffalo.

Powell, C. (2003). "Introduction to Seismology," Lecture, Center for Earthquake Research and Information, University of Memphis.

SAP2000 Nonlinear, version 7.10. (1999). Computers and Structures Inc, Berkeley, CA.

Kunnath, S.K. (2003). *IDASS.* http://cee.engr.urcdavis.edu/faculty/kunnath/kunnath.htm

Kunnath, S.K. (2003). *IDASS-Users Manual*. http://cee.engr.urcdavis.edu/faculty/kunnath/kunnath.htm

Tuttle, M. P., Schweig, E. S., Sims, J.D., Lafferty, R.H., Wolf, L.W., and Haynes, M.L. (2002). "The Earthquake Potential of the New Madrid Seismic Zone," *BSSA*, Seismological Society of America, 92(6), 2080-2089.

Wen, Y.K. (2003). Ground Motions http://mae.ce.uiuc.edu

Wen, Y.K., Ellingwood, B.R., and Bracci, J.M. (2004). "Vulnerability Function Framework for Consequence-based Engineering", *Technical Report # DS-4*, Mid-America Earthquake Center, University of Illinois at Urbana-Champaign.

Wen, Y.K., Wu, C.L. (2001). "Uniform Hazard Ground Motions for Mid-America Cities," *Earthquake Spectra,* 17(2), 359-384.

APPENDIX A

TERM DEFINITIONS

lc	Vertical distance between supports, in.	$A_{s,prov}$	Area of tension steel provided
t	Thickness of slab	ρ_{prov}	Ratio of tension steel provided
b_w	Web width	k_{prov}	k calculated based on area of steel provided
b_{actual}	Distance member must span	M_{prov}	Moment resistant provided
f'c	Specified compressive strength of concrete, psi	Overdesign	Percent of over strength a structural member has
fy	Specified yield strength of reinforcement	h	Overall thickness of member
d	Effective depth of section	h_f	Flange thickness
Cover	Distance between reinforcement and extreme section of member	l	Span length
Stirrup	Diameter of the stirrup	ln	Clear span
d_b	Bar diameter, in.	A_b	Area of beam section
Φ	Strength reduction factor	A_{slab}	Area of slab section
ϵ_{cu}	Strain in concrete	Yb	Distance between extreme fiber and centroid of beam section
ϵ_{sy}	Strain in longitudinal reinforcement in a compression zone	Ys	Distance between extreme fiber and centroid of slab section
k	$1-\sqrt{\frac{2\cdot M_d/\phi}{0.85\cdot f'c\cdot b\cdot d^2}}$	Q	$\frac{A_b\cdot Y_b + A_{slab}\cdot Y_s}{A_b + A_s}$
ρ	Ratio of tension reinforcement	Ib	Moment of inertia of beam section
ρ'	Ratio of compression reinforcement	Is	Moment of inertia of slab section
ρ_b	Reinforcement ratio producing balanced strain conditions	α	Ratio of flexural stiffness of beam section to flexural stiffness of slab section
β_1	Factor defined in ACI 318-99 10.2.7.3	w_u	Factored load per unit area
Mu	Factored moment	Mo	Total factored static moment
Mureduced	Factored moment after reduction	lmin	Minimum length
R	Reduction factor	β	Ratio of clear spans in long to short direction of two-way slabs

b	Width of member	Mcs	Column strip moment
k_{bal}	k at balanced strain conditions	Mms	Middle strip moment
As	Area of nonprestressed tension reinforcement	x	Shorter overall dimension of rectangular cross section
As, min	Minimum area of tension reinforcement required	Y	Longer overall dimension of rectangular cross section
b_{eff}	Effective compression flange width of structural member	C	Cross-sectional constant to define torsional properties
Ag	Gross area	Mu-slab	Factored moment in slab
F(xi)	Function evaluated at xi	P(LS/Sa)	Probability of exceeding a limit state given spectral acceleration
i	Data point number	Φ	Standard normal distribution
n	Number of data points	λ_{ICC}	ln(median(capacity drift))
zi	Standard normal variate corresponding to xi	$\lambda_{D/Sa}$	ln(demand drift_-0.5*$\beta_{D/Sa}$
xi	Inter-story drift value	$\beta_{D/Sa}$	sqrt(ln(1+Δx^2))
λ	Distribution parameter	β_{ICC}	sqrt(1+cov^2)
δ	Distribution parameter	βc	Modeling Uncertainty

APPENDIX B
SAMPLE DESIGN CALCULATIONS

While the design procedures for the beams, columns, and slab were provided in the previous sections, sample calculations are shown in the section below in order to aid in the understanding of the procedures used for design in this research.

3.6.1 Sample Beam Calculations

Finding Bf: smaller of

$$\frac{1}{4}l_c = 78"$$
$$16 \cdot t + b_w = 140"$$
$$b_{actual} = 312"$$

Given Quantities:

$$f'c = 4\,\text{ksi}$$
$$fy = 60\,\text{ksi}$$
$$b_w = 16"$$
$$d = 24" - \text{cover} - stirrup - \frac{d_b}{2} = 24 - 1.5 - 0.5 - 7/16 = 21.56"$$
$$\phi = 0.9$$
$$\varepsilon_{cu} = 0.003$$
$$\varepsilon_{sy} = 0.0021$$

Moment Redistribution (ACI 318-99:8.4):

$$R = 20 \cdot (1 - \frac{\rho - \rho'}{\rho_b})\%$$
$$\rho_b = \frac{0.85 f'c \cdot \beta_1}{f_y} \cdot \frac{87{,}000}{87{,}000 + f_y}$$

$$\rho_b = \frac{0.85 * 4{,}000 \cdot 0.85}{60{,}000} \cdot \frac{87{,}000}{87{,}000 + 60{,}000} = 0.029$$

$$\rho - \rho' = 0.5\rho_b = 0.014$$

$$R = 20 \cdot (1 - \frac{0.014}{0.029})\% = 10\% \text{ allowable moment reduction}$$

Negative Moment Reinforcement:

$$M_u = 3007.27 \text{ k-in}$$

$$M_{u,reduced} = 2706.54 \text{ k-in}$$

Calculate k:

$$k = 1 - \sqrt{1 - \frac{2 \cdot \frac{M_u}{\phi}}{0.85 \cdot f'c \cdot b \cdot d^2}}$$

$$k = 1 - \sqrt{1 - \frac{2 \cdot \frac{2706.54}{0.9}}{0.85 \cdot 4 \cdot 16 \cdot 21.56^2}} = 0.127$$

Calculate k_{bal}:

$$k_{bal} = \frac{0.85 \cdot \varepsilon_{cu}}{\varepsilon_{cu} + \varepsilon_{sy}}$$

$$k_{bal} = \frac{0.85 \cdot 0.003}{0.003 \cdot 0.0021} = 0.503$$

$$k \le 0.75 \cdot k_{val}$$

$0.127 \le 0.377$ use k instead of k_{bal}

Required Area of Steel:

$$A_s = \frac{M_u / \phi}{f_y \cdot d \cdot (1 - k/2)}$$

$$A_s = \frac{2706.54/0.9}{4 \cdot 21.56 \cdot (1 - 0.127/2)} = 2.48in^2$$

Minimum steel area:

$$A_{s\,min} = 6\sqrt{f'c/f_y} \cdot bw \cdot d$$

$$A_{s\,min} = 6\sqrt{4{,}000/60{,}000} \cdot 78 \cdot 21.56 = 1.90in^2$$

or

$$A_{s\,min} = \frac{200 \cdot beff \cdot d}{f_y}$$

$$A_{s\,min} = \frac{200 \cdot 78 \cdot 21.56}{60{,}000} = 5.30in^2$$

Try 4 #6 bars

$$A_{s,prov} = 2.4in^2$$

Calculate Moment Provided:

$$\rho_{prov} = \frac{A_{sprov}}{d \cdot b}$$

$$\rho_{prov} = \frac{2.4}{21.56 \cdot 16} = 0.006957$$

$$k_{prov} = \rho_{prov} \frac{f_y}{0.85 \cdot f'c}$$

$$k_{prov} = 0.006957 \frac{60{,}000}{0.85 \cdot 4{,}000} = 0.123$$

$$M_{prov} = A_s \cdot f_y \cdot d \cdot (1 - k_{prov}/2)$$

$$M_{prov} = 2.4 \cdot 60 \cdot 21.56 \cdot (1 - 0.123/2) = 2914k - in$$

$$overdesign = 7\%$$

2.6.2 Sample Slab Calculations

Calculate Slab Thickness:

Given Quantities:

$b_w = 16''$

$h_w = 16''$

$h = 20''$

$hf = 8$

$b = 50''$

$l = 26'$

$\ln = 24.67'$

$f_y = 60{,}000\,psi$

$f'c = 4{,}000\,psi$

Locate the Centroid:

$A_b = bw \cdot hw$

$A_b = 16 \cdot 16 = 256in^2$

$A_{slab} = hf \cdot b$

$A_{sslab} = 8 \cdot 50 = 400in^2$

$Y_b = \frac{hw}{2}$

$Y_b = \frac{16}{2} = 8''$

$Y_s = \frac{hf}{2} + hw$

$Y_s = \frac{8}{2} + 16 = 20''$

$Q = \frac{A_b \cdot Y_b + A_{slab} \cdot Y_s}{A_b + A_s}$

$Q = \frac{256 \cdot 8 + 400 \cdot 20}{256 + 400} = 15.32in$

Calculate I's:

$$I_b = \frac{1}{12}\cdot b_w \cdot {h_w}^3 + A_b \cdot (Q - Y_b)^2 + \frac{1}{12}\cdot b \cdot {h_f}^3 + A_{slab} \cdot (Q - Y_s)^2$$

$$I_b = \frac{1}{12}\cdot 16 \cdot 16^3 + 256 \cdot (15.32 - 8)^2 + \frac{1}{12}\cdot 50 \cdot 8^3 + 400 \cdot (15.32 - 20)^2 = 1.45\, ft^4$$

$$I_s = \frac{1}{12} l \cdot 12 \cdot hf^3$$

$$I_s = \frac{1}{12}\cdot 26 \cdot 12 \cdot 8^3 = 0.642\, ft^4$$

$$\alpha = \frac{I_b}{I_s}$$

$$\alpha = \frac{1.45}{0.642} = 2.26$$

Slab Thickness (ACI 318:9.5.3.3):

$$\alpha \succ 2$$

$$h = \frac{\ln(0.8 + {f_y}/{200{,}000})}{36 + 9 \cdot \beta}$$

$$h = \frac{24.67 \cdot 12 \cdot (0.8 + {60{,}000}/{200{,}000})}{36 + 9 \cdot 1} = 7.24"$$

From these calculations it is found that the required slab thickness is 7.24”, less than the 8” assumed thickness, therefore this assumption is acceptable. The slab reinforcement is calculated below using the direct design method. Section 13.6.1 of the ACI 318-99 describes the requirements for using the direct design method.

Calculate Slab Reinforcement:

Distribution of Moment within Panels:

$$w_u = 1.4(\frac{8}{12} \cdot 150 + 20) + 1.7 \cdot 50 = 253 psf$$

$$M_o = \frac{w_u \cdot l2 \cdot \ln^2}{8}$$

$$M_o = \frac{(253/1000) \cdot 26 \cdot 24.67^2}{8} = 500.43k - ft$$

$$ColumnStrip = \frac{1}{4} l \min$$

$$ColumnStrip = \frac{1}{4} \cdot 26 = 6.5'$$

$$MiddleStrip = l1 - 2 \cdot ColumnStrip$$

$$MiddleStrip = 26 - 2 \cdot 6.5 = 13'$$

Positive and Negative Panels:

Interior Spans:

$$Neg.FactoredMom = 0.65 \cdot M_o = 325.28k - ft$$

$$Pos.FactoredMom = 0.35 \cdot M_o = 175.15k - ft$$

$$Sum = NegFactoredMom + Pos.FactoerdMom = 500.43$$

End Spans: Slab with beams between all supports.

$$InteriorNeg.FactoredMom = 0.70 \cdot M_o = 350.30k - ft$$

$$Pos.FactoredMom = 0.57 \cdot M_o = 285.24k - ft$$

$$ExteriorNeg.FactoredMom = 0.16 \cdot M_o = 80.10k - ft$$

Factored Moment in Column Strip:

ACI 318-99: 13.6.4.1

$$M_{cs} = 0.75 \cdot InteriorNeg.FactoredMom = 262.73k - ft$$

ACI 318-99: 13.6.4.2

Assume a rectangular beam section because the negative moment is based on a rectangular section.

$$x = \frac{16}{12} = 1.33'$$

$$y = \frac{24}{12} = 2'$$

$$C = \Sigma(1 - 0.63 \cdot {}^{x}\!/\!_{y}) \cdot \frac{x^3 \cdot y}{3}$$

$$C = (1 - 0.63 \cdot {}^{1.33}\!/\!_{2}) \cdot \frac{1.33^3 \cdot 2}{3} = 0.92$$

$$\beta_t = \frac{E_{cb} \cdot C}{2 \cdot E_{cs} \cdot I_s} = 0.71$$

Use interpolation in order to determine a value of 77.34% of the exterior negative factored moment that must be resisted by the column strip.

$$M_{cs} = 0.7734 \cdot 80.10 = 61.93k - ft$$

ACI 318-99: 13.6.4.4

$$M_{cs} = 0.75 \cdot Pos.FactoredMom$$

$$M_{cs} = 0.75 \cdot 285.24 = 213.93k - ft$$

ACI 318-99: 13.6.5-Moment to be carried by both the beam and the slab.

$$M_b = 0.85 \cdot InteriorNeg.FactoredMom = 223.32k - ft$$

$$M_b = 0.85 \cdot ExteriorNeg.FactoredMom = 52.64k - ft$$

$$M_b = 0.85 \cdot Pos.FactoredMom = 181.84k - ft$$

$$M_s = 0.15 \cdot InteriorNeg.FactoredMom = 39.41k - ft$$

$$M_s = 0.15 \cdot ExteriorNeg.FactoredMom = 9.29k - ft$$

$$M_s = 0.15 \cdot Pos.FactoredMom = 32.09k - ft$$

ACI 318-99: 13.6.6-Middle Strip Moments

The middle strip section of the slab must be able to resist the moment that is not placed on the column strip section of the slab.

$$M_{ms} = 87.58k - ft$$
$$M_{ms} = 71.31k - ft$$
$$M_{ms} = 18.14k - ft$$

The sample calculations below show the reinforcement area needed in the interior column strip for resisting negative moment demands. These calculations were repeated for the exterior negative factored moment as well as the positive factored moment for both the column and middle strips.

Given Quantities:

$$M_{u-slab} = {M_s \cdot 12}/{13} = 36.38 {k - in}/{ft}$$
$$b = 12"$$
$$A_g = 96in^2$$
$$\phi = 0.9$$
$$d = 7"$$
$$h = 8"$$

Calculate k:

$$k = 1 - \sqrt{\frac{2 \cdot {M_d}/{\phi}}{0.85 \cdot f'c \cdot b \cdot d^2}}$$
$$k = 1 - \sqrt{\frac{2 \cdot ({36.38}/{0.9})}{0.85 \cdot 4 \cdot 12 \cdot 7^2}} = 0.02$$

Calculate k_{bal}:

$$k_{bal} = \beta_1 \cdot \frac{\varepsilon_{cu}}{\varepsilon_{cu} + \varepsilon_{sy}}$$

$$k_{bal} = 0.85 \cdot \frac{0.003}{0.003 + 0.0021} = 0.50$$

$$k \le 0.75 \cdot k_{bal}$$

$$0.02 \le 0.377$$

Use k for design not k_{bal}

Calculate the Required Area of Steel:

$$A_s = \frac{M_d / \phi}{f_y \cdot d \cdot (1 - k/2)}$$

$$A_s = \frac{36.38 / 0.9}{4 \cdot 7 \cdot (1 - 0.02/2)} = 0.10 in^2 / ft$$

Calculate Minimum Required Area of Steel:

$$A_s = 0.0018 \cdot h \cdot 12$$

$$A_s = 0.0018 \cdot 8 \cdot 12 = 0.17 in^2 / ft$$

The minimum area of steel required is larger than that required by the moment demands placed onto the slab, therefore the minimum area of steel required is utilized throughout this portion of the slab. It was found that this minimum area of steel reinforcement controlled throughout the entire slab system.

VITA

Lauren Rae Beason, the author, was born July 6, 1980, in Lubbock, Texas. She graduated from A&M Consolidated High School, located in College Station, Texas. The author studied civil engineering at Texas A&M University, receiving a Bachelor of Science degree in civil engineering May 2002. After graduation, she enrolled in graduate school to obtain a Master of Science in civil engineering - structures. While working on her degree, she worked as a Research Assistant for Dr. Joseph Bracci.

The author's permanent address is as follows:

2105 Fairfax
College Station, Texas 77845
Telephone: (979) 696-3544